University of Alberta

Organization of the cerebellum: correlating biochemistry, physiology and anatomy in the ventral uvula of pigeons

by

David James Graham

A thesis submitted to the Faculty of Graduate Studies and Research
in partial fulfillment of the requirements for the degree of

Master of Science

Centre for Neuroscience

Fall 2011
Edmonton, Alberta

Abstract

The fundamental unit of organization in the cerebellum is the parasagittal zone, which can be seen in anatomical connections, physiological response properties, and molecular composition. This parasagittal arrangement is evolutionarily conserved and appears necessary for information processing. However, the relationship between these parasagittal zones and cerebellar function remains unclear. The goal of this thesis is to relate the zonal organization of various features involved in visual motion processing in the vestibulocerebellum by using immunochemical, electrophysiological and neuroanatomical techniques. Zebrin II (aldolase C) is heterogeneously expressed by Purkinje cells in alternating sagittal stripes of high and low (or no) expression. We demonstrate a clear relationship between zebrin II stripes, Purkinje cell response properties, and the visual climbing fibre afferents to the medial vestibulocerebellum. By examining the molecular, anatomical and physiological basis of parasagittal zones, we can uncover the basic principle of organization and function of the cerebellum.

Acknowledgements

I would like to thank my supervisor and mentor, Dr. Doug Wylie. Throughout my entire degree, he was a constant source of motivation, guidance, friendship, and even the occasional crossword puzzle partner. He made science fun, while ensuring that my standards were as high as his. I will always cherish and appreciate the opportunities he afforded me. I would also like to thank Dr. Janelle Pakan, for bringing me into the lab, and patiently instructing me on how to do science. I could not have finished this without her. Cristian Gutierrez and Dr. Andrew Iwaniuk, thank you for keeping me sane throughout. Your insights, encouragement and laughs made the lab a fun place to be. Thank you to Drs. Dallas Treit and Karim Fouad, and all the members at the Centre for always being there to answer the questions Doug thought too stupid to answer.

Finally, special thanks go to my friends and family for always being there for me. Mom and Dad, I could write another thesis just to thank you for all you've done for me over the years. Ryan, Scott, Kevin and Adam, thank you for indulging my sense of humour and keeping me real. Thank you especially Sarah for being the best girl in the world, and putting up with my inanity for the past 3 years. You're more than I deserve. I love you all very much.

> "We like to praise birds for flying. But how much of it is actually flying, and how much of it is just sort of coasting from the previous flap?" –Jack Handy

Table of Contents:

List of Tables:

List of Figures:

List of Abbreviations:

AOS	accessory optic system
BDA	biotinylated dextran amine
CF	climbing fibre
dc	dorsal cap of Kooy of the inferior olive
dl	dorsal lamella of the inferior olive
DTN, MTN, LTN	dorsal, medial, and lateral terminal nuclei
gl	granular layer of the cerebellum
Hsp25	heat-shock protein 25
IO	inferior olive
IXcd	folium IXcd of the cerebellum
LM (l, m, i)	nucleus lentiformis mesencephali, (lateral, medial, intercalated)
mcIO	medial column of the inferior olive
MF	mossy fibre
ml	molecular layer of the cerebellum
MLd	lateral mesencephalic nucleus, pars dorsalis
MST	middle superior temporal area
nBOR (d,p.l)	nucleus of the basal optic root (dorsal, proper, lateral)
NOT	nucleus of the optic tract
N-T	nasal-to-temporal
pcl	Purkinje cell layer of the cerebellum
rHA	rotation about an horizontal axis

rVA	rotation about the vertical axis
T-N	temporal-to-nasal
VbC	vestibulocerebellum
vl	ventral lamella of the inferior olive
vlo	ventrolateral outgrowth of the inferior olive
VTA	ventral tegmental area
VTRZ	visual relay tegmental zone
wm	white matter of cerebellum
X	folium X of the cerebellum
ZII+/-	zebrin II immunopositive, immunonegative

Chapter 1: **Introduction**

Cerebellum literally means "little brain," and though up to 80% of all neurons in the brain are found in the cerebellum (Lange, 1975; Herculano-Houzel, 2010), historically, the functional role of the cerebellum has received little attention. The cerebellar cortex consists of three layers throughout its extent: a molecular layer, a Purkinje cell (PC) layer and a granule cell layer (Fig. 1.1). Even though this basic cerebellar anatomy was established a century ago by work of early neuroscientists such as Ramon y Cajal (1911), today we are still far from understanding how the cerebellum actually functions, and exactly what it does. Due in part to its seemingly simple and uniform structure, conventional theories on cerebellar function have looked no further than its role in motor coordination (for review, see Glickstein et al., 2009); however, recent research has revealed that the cerebellum is more structurally and functionally complex than traditionally thought. This has lead to a fascinating new understanding of cerebellar organization. Researchers now know that the cerebellum consists of an array of parasagittal zones oriented parallel to the midline, and is far from being a homogenous, uniform structure (Voogd and Bigare, 1980; Arends and Voogd, 1989; Hawkes et al., 1993; Hawkes and Mascher, 1994; Tan et al., 1995b; Voogd et al., 1996; Hawkes, 1997; Herrup and Kuemerle, 1997; Voogd and Ruigrok, 1997; Voogd and Glickstein, 1998; Rivkin and Herrup, 2003; Pijpers et al., 2005;

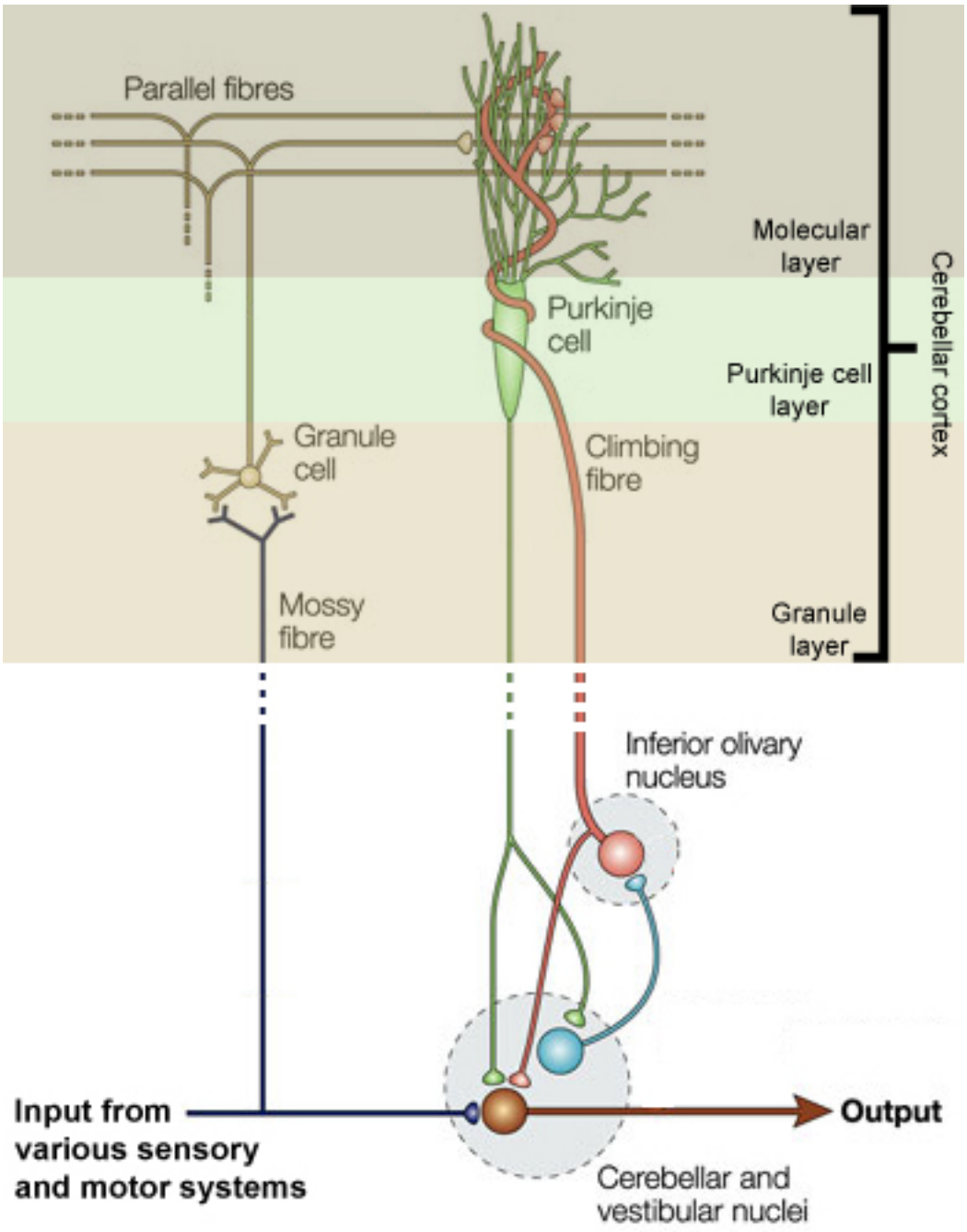

Figure 1.1 Simplified diagram of the cerebellar circuit. Three layers are seen throughout the cerebellar cortex of all vertebrate species. Afferents to the cerebellar cortex come from various sources via mossy fibres or climbing fibres. Purkinje cell axons are the only efferents of the cerebellar cortex, and synapse onto cerebellar and vestibular nuclei. (adapted from Ito, 2002)

Ito, 2006). This parasagittal organization can be seen in anatomical connections, functional zones, and biochemical markers (for review see: Hawkes and Gravel, 1991; Hawkes, 1992; 1997; Tan et al., 1995b; Herrup and Kuemerle, 1997).

The pigeon vestibulocerebellum (VbC) is an ideal structure in which to study the parasagittal nature of cerebellar organization for several reasons. First, the anatomical connections of the VbC have been well documented (see below, Sec. 1.2; Fig. 1.3). The parasagittal organization of the afferent input from the medial column of the inferior olive (mcIO) to the VbC *via* climbing fibres is extremely well understood (Wylie et al., 1999c; Crowder et al., 2000; Pakan et al., 2005), and the topography of the mcIO has been established with single-unit recording (Winship and Wylie, 2001). It is also known that the mossy fibre afferents from the accessory optic system (AOS) and pretectum provide the majority of visual inputs to the VbC, and the nuclei that provide these inputs have been well described (Wylie and Frost, 1990; 1999b; Wylie and Crowder, 2000; Crowder and Wylie, 2001; 2002; Crowder et al., 2003b; Winship et al., 2006a). Second, the functional characteristics of the pigeon VbC have been researched in depth. PCs in the VbC are responsive to different types of optic flow (see below, Sec. 1.1), and it has been shown that these response properties are organized into parasagittal zones (see Fig. 1.4; Wylie and Frost, 1991; Wylie et al., 1993; 1994; 1999c; De Zeeuw et al., 1994; Lau et al., 1998; Crowder et al., 2000; Winship and Wylie, 2003; Voogd and Wylie, 2004). Finally, it has recently been shown that some biochemical markers are expressed as alternating immunopositive and

immunonegative stripes throughout the cerebellum (see below, sec. 1.3; for review, see Hawkes & Herrup 1995). Of these molecular markers, the most thoroughly characterized is the metabolic isoenzyme aldolase C (also known as zebrin II [ZII]) which is expressed almost exclusively by PCs, including their dendrites, somata, axons and axon terminals (Brochu et al., 1990; Ahn et al., 1994; Hawkes and Herrup, 1995; Pakan et al., 2007). There are alternating, sagittally oriented stripes of ZII-immunopositive (ZII+) and ZII-immunonegative (ZII-) Purkinje cells throughout the cerebellar cortex. The most medial positive stripe is designated P1+, followed by the most medial negative stripe P1-, and the number increases as the stripes move laterally to P7+ and P7- (Brochu et al., 1990; Ozol et al., 1999; Sillitoe and Hawkes, 2002; Sillitoe et al., 2005). The spatial pattern and number of ZII stripes is evolutionarily conserved (Marzban and Hawkes, 2010), suggesting it has an important role in fundamental cerebellar function. The underlying question, however, is how the inherent parasagittal expression patterns of these molecules are related to cerebellar function. In this regard, the VbC provides an interesting opportunity to investigate the relationship between its well known anatomical and functional organization and biochemical markers. This will hopefully lead to a better understanding of the general principles underlying basic cerebellar architecture.

This thesis examines the anatomical, functional and biochemical properties of the pigeon VbC. Through the use of electrophysiological recording techniques, immunohistochemical techniques, and anatomical tracers, this thesis aims to reveal the underlying parasagittal organization of the cerebellum.

1.1 Optic Flow

1.1.1 *Introduction to Optic Flow*

Optic flow is the pattern of visual motion that occurs across the entire retina as a result of self-motion (Gibson, 1954), and it provides proprioceptive information about an organism's progress through the environment (Gibson, 1966; Lee, 1980; Lishman, 1981; Koenderink and van Doorn, 1987; Harris and Rogers, 1999; Lappe et al., 1999; Warren et al., 2001; Collett, 2002; Frenz et al., 2003; Baumberger and Fluckiger, 2004; Galbraith et al., 2005; Nomura et al., 2005). Figure 1.2 illustrates the pattern of visual motion across the retina using optic flow fields which are depicted as a sphere surrounding the moving organism. In figure 1.2A, rotation of the organism to the left causes rightward optic flow across the retina, and circular optic flow would be present along the axis of rotation. The pattern of optic flow shown in figure 1.2B is caused by backward translation in a straight line. The resulting focus of *contraction* is created as visual motion vectors converge in front of the organism on a point opposite to the direction of translation. In the direction of the translation vector, along the same axis, is a focus of *expansion* (not shown), a point from which all visual images radiate outward. However, within an organism's environment, analysis of optic flow fields is rarely as simple as the examples given. The retina itself does not remain stationary as it is mounted within a number of mobile supports (e.g. eyeball, head, torso, hips), and therefore naturally occurring optic

flow patterns contain both rotational and translational elements (van den Berg, 2000). Thus, a system of neural mechanisms must be in place to process the complex information produced by optic flow fields.

Gibson (1954) emphasized that vision can act as a proprioceptive sense to help control orientation and locomotion through the environment. Optic flow patterns are critical in this respect, as they contribute information needed for generating compensatory eye movements and head movements necessary for retinal image stabilization. We now know information provided by optic flow is used to process time to collision, heading of self-motion, object motion and object segmentation (Andersen and Atchley, 1997; Andersen, 1997; Lappe et al., 1999), and the control of posture and locomotion (Warren et al., 2001). Several studies have found that the AOS, the oculomotor nuclei, the vestibular nuclei, the IO and the VbC are involved in the analysis of optic flow and the generation of optokinetic responses (for reviews see Simpson, 1984; Graf et al., 1988; Simpson et al., 1988c; Grasse and Cynader, 1990). The role of the AOS in the optokinetic response is discussed below (Sec. 1.1.3).

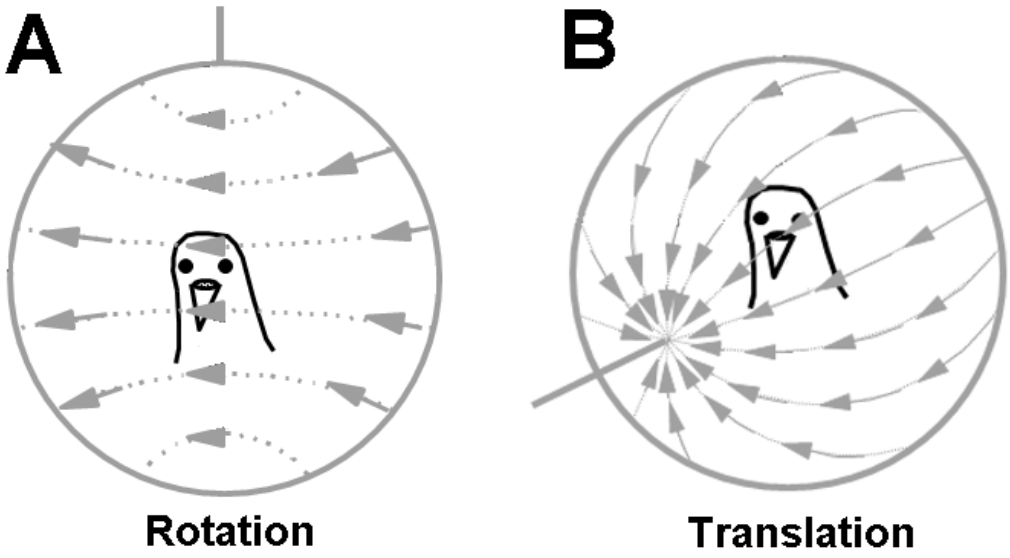

Figure 1.2 Optic flow-fields generated by self-rotation and self-translation. Arrows, as projected onto a sphere, represent the directions of local image motion in the optic flow-field. **A** shows a circular flow-field created by rotating about a vertical axis. The flow-field motion is opposite to the direction of head rotation. **B** shows optic flow produced by backward translation along an axis. At the 'pole' opposite the direction of translation, the arrows converge to a point; the focus of *contraction*. Likewise, at the opposite pole (not shown) the vectors would radiate outward at a point; the focus of *expansion*. At the equators of the sphere, the flow-field is laminar, with all vectors pointing in approximately the same direction.

1.1.2 *Optic Flow Pathways: Anatomy and Physiology of the AOS and Pretectum*

The role of the AOS and pretectum in the analysis of the visual effects of self-motion, and the nuclei involved in this process has been described in several vertebrate species (see Figure 1.3; for review, see Simpson, 1984). In mammals the medial, lateral, and dorsal terminal nuclei (MTN, LTN, and DTN, respectively) of the AOS are located near the mesodiencephalic junction, and receive direct retinal projections. There are also neurons responsive to optic flow in the associated nucleus of the optic tract (NOT) of the pretectum which is located immediately adjacent to DTN (Oyster et al., 1980; Ballas et al., 1981; Farmer and Rodieck, 1982; Weber, 1985). These nuclei then send efferent projections to neurons in the dorsal cap of Kooy and the ventrolateral outgrowth of the IO (Giolli et al., 1984, 1985; Blanks et al., 1995), which in turn send CF input to PCs in the VbC (Gerrits and Voogd, 1982; Hess and Voogd, 1986; Voogd et al., 1987a,b; Ruigrok et al., 1992; Tan et al., 1995a; Sugihara et al., 2004; Sugihara and Shinoda, 2004). AOS nuclei also project to a group of neurons in the ventral tegmental area (also known as the visual tegmental relay zone) which also sends input to the dorsal cap of Kooy (Maekawa and Takeda, 1979). PCs in the VbC project primarily to deep cerebellar and vestibular nuclei in the brainstem (Wylie et al., 1994; Tan et al., 1995b). The AOS and pretectum also provide direct input to vestibular and premotor nuclei (Giolli et al., 1984, 1985; Blanks et al., 1995). Therefore, optic flow information provided by the

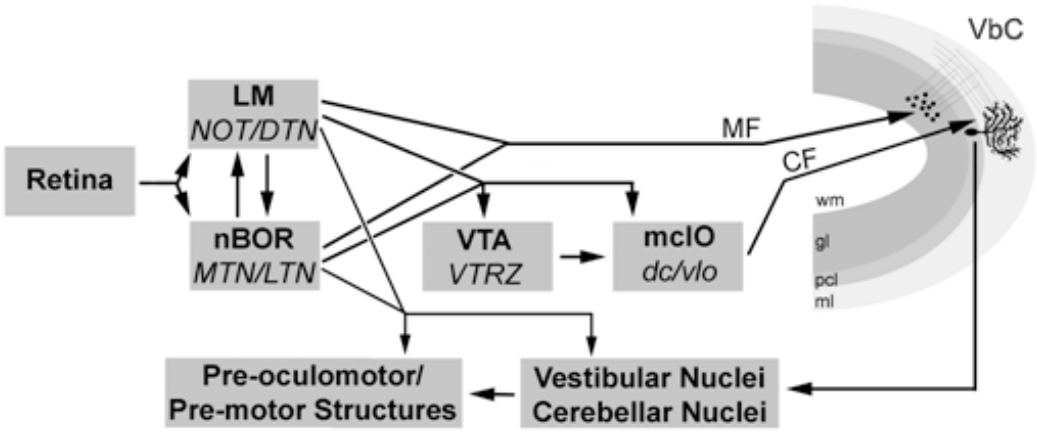

Figure 1.3 Simplified wiring diagram of the afferent and efferent connections of the Accessory Optic System (AOS) and associated pretectal pathways to the vestibulocerebellum. Avian and mammalian (in italics) nomenclature is included. LM, nucleus lentiformis mesencephali; nBOR, nucleus of the basal optic root; VTA, ventral tegmental area; mcIO, medial column of the inferior olive; VbC, vestibulocerebellum; MF, mossy fibre; CF, climbing fibre; wm, cerebellar white matter; gl, granule layer; pcl, Purkinje cell layer; ml, molecular layer; NOT, nucleus of the optic tract; DTN, dorsal terminal nucleus; MTN, medial terminal nucleus; LTN, lateral terminal nucleus; VTRZ, visual tegmental relay zone; dc, dorsal cap of Kooy of the inferior olive; vlo, ventrolateral outgrowth of the inferior olive.

AOS and associated pretectal nuclei to premotor and vestibular structures is both indirect (via the olivocerebellar pathway) and direct (via retinal recipient nuclei).

Retinal recipient nuclei within the AOS and in the pretectum have also been identified in birds (see Fig. 1.3). Within the AOS, the nucleus of the basal optic root (nBOR) receives direct retinal input from displaced ganglion cells of the retina (Karten et al., 1977; Reiner et al., 1979; Fite et al., 1981), and is comprised of three subdivisions based on cell morphology: nBOR dorsal, lateral, and proper (nBORd, nBORl, and nBOR, respectively; Brecha et al., 1980). Wylie et al. (1999a) suggested that nBORd may be an avian analogue of the visual tegmental relay zone (VTRZ). The nucleus lentiformis mesencephali (LM) in the pretectum receives retinal input and can be divided into two subnuclei: the LM pars lateralis and pars medialis (LMl and LMm, respectively; Gamlin and Cohen, 1988a,b). Both the nBOR and LM project to the mcIO (an olivary structure homologous to the dorsal cap of Kooy), which in turn projects to PCs in the VbC via CFs (Brecha et al., 1980; Gamlin and Cohen, 1988b; Wylie et al., 1997). In birds, the AOS (nBOR) and pretectum (LM) also send direct bilateral projections to the granule layer in folium IXcd (but not X) via MFs, therefore allowing both direct and indirect (via olivocerebellar pathway) input to the VbC (Wylie et al., 1997). VbC efferents also project primarily to the cerebellar and vestibular nuclei, as in mammals.

Because the AOS and pretectal neurons have been studied in many different species, the visual response properties of these neurons have been well

described (salamanders: Manteuffel, 1982, 1984; frogs: Cochran et al., 1984; Gruberg and Grasse, 1984; turtles: Rosenberg and Ariel, 1990; rabbits: Collewijn 1975; Maekawa et al., 1984; Simpson et al., 1979; rats: Natal and Britto, 1987; 1988; cats: Hoffmann and Schoppmann, 1981; Grasse and Cynader, 1984, 1990; opossum: Volchan et al., 1989; monkey: Hoffmann et al., 1988; Mustari and Fuchs, 1989; Westheimer and Blair, 1974; chicken: Burns and Wallman, 1981; McKenna and Wallman, 1981, 1985b; pigeon: Britto et al., 1981; Morgan and Frost, 1981; Winterson and Brauth, 1985; Gioanni et al., 1984; Wylie and Frost, 1990; 1999b; Wolf-Oberhollenzer and Kirschfeld, 1994; Wylie, 2000; wallaby: Ibboston et al., 1994; Ibbotson and Price, 2001). AOS and pretectal neurons are known to have extremely large receptive fields that lack inhibitory surrounds, and exhibit direction-selectivity to large-field visual stimuli moving in the contralateral visual field.

With respect to the pigeon, most nBOR and LM neurons show the greatest excitation to visual motion in a *preferred* direction, and are strongly inhibited by visual motion in the opposite, *anti-preferred* direction (Winterson and Brauth, 1985; Wolf-Oberhollenzer and Kirschfeld, 1994; Wylie and Frost, 1996; 1999b; Wylie, 2000; Wylie and Crowder, 2000; Crowder and Wylie, 2002). Specifically, about 50% of LM neurons prefer forward (temporal-to-nasal) visual motion, while fewer neurons prefer up, down, and backward (nasal-to-temporal) visual motion (~17% each; McKenna and Wallman, 1985; Winterson and Brauth, 1985; Fite et al., 1989; Fan et al., 1995; Wylie and Crowder, 2000). In contrast, most neurons in nBOR prefer up, down or backward visual motion (~32% each), with

fewer preferring forward visual motion (<5%; Burns and Wallman, 1981; Morgan and Frost, 1981; Gioanni et al., 1984; Rosenberg and Ariel, 1990; Wylie and Frost, 1990). The nBOR is topographically organized in terms of direction preference of visual motion. The dorsal portion of the nucleus contains cells responsive to upward visual motion, while cells responsive to downward visual motion are located ventrally. Cells responsive to backward visual motion are found along the most ventral and lateral surface of the nBOR, and cells responsive to forward visual motion are located in the posterior-dorsolateral margin of the nucleus (Burns and Wallman, 1981; Wylie and Frost, 1990). With respect to the LM, a consistent functional topographical organization has not yet been established.

1.1.3 *The Role of the AOS and Pretectum in the Optokinetic Response*

The optokinetic response (OKR) involves eye movements with an alternation of slow pursuit in one direction and a quick return in the opposite direction in order to stabilize movement of the entire visual field on the retina. The OKR minimizes optic flow across the retina by producing eye and/or head movements in the direction of motion. The OKR and the vestibulo-occular reflex work in harmony to help maintain a stable image upon the retina (Simpson, 1984; Waespe and Henn, 1987; Simpson et al., 1988c). This image stabilization is important for two reasons. First, it has been shown that a stationary retinal image is necessary for visual acuity (Westheimer and McKee, 1975). Second, the

velocity discrimination of moving targets is more accurately determined when the background visual field is stationary on the retina (Nakayama, 1981).

Several studies suggest that the AOS and pretectum play a major role in the control of OKR. Lesions to the AOS or pretectum severely impair OKR, while lesions to nuclei in other visual systems (e.g. geniculostriate or tectofugal structures) do not have a severe effect on OKR (Gioanni et al., 1983a,b; Simpson, 1984; McKenna and Wallman, 1985; Simpson et al., 1988). In birds, lesions to nBOR abolished monocular horizontal OKR in response to backward motion as well as vertical motion (Wallman et al., 1981; Gioanni et al., 1983b), while LM lesions abolished monocular horizontal OKN in response to forward motion (Gioanni et al., 1983a). As discussed previously, most neurons in the nBOR prefer up, down, or backwards optic flow, whereas most LM neurons prefer forward optic flow. Thus, these lesion results correspond well with the visual response properties of neurons in the nBOR and LM.

1.2 Organization of the Vestibulocerebellum

Information from the nBOR and LM is integrated in the mcIO and VbC to form large panoramic receptive fields sensitive to specific types of optic flow. Using the nomenclature of Karten and Hodos (1967), the pigeon VbC is comprised of the two most ventral folia of the posterior vermis, folia IXcd and X. The medial halves of these two folia are referred to as the uvula and nodulus, respectively, while the lateral halves are referred to as the flocculus, and merge rostrally to form the auricle of the cerebellum (Larsell, 1948; Larsell and

Whitlock, 1952). Several studies have shown that optic flow pathways to the VbC are involved in OKR and the vestibulooccular reflex (Simpson, 1984; McKenna and Wallman, 1985; Waespé and Henn, 1987; Simpson et al., 1988).

1.2.1 *Visual Afferents and Electrophysiological Response Properties*

LM and nBOR project directly to the mcIO, as previously discussed (see section 1.1.1). Wylie (2001) found that the caudal mcIO receives greater projections from the LM, whereas the nBOR has greater projections to the rostral mcIO. Given the visual motion preferences of the LM and nBOR discussed above, the specific projections from these nuclei to the mcIO correspond with the optic flow preferences of the neurons in the mcIO (Wylie, 2001; Winship and Wylie, 2003; see also Chapter 3).

Within the VbC, previous studies have shown that the complex spike activity (CSA) of PCs is modulated in response to particular patterns of optic flow (Simpson et al., 1981; 1989; Graf et al., 1988; Leonard et al., 1988; Kano et al., 1990a,b; Kusunoki et al., 1990; Shojaku et al., 1991; Wylie and Frost, 1991; 1993; 1999a; Wylie et al., 1993; 1998a). Furthermore, these PCs have binocular, panoramic receptive fields, and they have been shown to be topographically organized according to their preference for specific types of optic flow (Wylie et al., 1993; 1999c; Wylie and Frost, 1999a; Crowder et al., 2000). The CSA of these PCs is modulated best by optic flow generated around particular axes of rotation (e.g. Fig. 1.2A) or along particular axes of translation (e.g. Fig. 1.2B). While the medial VbC (the ventral uvula and nodulus) responds to different types

of translational optic flow, the lateral VbC (the flocculus) responds to different types of rotational optic flow.

In pigeons, there are two types of neurons sensitive to rotational optic flow in the flocculus: neurons that prefer rotational optic flow about the vertical axis (*rVA* neurons), and neurons that prefer rotational optic flow about a horizontal axis (*rHA* neurons; Graf et al., 1988; Wylie and Frost, 1993). The organization of these cells within the flocculus has been extensively studied (see Fig. 1.4; Wylie et al., 1999c; 2003a; Winship and Wylie, 2003; Pakan et al., 2005). In the uvula/nodulus, there are four types of neurons sensitive to translation: *ascent* and *descent* neurons respond best to downward and upward optic flow along the vertical axis, respectively, and *contraction* and *expansion* neurons respond best to forward and backward optic flow along a horizontal axis, respectively (Wylie and Frost, 1999b). As with rotational neurons in the flocculus, the translation neurons are topographically organized into zones in the VbC (see Fig. 1.4; Chapter 2). CF afferents to PCs in the flocculus and uvula/nodulus arise from the medial and lateral mcIO, respectively (Lau et al., 1998). The topographical organization of these inputs to each individual type of neuron in the flocculus and uvula/nodulus have also been determined (Wylie et al., 1999c; Crowder et al., 2000; Pakan et al., 2005; see Chapter 3).

Studies in mammals show that optokinetic responses of PCs are almost identical to that of pigeons, and are evolutionarily conserved across species (for review, see Voogd and Wylie, 2004; Simpson et al., 1981; Graf et al., 1988). The function of the uvula/nodulus is very similar across several species (Wylie and

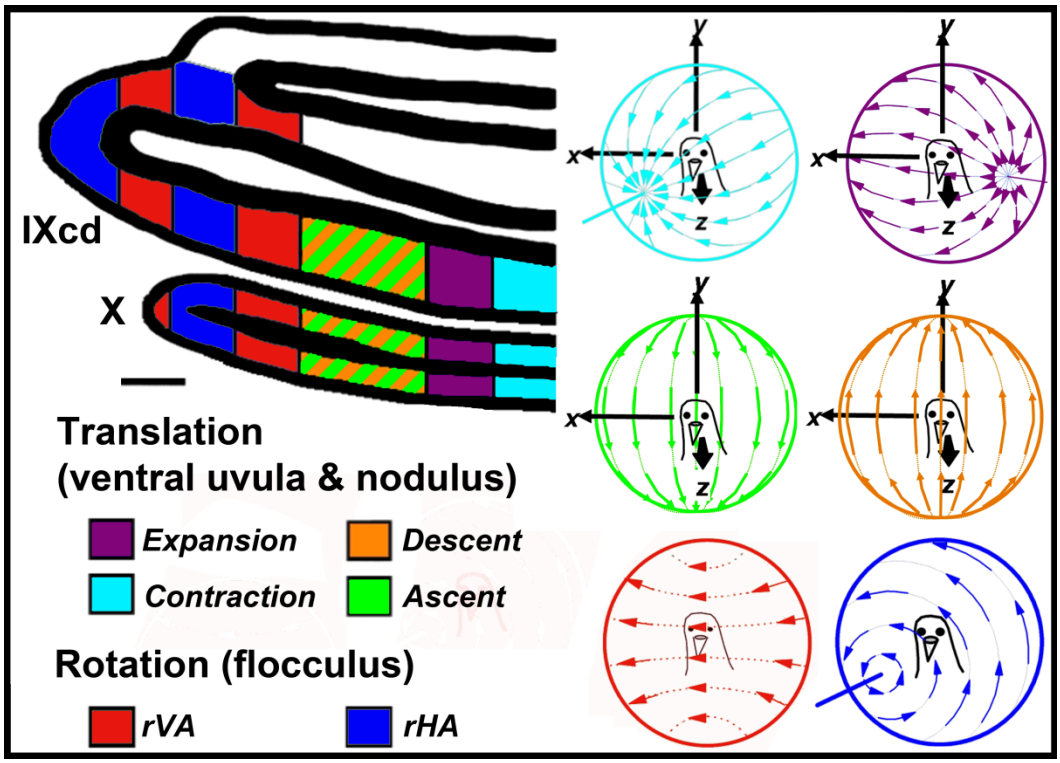

Figure 1.4 Topography of electrophysiological zones in the vestibulocerebellum (VbC) of pigeons. Distribution of Purkinje cells responsive to translational or rotational optic flow in the VbC is shown. There are four functional classes of Purkinje cells responsive to patterns of optic flow resulting from self-translation in the medial VbC (i.e. uvula/nodulus): *contraction* (light blue), *expansion* (purple), *ascent* (green), and *descent* (orange) (based on Wylie et al. 2003b). In the lateral VbC (i.e. flocculus), interdigitated areas of Purkinje cells responsive to patterns of optic flow resulting from self-rotation about either the vertical axis (*rVA*; red) or an horizontal axis (*rHA*; dark blue) are shown (Wylie et al. 1993; Wylie and Frost, 1993).

Frost, 1993; Barmack and Shojaku, 1995), though most studies in mammals have focused on the simple spike activity of otolith (vestibular) afferents resulting from linear acceleration (e.g. Angelaki and Hess, 1994; 1995a,b; Yakusheva et al., 2008), instead of determining the CSA of PCs in response to translational optic flow patterns.

1.3 Correlating Anatomical, Physiological, and Biochemical Patterns

More than thirty years ago, it was established that the fundamental organization of the cerebellum consists of sagittal zones (Voogd and Bigaré, 1980), which is reflected in the topography of the afferent inputs and functional properties of the cerebellar cortex (for review, see Voogd and Glickstein, 1998), and the molecular makeup of neurons in the cerebellum (for review see Hawkes and Gravel, 1991; Hawkes and Herrup, 1995; Herrup and Kuemerle, 1997). Recently, studies have attempted to determine the functional significance of these biochemical zones with respect to the pattern of afferent inputs and physiological properties in the cerebellum.

1.3.1 *Zebrin II and Climbing Fibre Zones*

In mammals, the relationship between the ZII expression pattern of Purkinje cells and the organization of climbing fibres originating in the inferior olive has recently been examined extensively (e.g. Gravel et al., 1987; Hawkes and Leclerc, 1989; Gravel and Hawkes, 1990; Hawkes et al., 1993; Voogd and

Ruigrok, 2004; Pijpers et al., 2006; Sugihara and Quy, 2007). For example, a study by Voogd et al. (2003) micro-injected a tracer into individual zones defined by the somatotopy of climbing fibre responses to examine climbing fibre collateralization in the rat cerebellar hemisphere. They found that injections of tracer into a zone of a given ZII signature (either ZII+ or ZII-) resulted in climbing fibre collaterals in ZII zones of the same signature. In a comprehensive study of the entire cerebellum, Sugihara and Shinoda (2004) established a relationship between olivocerebellar afferents and ZII expression patterns by microinjecting an anterograde tracer into various inferior olivary subnuclei in rats, and comparing the resulting climbing fibre labelling to ZII zones. They found that ZII-positive and ZII-negative zones received climbing fibres from different subnuclei of the inferior olive. In comparing the olivocerebellar origins of the climbing fibres that projected to ZII-positive and ZII-negative zones, Sugihara and Shinoda (2004) built upon the hypothesis of Voogd et al. (2003), suggesting that ZII-negative stripes receive climbing fibre input carrying somatosensory information, whereas ZII-positive stripes receive climbing fibre input carrying information from visual, auditory and other sensory systems (see also Voogd et al., 2003; Voogd and Ruigrok, 2004; Sugihara and Quy, 2007; Sugihara and Shinoda, 2007). However, this theory has been challenged by a recent study in pigeons, showing that olivocerebellar afferents from physiologically distinct subzones in the mcIO span a ZII+ and ZII- pair in the VbC (Pakan and Wylie, 2008). Specifially, localized injections of anterograde tracer into the area of the mcIO responsive to *rVA* optic flow resulted in CFs in

ZII zones P4+/- and P6+/-, whereas injections into the area of the mcIO responsive to *rHA* optic flow resulted in CFs that spanned ZII zones P5+/- and P7+/-.

1.3.2 ***Zebrin II and Mossy Fibres Zones***

Fewer studies have looked at mossy fibre afferent organization in the cerebellum. These studies have shown that mossy fibres terminals are also parasagittally organized in the granular layer from a number of projections, including spinocerebellar, cuneocerebellar, reticulocerebellar, and pontocerebellar pathways (for review see Voogd and Ruigrok, 1997; Voogd and Glickstein, 1998). The relationship of these mossy fibre terminals to the ZII expression pattern appears to be less clear than that of climbing fibres. In mammals, spinocerebellar and cuneocerebellar mossy fibre terminal zones in the anterior cerebellum either align with stripes defined by ZII expression, or are partially distributed within a ZII-negative stripe (Gravel and Hawkes, 1990; Akintunde and Eisenman, 1994; Ji and Hawkes, 1994; 1995). Pijpers et al., (2006) injected retrograde tracers into confined regions of the cerebellar cortex and found that resulting mossy fibre collaterals largely had the same ZII signature as the injection site (i.e. ZII-positive injection resulted in ZII-positive mossy fibre collaterals). They also found that climbing fiber collaterals were distributed as longitudinal strips, and were always accompanied by clusters of labeled mossy fibres rosettes in the subjacent granular layer, indicating a close relationship between mossy fibre and climbing fibre afferents. The picture becomes less clear

in the spinocerebellar system, where some studies have shown that mossy fibre projections of the lumbar spinal cord correlate well with ZII bands, whereas others have shown no relationship between ZII and spinocerebellar afferents (Gravel and Hawkes, 1990; Matsushita et al., 1991; Ji and Hawkes, 1994).

In birds, only one study has compared mossy fibre afferents to ZII. Pakan et al. (2010) injected anterograde tracers into LM and nBOR of pigeons to investigate the organization of mossy fiber terminals in relation to ZII. They found that parasagittal clusters of mossy fiber terminals were concentrated in the granule layer subjacent to ZII+ regions in folium IXcd. It remains to be seen if mossy fibres from other sensory systems are correlated with ZII patterns.

1.3.3 ***Zebrin II and Functional Zones***

The parasagittal organization of the cerebellar cortex is also evident in the topography of physiological response properties of Purkinje cells (Oscarsson and Sjolund, 1977; Cicirata et al., 1992; Chockkan and Hawkes, 1994; Wylie et al., 1995; Cheron et al., 1996; Escudero et al., 1996; Peeters et al., 1999). A few studies have suggested that functional zones in the cerebellum and the ZII expression pattern frequently align. For example, the relationship between ZII zones and boundaries in the tactile receptive field map has been investigated in several studies (e.g. Chockkan and Hawkes, 1994; Bower, 1997; Hallem et al., 1999). Theses studies showed that a zone defined by a specific electrophysiological response was confined to either a ZII+ or ZII- band, but never both. Sugihara et al. (2007) simultaneously measured the CSA at several

sites within and between different ZII stripes, and found that synchrony was higher among PCs within either a ZII+ or a ZII- band. Mostofi et al. (2010) used an eye-blink conditioning paradigm in the rabbit cerebellum to show that periocular-evoked CSA was localized to a particular ZII stripe. A recent study has shown that functional zones responsive to different types of rotational optic flow span a ZII+ and ZII- pair in the VbC of pigeons (Pakan et al., 2011). Specifically, the CSA of PCs responsive to *rVA* optic flow was confined to ZII zones P4+/- and P6+/-, whereas the CSA of PCs responsive to *rHA* optic flow was confined to ZII zones P5+/- and P7+/-.

In following with the work done in the pigeon flocculus (Pakan and Wylie, 2008; Pakan et al., 2011), this thesis will compare the ZII expression pattern in the pigeon uvula/nodulus to the visual climbing fibre projections from the lateral mcIO (Chapter 3), and the Purkinje cell response properties (Chapter 2) of this region.

1.4 Summary and Outline of Chapters

Up to 80% of the neurons in the central nervous system are found in the cerebellum (Lange, 1975; Herculano-Houzel, 2010). The cerebellum integrates information from various sensory and motor systems, yet how the cerebellum organizes and processes this information is still poorly understood. This thesis investigates the parasagittal organization in the VbC by examining properties of the optic flow pathways from the AOS and associated pretectum, and discussing them in terms of the anatomical, physiological, and molecular organization of the

cerebellum. Though it has been known for many years that many biochemical markers are expressed as "stripes" throughout the cerebellum, the importance of these stripes has only begun to be elucidated (for review see: Hawkes and Gravel, 1991; Hawkes and Eisenman, 1997; Herrup and Kuemerle, 1997). The importance of the parasagittal pattern as revealed by molecular markers is emphasized by its close relationship to cerebellar projection patterns and functional properties of the cerebellum. Nowhere is this more evident than in the ZII expression pattern in PCs and its undeniable link to afferent organization and function in the cerebellum. Whether there is a physiological distinction between ZII+ and ZII- will be a topic of discussion throughout this thesis.

This thesis includes two studies of the physiological response properties of PCs, anatomical afferents and molecular organization of the visual pathways from the AOS and pretectum to the cerebellum. In Chapter 2, using electrophysiological recording techniques, we seek to determine the relationship between the response properties of Purkinje cells and the ZII parasagittal expression pattern in the medial VbC. A previous study in the pigeon flocculus showed that a physiologically distinct zone in the pigeon flocculus spanned a single ZII+ and ZII- pair (Pakan et al., 2011). We will examine whether or not a single physiological zone in the uvula/nodulus shows this same relationship to ZII. Chapter 3 will examine the correlation of ZII expression with olivocerebellar climbing fibre afferents in the VbC. In pigeons, the optic flow preferences of sub-regions in the mcIO have been determined (Wylie et al., 1999a; Crowder et al., 2000; Winship and Wylie, 2003), and the climbing fibre projections of two

functionally distinct sub-regions in the medial mcIO have been shown to span a single ZII+ and ZII- pair in the flocculus (Pakan and Wylie, 2008). Using anterograde tracers, we examine the organization of climbing fibre afferents from physiologically distinct regions in the lateral mcIO, and correlate this organization to the parasagittal zebrin expression pattern. These experiments will help determine the functional significance of the Purkinje cell marker ZII, and contribute to the understanding of the fundamental organization of the cerebellum.

1.5 References

Ahn AH, Dziennis S, Hawkes R, Herrup K. 1994. The cloning of zebrin II reveals its identity with aldolase C. Development 120(8):2081-2090.

Akintunde A, Eisenman LM. 1994. External cuneocerebellar projection and Purkinje cell zebrin II bands: a direct comparison of parasagittal banding in the mouse cerebellum. J Chem Neuroanat 7(1-2):75-86.

Andersen GJ, Atchley P. 1997. Smoothness of the velocity field and three-dimensional surface detection from optic flow. Percept Psychophys 59(3):358-369.

Andersen RA. 1997. Neural mechanisms of visual motion perception in primates. Neuron 18(6):865-872.

Angelaki DE, Hess BJ. 1994. The cerebellar nodulus and ventral uvula control the torsional vestibulo-ocular reflex. J Neurophysiol 72(3):1443-1447.

Angelaki DE, Hess BJ. 1995a. Lesion of the nodulus and ventral uvula abolish steady-state off-vertical axis otolith response. J Neurophysiol 73(4):1716-1720.

Angelaki DE, Hess BJ. 1995b. Inertial representation of angular motion in the vestibular system of rhesus monkeys. II. Otolith-controlled transformation that depends on an intact cerebellar nodulus. J Neurophysiol 73(5):1729-1751.

Arends J, Voogd J. 1989. Topographic aspects of the olivocerebellar system in the pigeon. Exp Brain Res, Series 17:52-57.

Ballas I, Hoffmann KP, Wagner HJ. 1981. Retinal projection to the nucleus of the optic tract in the cat as revealed by retrograde transport of horseradish peroxidase. Neurosci Lett 26(3):197-202.

Barmack NH, Shojaku H. 1995. Vestibular and visual climbing fiber signals evoked in the uvula-nodulus of the rabbit cerebellum by natural stimulation. J Neurophysiol 74, 2573–2589.

Baumberger B, Fluckiger M. 2004. The development of distance estimation in optic flow. Perception 33(9):1081-1099.

Blanks RH, Clarke RJ, Lui F, Giolli RA, Van Pham S, Torigoe Y. 1995. Projections of the lateral terminal accessory optic nucleus of the common marmoset (Callithrix jacchus). J Comp Neurol 354(4):511-532.

Bower JM. 1997. Control of sensory data acquisition. Int Rev Neurobiol 41:489-513.

Brecha N, Karten HJ, Hunt SP. 1980. Projections of the nucleus of the basal optic root in the pigeon: an autoradiographic and horseradish peroxidase study. J Comp Neurol 189(4):615-670.

Britto LR, Natal CL, Marcondes AM. 1981. The accessory optic system in pigeons: receptive field properties of identified neurons. Brain Res 206(1):149-154.

Brochu G, Maler L, Hawkes R. 1990. Zebrin II: a polypeptide antigen expressed selectively by Purkinje cells reveals compartments in rat and fish cerebellum. J Comp Neurol 291(4):538-552.

Burns S, Wallman J. 1981. Relation of single unit properties to the oculomotor function of the nucleus of the basal optic root (accessory optic system) in chickens. Exp Brain Res 42(2):171-180.

Cheron G, Escudero M, Godaux E. 1996. Discharge properties of brain stem neurons projecting to the flocculus in the alert cat. I. Medical vestibular nucleus. J Neurophysiol 76(3):1759-1774.

Chockkan V, Hawkes R. 1994. Functional and antigenic maps in the rat cerebellum: zebrin compartmentation and vibrissal receptive fields in lobule IXa. J Comp Neurol 345(1):33-45.

Cicirata F, Angaut P, Serapide MF, Panto MR, Nicotra G. 1992. Multiple representation in the nucleus lateralis of the cerebellum: an electrophysiologic study in the rat. Exp Brain Res 89(2):352-362.

Cochran SL, Dieringer N, Precht W. 1984. Basic optokinetic-ocular reflex pathways in the frog. J Neurosci 4(1):43-57.

Collett TS. 2002. Insect vision: controlling actions through optic flow. Curr Biol 12(18):R615-617.

Collewijn H. 1975. Direction-selective units in the rabbit's nucleus of the optic tract. Brain Res 100(3):489-508.

Crowder NA, Lehmann H, Parent MB, Wylie DR. 2003b. The accessory optic system contributes to the spatio-temporal tuning of motion-sensitive pretectal neurons. J Neurophysiol 90(2):1140-1151.

Crowder NA, Winship IR, Wylie DR. 2000. Topographic organization of inferior olive cells projecting to translational zones in the vestibulocerebellum of pigeons. J Comp Neurol 419(1):87-95.

Crowder NA, Wylie DR. 2001. Fast and slow neurons in the nucleus of the basal optic root in pigeons. Neurosci Lett 304(3):133-136.

Crowder NA, Wylie DR. 2002. Responses of optokinetic neurons in the pretectum and accessory optic system of the pigeon to large-field plaids. J Comp Physiol A Neuroethol Sens Neural Behav Physiol 188(2):109-119.

De Zeeuw CI, Wylie DR, DiGiorgi PL, Simpson JI. 1994. Projections of individual Purkinje cells of identified zones in the flocculus to the vestibular and cerebellar nuclei in the rabbit. J Comp Neurol 349(3):428-447.

Escudero M, Cheron G, Godaux E. 1996. Discharge properties of brain stem neurons projecting to the flocculus in the alert cat. II. Prepositus hypoglossal nucleus. J Neurophysiol 76(3):1775-1785.

Fan TX, Weber AE, Pickard GE, Faber KM, Ariel M. 1995. Visual responses and connectivity in the turtle pretectum. J Neurophysiol 73(6):2507-2521.

Farmer SG, Rodieck RW. 1982. Ganglion cells of the cat accessory optic system: morphology and retinal topography. J Comp Neurol 205(2):190-198.

Fite KV, Brecha N, Karten HJ, Hunt SP. 1981. Displaced ganglion cells and the accessory optic system of pigeon. J Comp Neurol 195(2):279-288.

Fite KV, Kwei-Levy C, Bengston L. 1989. Neurophysiological investigation of the pretectal nucleus lentiformis mesencephali in Rana pipiens. Brain Behav Evol 34(3):164-170.

Frenz H, Bremmer F, Lappe M. 2003. Discrimination of travel distances from 'situated' optic flow. Vision Res 43(20):2173-2183.

Galbraith JM, Kenyon GT, Ziolkowski RW. 2005. Time-to-Collision estimation from motion based on primate visual processing. IEEE Trans Pattern Anal Mach Intell 27(8):1279-1291.

Gamlin PD. 2006. The pretectum: connections and oculomotor-related roles. Prog Brain Res 151:379-405.

Gamlin PD, Cohen DH. 1988a. Projections of the retinorecipient pretectal nuclei in the pigeon (Columba livia). J Comp Neurol 269(1):18-46.

Gamlin PD, Cohen DH. 1988b. Retinal projections to the pretectum in the pigeon (Columba livia). J Comp Neurol 269(1):1-17.

Gerrits NM, Voogd J. 1982. The climbing fiber projection to the flocculus and adjacent paraflocculus in the cat. Neuroscience 7(12):2971-2991.

Gibson JJ. 1954. The visual perception of objective motion and subjective movement. Psychol Rev 61(5):304-314.

Gibson JJ. 1966. The problem of temporal order in stimulation and perception. J Psychol 62(2):141-149.

Gioanni H, Rey J, Villalobos J, Dalbera A. 1984. Single unit activity in the nucleus of the basal optic root (nBOR) during optokinetic, vestibular and

visuo-vestibular stimulations in the alert pigeon (Columbia livia). Exp Brain Res 57(1):49-60.

Gioanni H, Rey J, Villalobos J, Richard D, Dalbera A. 1983a. Optokinetic nystagmus in the pigeon (Columba livia). II. Role of the pretectal nucleus of the accessory optic system (AOS). Exp Brain Res 50(2-3):237-247.

Gioanni H, Villalobos J, Rey J, Dalbera A. 1983b. Optokinetic nystagmus in the pigeon (Columba livia). III. Role of the nucleus ectomamillaris (nEM): interactions in the accessory optic system (AOS). Exp Brain Res 50(2-3):248-258.

Giolli RA, Blanks RH, Lui F. 2006. The accessory optic system: basic organization with an update on connectivity, neurochemistry, and function. Prog Brain Res 151:407-440.

Giolli RA, Blanks RH, Torigoe Y. 1984. Pretectal and brain stem projections of the medial terminal nucleus of the accessory optic system of the rabbit and rat as studied by anterograde and retrograde neuronal tracing methods. J Comp Neurol 227(2):228-251.

Giolli RA, Blanks RH, Torigoe Y, Williams DD. 1985. Projections of medial terminal accessory optic nucleus, ventral tegmental nuclei, and substantia nigra of rabbit and rat as studied by retrograde axonal transport of horseradish peroxidase. J Comp Neurol 232(1):99-116.

Glickstein M, Strata P, Voogd J. 2009. Cerebellum: History. Neuroscience.

Graf W, Simpson JI, Leonard CS. 1988. Spatial organization of visual messages of the rabbit's cerebellar flocculus. II. Complex and simple spike responses of Purkinje cells. J Neurophysiol 60(6):2091-2121.

Grasse KL, Cynader MS. 1984. Electrophysiology of lateral and dorsal terminal nuclei of the cat accessory optic system. J Neurophysiol 51(2):276-93.

Grasse KL, Cynader MS. 1990. The accessory optic system in frontal-eyed animals. In Vision and Visual Dysfunction,Vol. IV, The Neuronal Basis of Visual Function. Leventhal A, editor. New York: MacMillan. pp. 111-139 p.

Gravel C, Eisenman LM, Sasseville R, Hawkes R. 1987. Parasagittal organization of the rat cerebellar cortex: direct correlation between antigenic Purkinje cell bands revealed by mabQ113 and the organization of the olivocerebellar projection. J Comp Neurol 265(2):294-310.

Gravel C, Hawkes R. 1990. Parasagittal organization of the rat cerebellar cortex: direct comparison of Purkinje cell compartments and the organization of the spinocerebellar projection. J Comp Neurol 291(1):79-102.

Gruberg ER, Grasse KL. 1984. Basal optic complex in the frog (Rana pipiens): a physiological and HRP study. J Neurophysiol 51(5):998-1010.

Hallem JS, Thompson JH, Gundappa-Sulur G, Hawkes R, Bjaalie JG, Bower JM. 1999. Spatial correspondence between tactile projection patterns and the distribution of the antigenic Purkinje cell markers anti-zebrin I and anti-zebrin II in the cerebellar folium crus IIA of the rat. Neuroscience 93(3):1083-1094.

Harris JM, Rogers BJ. 1999. Going against the flow. Trends Cogn Sci 3(12):449-450.

Hawkes R. 1992. Antigenic markers of cerebellar modules in the adult mouse. Biochem Soc Trans 20(2):391-395.

Hawkes R. 1997. An anatomical model of cerebellar modules. Prog Brain Res 114:39-52.

Hawkes R, Blyth S, Chockkan V, Tano D, Ji Z, Mascher C. 1993. Structural and molecular compartmentation in the cerebellum. Can J Neurol Sci 20 Suppl 3:S29-35.

Hawkes R, Eisenman LM. 1997. Stripes and zones: the origins of regionalization of the adult cerebellum. Perspect Dev Neurobiol 5(1):95-105.

Hawkes R, Gravel C. 1991. The modular cerebellum. Prog Neurobiol 36(4):309-327.

Hawkes R, Herrup K. 1995. Aldolase C/zebrin II and the regionalization of the cerebellum. J Mol Neurosci 6(3):147-158.

Hawkes R, Leclerc N. 1989. Purkinje cell axon collateral distributions reflect the chemical compartmentation of the rat cerebellar cortex. Brain Res 476(2):279-290.

Hawkes R, Mascher C. 1994. The development of molecular compartmentation in the cerebellar cortex. Acta Anat (Basel) 151(3):139-149.

Herculano-Houzel S. 2010. Coordinated scaling of cortical and cerebellar numbers of neurons. Front Neuroanat 4(12):1-8.

Herrup K, Kuemerle B. 1997. The compartmentalization of the cerebellum. Annu Rev Neurosci 20:61-90.

Hess DT, Voogd J. 1986. Chemoarchitectonic zonation of the monkey cerebellum. Brain Res 369(1-2):383-387.

Hoffmann KP, Distler C, Erickson RG, Mader W. 1988. Physiological and anatomical identification of the nucleus of the optic tract and dorsal terminal nucleus of the accessory optic tract in monkeys. Exp Brain Res 69(3):635-644.

Hoffmann KP, Schoppmann A. 1981. A quantitative analysis of the direction-specific response of Neurons in the cat's nucleus of the optic tract. Exp Brain Res 42(2):146-157.

Ibbotson MR, Mark RF, Maddess TL. 1994. Spatiotemporal response properties of direction-selective neurons in the nucleus of the optic tract and dorsal terminal nucleus of the wallaby, Macropus eugenii. J Neurophysiol 72(6):2927-2943.

Ibbotson MR, Price NS. 2001. Spatiotemporal tuning of directional neurons in mammalian and avian pretectum: a comparison of physiological properties. J Neurophysiol 86(5):2621-2624.

Ito M. 2002. The molecular organization of cerebellar long-term depression. Nat Rev Neurosci 3(11):896-902.

Ito M. 2006. Cerebellar circuitry as a neuronal machine. Prog Neurobiol 78(3-5):272-303.

Ji Z, Hawkes R. 1994. Topography of Purkinje cell compartments and mossy fiber terminal fields in lobules II and III of the rat cerebellar cortex: spinocerebellar and cuneocerebellar projections. Neuroscience 61(4):935-954.

Ji Z, Hawkes R. 1995. Developing mossy fiber terminal fields in the rat cerebellar cortex may segregate because of Purkinje cell compartmentation and not competition. J Comp Neurol 359(2):197-212.

Kano M, Kano MS, Kusunoki M, Maekawa K. 1990a. Nature of optokinetic response and zonal organization of climbing fiber afferents in the vestibulocerebellum of the pigmented rabbit. II. The nodulus. Exp Brain Res 80(2):238-251.

Kano MS, Kano M, Maekawa K. 1990b. Receptive field organization of climbing fiber afferents responding to optokinetic stimulation in the cerebellar nodulus and flocculus of the pigmented rabbit. Exp Brain Res 82(3):499-512.

Karten H, Hodos W. 1967. A stereotaxic Atlas of the Brain of the Pigeon (Columba livia). Baltimore: Johns Hopkins Press.

Karten JH, Fite KV, Brecha N. 1977. Specific projection of displaced retinal ganglion cells upon the accessory optic system in the pigeon (Columbia livia). Proc Natl Acad Sci U S A 74(4):1753-1756.

Koenderink JJ, van Doorn AJ. 1987. Facts on optic flow. Biol Cybern 56(4):247-254.

Kusunoki M, Kano M, Kano MS, Maekawa K. 1990. Nature of optokinetic response and zonal organization of climbing fiber afferents in the vestibulocerebellum of the pigmented rabbit. I. The flocculus. Exp Brain Res 80(2):225-237.

Lange W. 1975. Cell number and cell density in the cerebellar cortex of man and some other mammals. Cell Tissue Res 157(1):115-124.

Lappe M, Bremmer F, van den Berg AV. 1999. Perception of self-motion from visual flow. Trends Cogn Sci 3(9):329-336.

Larsell O. 1948. The development and subdivisions of the cerebellum of birds. J Comp Neurol 89:123-182.

Larsell O, Whitlock DG. 1952. Further observations on the cerebellum of birds. J Comp Neurol 97(3):545-566.

Lau KL, Glover RG, Linkenhoker B, Wylie DR. 1998. Topographical organization of inferior olive cells projecting to translation and rotation zones in the vestibulocerebellum of pigeons. Neuroscience 85(2):605-614.

Lee DN. 1980. The optic flow field: the foundation of vision. Philos Trans R Soc Lond B Biol Sci 290(1038):169-179.

Leonard CS, Simpson JI, Graf W. 1988. Spatial organization of visual messages of the rabbit's cerebellar flocculus. I. Typology of inferior olive neurons of the dorsal cap of Kooy. J Neurophysiol 60(6):2073-2090.

Lishman JR. 1981. Vision and the optic flow field. Nature 293(5830):263-264.

Maekawa K, Takeda T. 1979. Origin of descending afferents to the rostral part of dorsal cap of inferior olive which transfers contralateral optic activities to the flocculus. A horseradish peroxidase study. Brain Res 172(3):393-405.

Maekawa K, Takeda T, Kimura M. 1984. Responses of the nucleus of the optic tract neurons projecting to the nucleus reticularis tegmenti pontis upon optokinetic stimulation in the rabbit. Neurosci Res 2(1-2):1-25.

Manteuffel G. 1984. Electrophysiology and anatomy of direction-specific pretectal units in Salamandra salamandra. Exp Brain Res 54(3):415-425.

Marzban H, Hawkes R. 2010. On the Architecture of the Posterior Zone of the Cerebellum. Cerebellum. Accepted for publication Sept 14 2010.

Matsushita M, Ragnarson B, Grant G. 1991. Topographic relationship between sagittal Purkinje cell bands revealed by a monoclonal antibody to zebrin I and spinocerebellar projections arising from the central cervical nucleus in the rat. Exp Brain Res 84(1):133-141.

McKenna OC, Wallman J. 1985. Accessory optic system and pretectum of birds: comparisons with those of other vertebrates. Brain Behav Evol 26(2):91-116.

Morgan B, Frost BJ. 1981. Visual response characteristics of neurons in nucleus of basal optic root of pigeons. Exp Brain Res 42(2):181-188.

Mostofi A, Holtzman T, Grout AS, Yeo CH, Edgley SA. 2010. Electrophysiological localization of eyeblink-related microzones in rabbit cerebellar cortex. J Neurosci 30(26) 8920–8930.

Mustari MJ, Fuchs AF. 1989. Response properties of single units in the lateral terminal nucleus of the accessory optic system in the behaving primate. J Neurophysiol 61(6):1207-1220.

Nakayama K. 1981. Differential motion hyperacuity under conditions of common image motion. Vision Res 21(10):1475-1482.

Natal CL, Britto LR. 1987. The pretectal nucleus of the optic tract modulates the direction selectivity of accessory optic neurons in rats. Brain Res 419(1-2):320-323.

Natal CL, Britto LR. 1988. The rat accessory optic system: effects of cortical lesions on the directional selectivity of units within the medial terminal nucleus. Neurosci Lett 91(2):154-159.

Nomura Y, Mulavara AP, Richards JT, Brady R, Bloomberg JJ. 2005. Optic flow dominates visual scene polarity in causing adaptive modification of locomotor trajectory. Brain Res Cogn Brain Res.

Oscarsson O, Sjolund B. 1977. The ventral spino-olivocerebellar system in the cat. I. Identification of five paths and their termination in the cerebellar anterior lobe. Exp Brain Res 28(5):469-486.

Oyster CW, Simpson JI, Takahashi ES, Soodak RE. 1980. Retinal ganglion cells projecting to the rabbit accessory optic system. J Comp Neurol 190(1):49-61.

Ozol K, Hayden JM, Oberdick J, Hawkes R. 1999. Transverse zones in the vermis of the mouse cerebellum. J Comp Neurol 412(1):95-111.

Pakan JM, Graham DJ, Gutiérrez-Ibáñez C, Wylie DR. 2011. Organization of the cerebellum: Correlating zebrin immunochemistry with optic flow zones in the pigeon flocculus. Vis Neurosci 28(2):163-174.

Pakan JM, Graham DJ, Wylie DR. 2010. Organization of visual mossy fiber projections and zebrin expression in the pigeon vestibulocerebellum. J Comp Neurol 518(4):175–198.

Pakan JM, Iwaniuk AN, Wylie DR, Hawkes R, Marzban H. 2007. Purkinje cell compartmentation as revealed by zebrin II expression in the cerebellar cortex of pigeons (Columba livia). J Comp Neurol 501(4):619–630.

Pakan JM, Todd KG, Nguyen AP, Winship IR, Hurd PL, Jantzie LL, Wylie DR. 2005. Inferior olivary neurons innervate multiple zones of the flocculus in pigeons (Columba livia). J Comp Neurol 486(2):159-168.

Pakan JM, Wylie DR. 2008. Congruence of zebrin II expression and functional zones defined by climbing fiber topography in the flocculus. Neurosci 157(1):57–69.

Paukert M, Huang YH, Tanaka K, Rothstein JD, Bergles DE. 2010. Zones of enhanced glutamate release from climbing fibers in the mammalian cerebellum. J Neurosci 30(21):7290–7299.

Peeters RR, Verhoye M, Vos BP, Van Dyck D, Van Der Linden A, De Schutter E. 1999. A patchy horizontal organization of the somatosensory activation of the rat cerebellum demonstrated by functional MRI. Eur J Neurosci 11(8):2720-2730.

Pijpers A, Apps R, Pardoe J, Voogd J, Ruigrok TJ. 2006. Precise spatial relationships between mossy fibers and climbing fibers in rat cerebellar cortical zones. J Neurosci 26(46):12067-12080.

Pijpers A, Voogd J, Ruigrok TJ. 2005. Topography of olivo-cortico-nuclear modules in the intermediate cerebellum of the rat. J Comp Neurol 492(2):193-213.

Ramon y Cajal S. 1911. . In: Azoulay L, editor. Histologie du systeme nerveux de l'homme et des vertebres, vol II. Paris: Maloine. p 196–212.

Reiner A, Brecha N, Karten HJ. 1979. A specific projection of retinal displaced ganglion cells to the nucleus of the basal optic root in the chicken. Neuroscience 4(11):1679-1688.

Rivkin A, Herrup K. 2003. Development of cerebellar modules: extrinsic control of late-phase zebrin II pattern and the exploration of rat/mouse species differences. Mol Cell Neurosci 24(4):887-901.

Rosenberg AF, Ariel M. 1990. Visual-response properties of neurons in turtle basal optic nucleus in vitro. J Neurophysiol 63(5):1033-1045.

Ruigrok TJ. 2003. Collateralization of climbing and mossy fibers projecting to the nodulus and flocculus of the rat cerebellum. J Comp Neurol 466(2):278-298.

Ruigrok TJ, Osse RJ, Voogd J. 1992. Organization of inferior olivary projections to the flocculus and ventral paraflocculus of the rat cerebellum. J Comp Neurol 316(2):129-150.

Schonewille M, Luo C, Ruigrok TJ, Voogd J, Schmolesky MT, Rutteman M, Hoebeek FE, De Jeu MT, De Zeeuw CI. 2006. Zonal organization of the mouse flocculus: physiology, input, and output. J Comp Neurol 497(4):670-682.

Shojaku H, Barmack NH, Mizukoshi K. 1991. Influence of vestibular and visual climbing fiber signals on Purkinje cell discharge in the cerebellar nodulus of the rabbit. Acta Otolaryngol Suppl 481:242-246.

Sillitoe RV, Hawkes R. 2002. Whole-mount immunohistochemistry: a high-throughput screen for patterning defects in the mouse cerebellum. J Histochem Cytochem 50(2):235-244.

Sillitoe RV, Marzban H, Larouche M, Zahedi S, Affanni J, Hawkes R. 2005. Conservation of the architecture of the anterior lobe vermis of the cerebellum across mammalian species. Prog Brain Res 148:283-297.

Simpson JI. 1984. The accessory optic system. Annu Rev Neurosci 7:13-41.

Simpson JI, Graf W, Leonard CS. 1981. The coordinate system of visual climbing fibres to the flocculus. In: Progress in oculomotor research. Fuchs A, Becker W, editors. Amsterdam/New York/Oxford: Elsevier/North Holland.

Simpson JI, Leonard CS, Soodak RE. 1988. The accessory optic system. Analyzer of self-motion. Ann N Y Acad Sci 545:170-179.

Simpson JI, Soodak RE, Hess R. 1979. The accessory optic system and its relation to the vestibulocerebellum. Prog Brain Res 50:715-724.

Simpson JI, Van der Steen J, Tan J, Graf W, Leonard CS. 1989. Representations of ocular rotations in the cerebellar flocculus of the rabbit. Prog Brain Res 80:213-223; discussion 211-212.

Sugihara I, Ebata S, Shinoda Y. 2004. Functional compartmentalization in the flocculus and the ventral dentate and dorsal group y nuclei: an analysis of single olivocerebellar axonal morphology. J Comp Neurol 470(2):113-133.

Sugihara I, Marshall SP, Lang EJ. 2007. Relationship of complex spike synchrony bands and climbing fiber projection determined by reference to aldolase C compartments in crus IIa of the rat cerebellar cortex. Journal Comp Neurol 50(1):13–29.

Sugihara I, Quy PN. 2007. Identification of aldolase C compartments in the mouse cerebellar cortex by olivocerebellar labelling. J Comp Neurol 500(6):1076-1092.

Sugihara I, Shinoda Y. 2004. Molecular, topographic, and functional organization of the cerebellar cortex: a study with combined aldolase C and olivocerebellar labelling. J Neurosci 24(40):8771-8785.

Sugihara I, Shinoda Y. 2007. Molecular, topographic, and functional organization of the cerebellar nuclei: analysis by three-dimensional mapping of the olivonuclear projection and aldolase C labelling. J Neurosci 27(36):9696-9710.

Tan J, Gerrits NM, Nanhoe R, Simpson JI, Voogd J. 1995a. Zonal organization of the climbing fiber projection to the flocculus and nodulus of the rabbit: a

combined axonal tracing and acetylcholinesterase histochemical study. J Comp Neurol 356(1):23-50.

Tan J, Simpson JI, Voogd J. 1995b. Anatomical compartments in the white matter of the rabbit flocculus. J Comp Neurol 356(1):1-22.

van den Berg AV. 2000. Human ego-motion perception. Int Rev Neurobiol 44:3-25.

Volchan E, Rocha-Miranda CE, Picanco-Diniz CW, Zinsmeisser B, Bernardes RF, Franca JG. 1989. Visual response properties of pretectal units in the nucleus of the optic tract of the opossum. Exp Brain Res 78(2):380-386.

Voogd J. 1975. Bolk's subdivision of the mammalian cerebellum. Growth centres and functional zones. Acta Morphol Neerl Scand 13(1-2):35-54.

Voogd J, Bigaré F. 1980. Topographical distribution of olivary and cortico nuclear fibers in the cerebellum: a review. Courville J, de Montigny C, Lamarre Y, editors. New York: Raven. 207-234 p.

Voogd J, Gerrits N, Hess DT. 1987a. Parasagittal zonation of the cerebellum in Macaques: an analysis based on acetylcholinesterase histochemistry. In: Glickstein M, Stein J, editors. Cerebellum and Neuronal Plasticity. New York: Plenum. p 15-39.

Voogd J, Gerrits NM, Ruigrok TJ. 1996. Organization of the vestibulocerebellum. Ann N Y Acad Sci 781:553-579.

Voogd J, Glickstein M. 1998. The anatomy of the cerebellum. Trends Neurosci 21(9):370-375.

Voogd J, Hess DT, Marani E. 1987b. The parasagittal zonation of the cerebellar cortex in cat and monkey. Topography, distribution of acetycholinesterase and development. . In: King JS, editor. New Concepts in Cerebellar Neurobiology. New York: Liss. p 15.

Voogd J, Pardoe J, Ruigrok TJ, Apps R. 2003. The distribution of climbing and mossy fiber collateral branches from the copula pyramidis and the paramedian lobule: congruence of climbing fiber cortical zones and the pattern of zebrin banding within the rat cerebellum. J Neurosci 23(11):4645-4656.

Voogd J, Ruigrok TJ. 1997. Transverse and longitudinal patterns in the mammalian cerebellum. Prog Brain Res 114:21-37.

Voogd J, Ruigrok TJ. 2004. The organization of the corticonuclear and olivocerebellar climbing fiber projections to the rat cerebellar vermis: the congruence of projection zones and the zebrin pattern. J Neurocytol 33(1):5-21.

Voogd J, Wylie DR. 2004. Functional and anatomical organization of floccular zones: a preserved feature in vertebrates. J Comp Neurol 470(2):107-112.

Waespe W, Henn V. 1987. Gaze stabilization in the primate. The interaction of the vestibulo-ocular reflex, optokinetic nystagmus, and smooth pursuit. Rev Physiol Biochem Pharmacol 106:37-125.

Wallman J, Adams JI, Trachtman JN. 1981. The eyes of young chickens grow toward emmetropia. Invest Ophthalmol Vis Sci 20(4):557-561.

Warren WH, Jr., Kay BA, Zosh WD, Duchon AP, Sahuc S. 2001. Optic flow is used to control human walking. Nat Neurosci 4(2):213-216.

Weber JT. 1985. Pretectal complex and accessory optic system of primates. Brain Behav Evol 26(2):117-140.

Westheimer G, Blair SM. 1974. Unit activity in accessory optic system in alert monkeys. Invest Ophthalmol 13(7):533-534.

Westheimer G, McKee SP. 1975. Visual acuity in the presence of retinal-image motion. J Opt Soc Am 65(7):847-50.

Winship IR, Crowder NA, Wylie DR. 2006a. Quantitative reassessment of speed tuning in the accessory optic system and pretectum of pigeons. J Neurophysiol 95(1):546-551.

Winship IR, Hurd PL, Wylie DR. 2005. Spatiotemporal tuning of optic flow inputs to the vestibulocerebellum in pigeons: differences between mossy and climbing fiber pathways. J Neurophysiol 93(3):1266-1277.

Winship IR, Wylie DR. 2001. Responses of neurons in the medial column of the inferior olive in pigeons to translational and rotational optic flowfields. Exp Brain Res 141(1):63-78.

Winship IR, Wylie DR. 2003. Zonal organization of the vestibulocerebellum in pigeons (Columba livia): I. Climbing fiber input to the flocculus. J Comp Neurol 456(2):127-139.

Winterson BJ, Brauth SE. 1985. Direction-selective single units in the nucleus lentiformis mesencephali of the pigeon (Columba livia). Exp Brain Res 60(2):215-226.

Wolf-Oberhollenzer F, Kirschfeld K. 1994. Motion sensitivity in the nucleus of the basal optic root of the pigeon. J Neurophysiol 71(4):1559-1573.

Wylie DR. 2000. Binocular neurons in the nucleus lentiformis mesencephali in pigeons: responses to translational and rotational optic flowfields. Neurosci Lett 291(1):9-12.

Wylie DR. 2001. Projections from the nucleus of the basal optic root and nucleus lentiformis mesencephali to the inferior olive in pigeons (Columba livia). J Comp Neurol 429(3):502-513.

Wylie DR, Bischof WF, Frost BJ. 1998a. Common reference frame for neural coding of translational and rotational optic flow. Nature 392(6673):278-282.

Wylie DR, Brown MR, Barkley RR, Winship IR, Crowder NA, Todd KG. 2003a. Zonal organization of the vestibulocerebellum in pigeons (Columba livia): II. Projections of the rotation zones of the flocculus. J Comp Neurol 456(2):140-153.

Wylie DR, Crowder NA. 2000. Spatiotemporal properties of fast and slow neurons in the pretectal nucleus lentiformis mesencephali in pigeons. J Neurophysiol 84(5):2529-2540.

Wylie DR, De Zeeuw CI, DiGiorgi PL, Simpson JI. 1994. Projections of individual Purkinje cells of identified zones in the ventral nodulus to the vestibular and cerebellar nuclei in the rabbit. J Comp Neurol 349(3):448-463.

Wylie DR, De Zeeuw CI, Simpson JI. 1995. Temporal relations of the complex spike activity of Purkinje cell pairs in the vestibulocerebellum of rabbits. J Neurosci 15(4):2875-2887.

Wylie DR, Frost BJ. 1990. The visual response properties of neurons in the nucleus of the basal optic root of the pigeon: a quantitative analysis. Exp Brain Res 82(2):327-336.

Wylie DR, Frost BJ. 1991. Purkinje cells in the vestibulocerebellum of the pigeon respond best to either translational or rotational wholefield visual motion. Exp Brain Res 86(1):229-232.

Wylie DR, Frost BJ. 1993. Responses of pigeon vestibulocerebellar neurons to optokinetic stimulation. II. The 3-dimensional reference frame of rotation neurons in the flocculus. J Neurophysiol 70(6):2647-2659.

Wylie DR, Frost BJ. 1996. The pigeon optokinetic system: visual input in extraocular muscle coordinates. Vis Neurosci 13(5):945-953.

Wylie DR, Frost BJ. 1999a. Complex spike activity of Purkinje cells in the ventral uvula and nodulus of pigeons in response to translational optic flow. J Neurophysiol 81(1):256-266.

Wylie DR, Frost BJ. 1999b. Responses of neurons in the nucleus of the basal optic root to translational and rotational flowfields. J Neurophysiol 81(1):267-276.

Wylie DR, Glover RG, Aitchison JD. 1999a. Optic flow input to the hippocampal formation from the accessory optic system. J Neurosci 19(13):5514-5527.

Wylie DR, Kripalani T, Frost BJ. 1993. Responses of pigeon vestibulocerebellar neurons to optokinetic stimulation. I. Functional organization of neurons discriminating between translational and rotational visual flow. J Neurophysiol 70(6):2632-2646.

Wylie DR, Linkenhoker B, Lau KL. 1997. Projections of the nucleus of the basal optic root in pigeons (Columba livia) revealed with biotinylated dextran amine. J Comp Neurol 384(4):517-536.

Wylie DR, Winship IR, Glover RG. 1999c. Projections from the medial column of the inferior olive to different classes of rotation-sensitive Purkinje cells in the flocculus of pigeons. Neurosci Lett 268(2):97-100.

Yakusheva T, Blazquez PM, Angelaki DE. 2008. Frequency-selective coding of translation and tilt in macaque cerebellar nodulus and uvula. J Neurosci 28:9997-10009.

Chapter 2: Correlating Zebrin Expression with Physiologically Defined Zones in the Ventral Uvula in Pigeons

We now know that the fundamental organization of the cerebellum consists of sagittal zones (e.g. Voogd and Bigaré, 1980). This can be seen in the pattern of afferent inputs from climbing fibres (CFs) and mossy fibres, projection patterns of Purkinje cells (PCs), and PC response properties (Voogd, 1967; Voogd et al., 1969; Ekerot and Larson, 1973; Andersson and Oscarsson, 1978; Llinas and Sasaki, 1989; De Zeeuw et al., 1994; Voogd and Glickstein, 1998; Wu et al., 1999; Ruigrok, 2003; Apps and Garwicz, 2005). Furthermore, the expression of several molecular markers has also revealed a parasagittal organization in the cerebellum (for review see Hawkes and Gravel, 1991; Hawkes, 1992). Of these markers, the most thoroughly studied is zebrin II (ZII) which recognizes the 36-kDa glycolytic enzyme aldolase C (Brochu et al., 1990; Ahn et al., 1994; Hawkes and Herrup, 1995). In the cerebellum, ZII is heterogeneously expressed in PCs such that there are sagittal stripes of high expression (ZII+) interdigitated with stripes of little or no expression (ZII-). The spatial pattern and number of ZII stripes is highly conserved in the cerebella of birds and mammals (Pakan et al., 2007; Iwaniuk et al., 2009; Marzban and Hawkes, 2010) indicating that it is critical for fundamental cerebellar function.

Recently several studies have attempted to show how the sagittal ZII stripes are related to physiological properties of PCs (Gao et al., 2006; Sugihara et al., 2007; Mostofi et al., 2010; Paukert et al., 2010). In this regard, our lab has been investigating the pigeon vestibulocerebellum (VbC). The VbC is an ideal structure to examine the relationship between ZII expression and function for

several reasons: (i) the physiological response properties of PCs have been well documented (Wylie and Frost, 1991, 1993; 1999; Wylie et al., 1993, 1998); (ii) the anatomical connections are well established (Wylie et al., 1999a,b, 2003a,b; Crowder et al., 2000; Winship and Wylie, 2003; Pakan et al., 2005); and (iii) the VbC is demarcated by seven alternating ZII+ and ZII- stripes in the pigeon (see Fig. 2.1B; Pakan et al., 2007). As a general model, Voogd and Wylie (2004) have noted that the VbC in mammals and birds is strikingly similar with respect to anatomical connections and physiological response properties.

The VbC is important for the processing of optic flow information. Optic flow is the motion that occurs across the entire retina as a result of self-motion (Gibson 1954), and serves as a signal to generate the optokinetic response toward gaze-stabilization (for review, see Waespe and Henn, 1987). Shown in Figure 1A, the VbC consists of folia IXcd and X. The lateral half of the VbC is the flocculus, and the complex spike activity (CSA) of floccular PCs responds best to optic flow resulting from self-rotation. Shown first in rabbits (Simpson et al., 1981; Graf et al., 1988), PCs responsive to rotational optic flow prefer visual motion about one of two axes: either the vertical axis (*rVA* cells), or an horizontal axis (*rHA* cells). In pigeons, as in rabbits (DeZeeuw et al., 1994), there are two *rVA* zones interdigitated with two *rHA* zones (Winship and Wylie 2003; see Fig. 2.1A). The medial half of the VbC comprises the uvula (IXcd) and the nodulus (X). The CSA in the ventral uvula and nodulus responds best to optic flow resulting from self-translation (Wylie and Frost, 1999). There are four types of visually responsive PCs in the uvula and the nodulus: *ascent* and *descent* neurons respond best

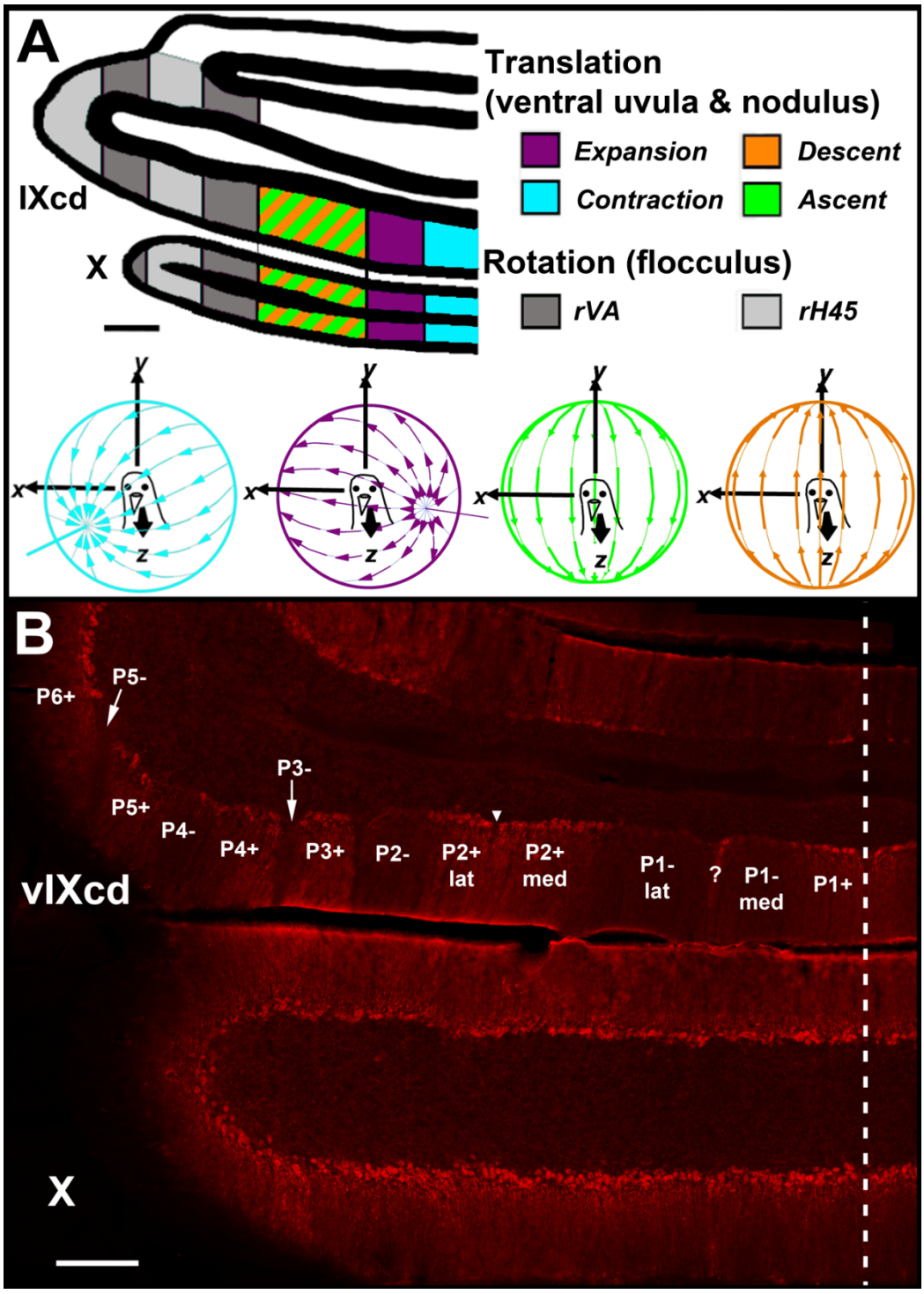

Figure 2.1 Zebrin II (ZII) organization and electrophysiological zones in the medial vestibulocerebellum (VbC) (i.e., ventral uvula and nodulus) of pigeons. A shows the four functional classes of Purkinje cells responsive to

patterns of optic flow resulting from self-translation in three-dimensional space: *contraction* (light blue), *expansion* (purple), *ascent* (green), and *descent* (orange) (based on Wylie et al. 2003b). In the lateral VbC (i.e. flocculus), Purkinje cells are responsive to patterns of optic flow resulting from self-rotation about either the vertical axis (*rVA*) or an horizontal axes oriented 45^{o} to the midline (*rH45*) as indicated by gray shading (Wylie et al. 1993; Wylie and Frost, 1993). **B** shows a coronal section through folia IXcd and X immunoreacted for ZII. The ZII stripes are numbered P1 to P7 (medial to lateral) from the midline (indicated by the dashed line). The ZII+/- pairs from P1+ to P5- are indicated in ventral IXcd as well as P6+. P6-, P7+, and P7- are found more rostrally (Pakan et al. 2007). P1- is divided into medial and lateral portions by a small satellite immunopositive band 1-2 Purkinje cells wide in the middle of P1- denoted "?". P2+ is divided into medial and lateral portions by a small immunonegative "notch" in the middle of P2+ (see inverted triangle). Folium X does not have ZII stripes, as all Purkinje cells are ZII+. Scale bars: = 500 μm in (A); 300 μm in (B).

to upward and downward translation along the vertical axis, respectively, while *contraction* and *expansion* neurons respond to backward and forward translation along horizontal axes. With respect to organization, studies from our lab (Wylie and Frost, 1993a; Wylie et al., 2003b) proposed three sagittal zones spanning the uvula/nodulus as shown in Figure 2.1A. *Contraction* cells were located most medially, *expansion* cells were located in a zone lateral to this and *descent* cells were located most laterally. There were fewer recordings of CSA from *ascent* cells, but they were grouped with the *descent* cells.

The pattern of ZII expression in the VbC is shown in Figure 2.1B. Folium X is uniformly ZII+ (as it is in mammals (e.g. Hawkes and Herrup, 1995)), while folium IXcd consists of an array of seven striking ZII+/- stripes. These are designated P1+/- through P7+/-; see Fig. 1B; Pakan et al. 2007). How the ZII stripes in the pigeon related to functional optic flow zones in Figure 2.1A has been the focus of recent research in our laboratory. Pakan et al. (2011) recorded the CSA of PCs in the flocculus, marked the locations of *rVA* and *rHA* recording sites, and showed that *rVA* neurons are localized to the P4+/- and P6+/- ZII stripes, whereas *rH45* neurons are localized to the P5+/- and P7+/- ZII stripes. Thus, a functional zone in the flocculus spans a ZII+/- stripe pair.

Whether the ZII defined zones in the ventral uvula reflect the unique physiological zonal organization that was found in the flocculus remains uncertain. In this study, we recorded PC CSA in the ventral uvula, marked the location of these recordings, and localized the recording sites to specific ZII stripes after using immunohistochemical techniques to view the expression of this

enzyme. Given the medio-lateral distribution of the translational optic flow zones in the ventral uvula (Fig. 2.1A; Wylie and Frost, 1993a; 1999; Wylie et al., 2003), we hypothesized that (i): *contraction* cells, which are found most medially, would be confined to the P1+/- ZII stripe, (ii) *descent* and *ascent* cells, which are found most laterally, would be confined to the P3+/- ZII stripe, and (iii) *expansion* cells, which are found in between these two zones, would be confined to the P2+/- ZII stripe. While we found that a functional zone in the ventral uvula spanned a ZII+/- pair, the distribution of the 4 types of cells responsive to self-translation did not exactly coincide with our hypothesis. Together, this study combined with that of Pakan et al. (2011) constitutes the first demonstration correlating ZII stripes and the physiological properties of PCs across an entire folium.

2.1 Methods

2.1.1 ***Surgery and Electrophysiological Recording Procedures in the Ventral Uvula and Nodulus***

The methods reported herein conformed to the guidelines established by the Canadian Council on Animal Care and were approved by the Biosciences Animal Care and Use Committee at the University of Alberta. Procedures were optimized for minimizing the number of animals used. Silver King and Homing pigeons (*Columba livia*), obtained from a local supplier, were anesthetized by an intramuscular injection of a ketamine (65 mg/kg) /xylazine (8 mg/kg) cocktail. Supplemental doses were administered as necessary. Animals were placed in a

stereotaxic device with pigeon ear bars and a beak bar adapter so that the orientation of the skull conformed to the atlas of Karten and Hodos (1967). The dorsal surface of the left cerebellum was accessed by removing the bone above folia VI and VII, as the medial VbC (folia IXcd and X) lies below these folia, and the transverse sinus prevents direct exposure of this area. Extracellular single unit recordings were then made using glass micropipettes filled with 2M NaCl (tip diameters of 3-5μm). Electrodes were advanced through folia VI-X using an hydraulic microdrive (Frederick Haer & Co. Millville, NJ). Raw signals were amplified, filtered (10-2000Hz), and digitized by a data analysis system (Cambridge Electronic Designs [CED] *1401plus*) at a sampling rate of 16667Hz. Using a *Spike2* (CED; programmed by Doug Wylie), spikes were sorted offline and peri-stimulus time histograms (PSTHs) were constructed.

The CSA of PCs was recorded from the molecular layer and cells were identified based on their characteristic spontaneous firing rate of about 1 spike/s. We determined the optic flow preferences of neurons as described in previous studies (Winship and Wylie, 2001, 2003; Wylie et al., 2003a,b; Pakan et al. 2011). Briefly, isolated units were first stimulated with a large handheld stimulus, which consisted of visual noise, to determine if the cell was sensitive to visual stimulation. By moving this stimulus in different areas of the panoramic binocular visual field, the optic flow preference of each unit was qualitatively determined. Visual stimuli were then back-projected onto a screen measuring 90^{o} X 75^{o} (width X height) that was positioned in the frontal visual field (from 45^{o} ipsilateral to 45^{o} contralateral azimuth), the contralateral visual field (from 45^{o}

contralateral azimuth to 135 ^{o} contralateral azimuth), or the ipsilateral visual field (from 45^{o} ipsilateral azimuth to 135^{o} ipsilateral azimuth; Fig. 2.2A). We refer to these as the frontal, contralateral and ipsilateral visual fields. The stimuli consisted of drifting sine or square wave gratings of an effective spatial and temporal frequency (0.125-0.5 cycles per degree, 0.125-0.5 Hz), generated by a VSG*Three* (Cambridge Research Services, Rochester, England). Direction tuning was established by measuring the responses to motion in 8 directions, 45^{o} apart (Fig. 2.2B). Responses were averaged over at least 3 sweeps, where each sweep consisted of 5 seconds of motion in one direction, a 4 second pause, and 5 seconds of motion in the opposite direction, followed by a 7 second pause (Fig. 2.2C and 2.2D). With these procedures, *contraction*, *expansion*, *ascent* and *descent* neurons are easy to distinguish (see Winship and Wylie, 2006): in the left VbC, *contraction* and *expansion* neurons show maximum excitation/[inhibition] to rightward/[leftward] motion and little modulation to vertical motion in the frontal visual field (Fig. 2.2E and 2.2F). *Contraction* neurons are differentiated from *expansion* neurons in the ipsi- and contralateral fields, where *contraction* neurons show maximum excitation/[inhibition] to temporal-to-nasal (T-N)/[N-T] motion while *expansion* neurons show maximum excitation/[inhibition] to N-T/[T-N] motion (Fig. 2.2E and 2.2F). *Descent* neurons show maximum excitation/[inhibition] to upward/[downward] motion in all visual fields (Fig. 2.2G) and *ascent* neurons show maximum excitation/[inhibition] to downward/[upward] motion (Fig. 2.2H). Both *ascent* and *descent* neurons show little modulation to horizontal motion (Fig. 2.2G and 2.2H; see Wylie et al.,

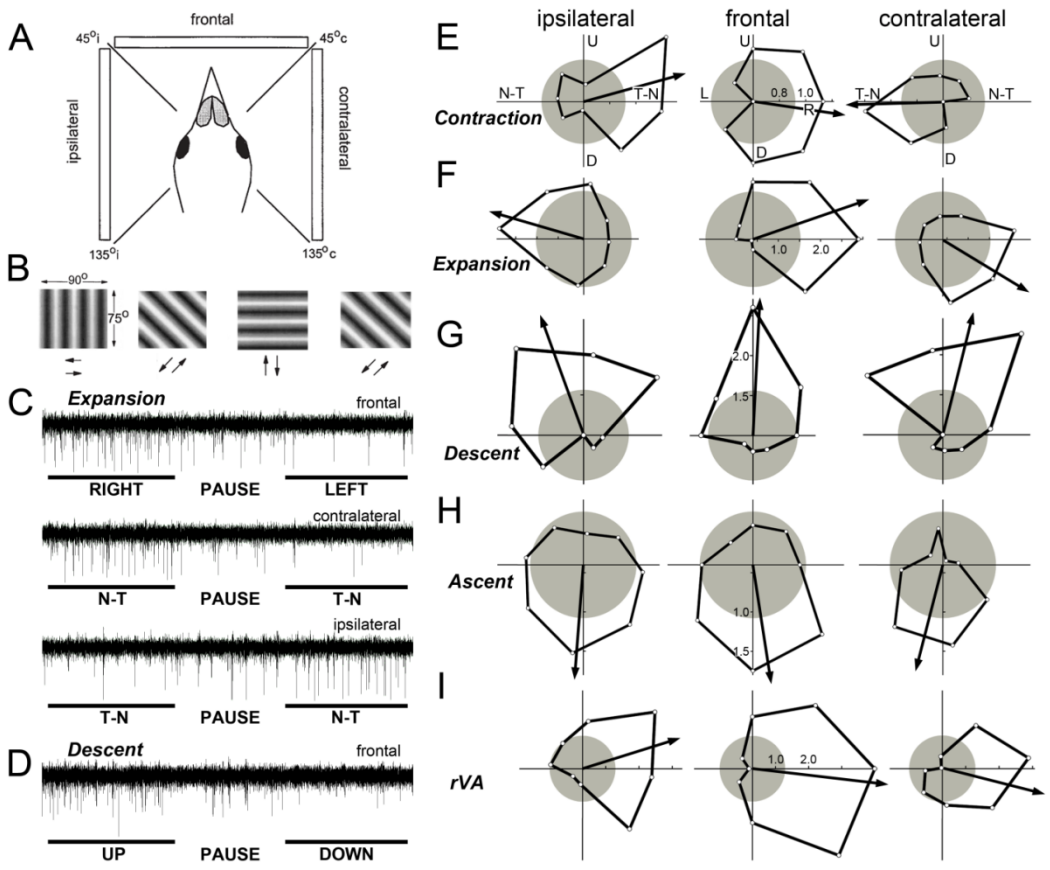

Figure 2.2. Complex spike activity (CSA) of Purkinje cells in the vestibulocerebellum in response to moving largefield stimuli presented in different regions of the visual field. A The screen was positioned at one of three locations relative to the bird: the ipsilateral, contralateral, and frontal regions (assuming recordings were made in the left VbC). **B** shows the four grating orientations used to determine tuning curves in each location. Drifting sine and square wave gratings were back-projected onto the screen that measured 90°×75° (width × height). Each grating moved in both directions, perpendicular to the orientation of the grating. Direction tuning curves were then constructed by

plotting the response as a function of the 8 directions of motion (**E-I**). **C** shows the recording of the responses of an *expansion* cell to a single sweep of horizontal motion in the frontal, contralateral and ipsilateral fields. **D** shows the recording of a *descent* cell to a single sweep of vertical motion in the frontal field. Each sweep consisted of 5 s of motion in one direction, followed by a 4 s pause, then 5 s of motion in the opposite direction. **E–I** show direction tuning curves of *contraction* (**E**), *expansion* (**F**), *descent* (**G**), *ascent* (**H**) and *rVA* (**I**) neurons for each of the three regions of the visual field (ipsilateral, frontal, contralateral). The tuning curves plot the firing rate as a function of direction of motion in polar coordinates. The gray circles represent the spontaneous rates, and the arrows indicate the preferred direction (i.e. the orientation of the mean vector). U, D, L, R = upward, downward, leftward and rightward motion; N-T, T-N = nasal-to-temporal and temporal-to-nasal motion, respectively.

2003). Using SigmaPlot, direction tuning curves were plotted (Fig. 2.2E-I), and a preferred direction (PD) for each unit was determined by calculating the mean vector:

$$PD = \tan^{-1}\left(\frac{\sum_n \left(FR_n \times \sin\theta_n\right)}{\sum_n \left(FR_n \times \cos\theta_n\right)}\right)$$

Where FR = firing rate and *n* = the eight directions of motion. A modulation index (MI) was also calculated for each unit:

$$MI = \left(\frac{max\ response - min\ response}{max\ response + min\ response}\right)$$

Thus, if the maximum response was twice that of the minimum response, MI = 0.33.

Several electrode penetrations were made to map out the locations of the different translational optic flow zones in the medial VbC. In order to mark some of the recording sites, and thus reconstruct the recording locations, we made injections of red and green fluorescent tracers at locations in the ventral uvula and nodulus from which we had recorded CSA to visual stimuli (e.g. Fig. 2.4A-C). For accurate placement of the injection electrodes and reconstruction of the electrode tracts to localize each recorded cell to a specific ZII zone, we relied on sterotaxic coordinates. The injection electrodes were micropipettes (tip diameter 20-30μm) containing 1% cholera toxin subunit B (CTB: either CTB-AlexaFluor 488 [green] or 594 [red] conjugate [Molecular Probes, Eugene, OR]). CTB was iontophoresed for 5-10 minutes (~10nL; +4 μamps, 7 seconds on, 7 seconds off).

The advantage of using CTB was that we could record with the injecting electrode to confirm the response type of the neuron. Note that the CTB injections were only used to mark the locations of recording sites. Because of the lengths of the recording sessions, which lasted a minimum of 12 hours, we were advised by the Biosciences Animal Care and Use Committee at the University of Alberta not to allow the animals to recover post-surgery. (Thus, CTB was not used as a retrograde tracer).

At the end of the experiments, the pigeons were deeply anesthetized with an overdose of sodium pentobarbital (100mg/kg) and immediately transcardially perfused with phosphate buffered saline (PBS; 0.9% NaCl, 0.1M phosphate buffer) followed by 4% paraformaldehyde in 0.1 M PBS (pH 7.4). The brain was extracted from the skull and immersed in paraformaldehyde for 7 days at 4°C. The brain was then embedded in gelatin and cryoprotected by placing it in 30% sucrose in 0.1M PBS until it sank. Using a microtome, frozen serial sections through the cerebellum in the coronal plane were cut (40μm thick) and collated into two series.

2.1.2 ***Zebrin II Immunohistochemistry***

ZII expression was visualized using established immunohistochemical techniques described previously (Pakan et al., 2007). Briefly, sections were rinsed thoroughly in 0.1M PBS and blocked with 10% normal donkey serum (Jackson Immunoresearch Laboratories, West Grove, PA) and 0.4% TritonX-100 in PBS for 1 hour. Tissue was then incubated in PBS containing 0.1% TritonX-100 and

the primary antibody, mouse monoclonal anti-zebrin II (kindly provided by Richard Hawkes, University of Calgary; Brochu, Maler et al. 1990) for 5 days at 4^{o}C. Sections were then rinsed several times in PBS and sections then incubated in a fluorescent secondary antibody. Because recording sites were marked with injections of green and red tracer in the same animal, alternate series were visualized with Dylite 594 (red) or Dylite 488 (green) conjugated donkey anti-mouse antibody (Jackson Immunoresearch Laboratories, West Grove, PA: diluted 1:100 in PBS, 2.5% normal donkey serum, and 0.4% TritonX-100) for 2 hours at room temperature. The tissue was then rinsed several times in PBS and mounted onto gelatinized slides for viewing.

2.1.3 *Microscopy and Image Analysis*

Sections were viewed with a compound light microscope (Leica DMRE) equipped with the appropriate fluorescence filters (rhodamine and FITC). Images were acquired using a Retiga EXi *FAST* Cooled mono 12-bit camera (Qimaging, Burnaby BC) and analyzed with OPENLAB imaging software (Improvision, Lexington MA). Adobe Photoshop was used to adjust for brightness and contrast.

2.2 Results

2.2.1 *Electrophysiological Recording of Visual Response Properties in the Ventral Uvula and Nodulus*

The data are based on experiments in 24 animals. The CSA at 125 sites in the left nodulus and uvula was recorded and localized. All units showed either significant directional tuning, and were identified as *contraction* (*n*=19), *expansion* (*n*=26), *ascent* (*n*=16), *descent* (*n*=48), *rVA* (*n*=10), or were not modulated by visual stimuli (NM; *n*=6). In Figure 2.2C, peri-stimulus time histograms (PSTHs) are shown for horizontal motion in the three fields for an *expansion* cell. Note the excitation (inhibition) to motion in the rightward (leftward) direction in the frontal field (top) and the excitation (inhibition) to N-T (T-N) motion in both the contralateral (middle) and ipsilateral (bottom) fields. Similarly in Figure 2.2D, a PSTH to vertical motion in the frontal field is shown for a *descent* cell. Note the excitation (inhibition) to upward (downward) motion. Representative directional tuning curves to largefield motion in the ipsilateral, frontal and contralateral fields are shown for single units of the different cell types in Figure 2.2E-I. Firing rate is plotted as a function of direction, and the preferred directions, determined from the mean vector, are indicated by the arrows. Figure 2.3A-F shows average normalized tuning curves for each of the cell types. In Figure 2.3G-I, the distribution of the PDs for each of the cell types are shown. The average MI for cells responsive to visual stimulation was 0.48 ± 0.017 (mean ± s.e.m.; range = 0.2-1.0). Of the 125 recording sites, 18 of these were in folium X, and 107 were in IXcd (13 *contraction*, 26 *expansion*, 15 *ascent*, 41 *descent*, 6 *rVA*, 6 NM).

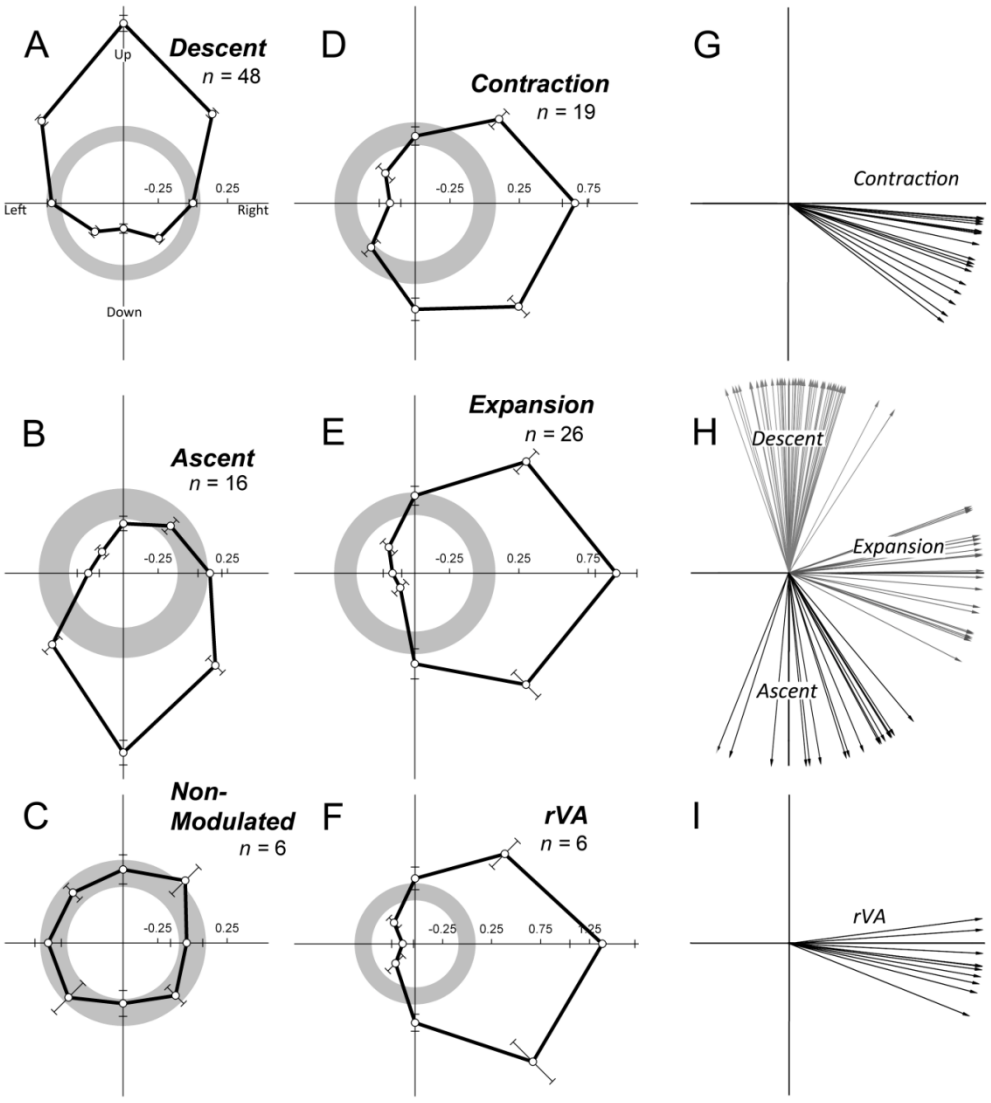

Figure 2.3. Average direction tuning curves and preferred direction of visual motion of Purkinje cells in the ventral uvula and nodulus. A-F shows the average direction tuning curves, as measured in the frontal field, for all cell types encountered (*descent, ascent, non-modulated, contraction, expansion, rVA*). These were averaged after subtracting the spontaneous rate (SR) from the firing rate in each direction from a given cell type. Average firing rate was plotted as a

function of direction of motion in polar coordinates, and the error bars represent +/- 1 standard error of the mean (s.e.m.). The grey circles indicate the average spontaneous rate (set to 0), +/- 1 s.e.m. **G-I** show the distributions of the preferred directions of all *contraction, expansion, descent, ascent* and *rVA* cells by calculating the mean vector (see Methods for details)**.**

2.2.2 *ZII Immunohistochemistry of Folium IXcd*

After ZII expression was visualized in the coronal sections throughout the cerebellum, using immunohistochemical techniques, the locations of the 107 recording sites in IXcd were assigned to a particular ZII stripe. In the cerebella of all animals, we observed the expected pattern of ZII immunoreactivity in folium IXcd (Figs. 2.1B, and 2.4) consisting of seven ZII+/- stripes. We used the nomenclature from Pakan et al. (2007), whereby the most medial positive stripe is designated as P1+ and the number increases as the stripes move laterally to P7+ (see Fig. 2.1B; Brochu et al., 1990; Eisenman & Hawkes, 1993; Ozol et al., 1999; Sillitoe & Hawkes, 2002; reviewed in Sillitoe et al., 2005). The width of individual stripes can vary both between animals as well as along the rostrocaudal axis of the cerebellum within animals. Therefore, in designating the stripe numbers, it was important to complete an examination of all sections throughout the rostrocaudal extent of IXcd. Nonetheless, the seven ZII+/- stripe pairs were easily identifiable. Abutting the midline is a wide ZII+ stripe (P1+) followed by a wide ZII- stripe (P1-). The P1- stripe is separated into medial (P1-med) and lateral (P1-lat) portions by a thin ZII+ stripe that is one to three PCs wide (see "?" in Figs. 2.1B, 2.4A and 2.4B). P2+ is consistently wide throughout the rostrocaudal extent of IXcd, and is separated into medial (P2+med) and lateral (P2+lat) portions by a small "notch" about 50 μm wide in the middle that appeared to contain no PCs (Pakan et al., 2010; see inverted triangle in Fig. 2.1B, 2.4A and 2.4B). The P3+/- stripe pair was relatively thin, with the P3- stripe becoming thinner rostrally. The more lateral stripes, P4+ to P7- (Fig. 2.1B) are

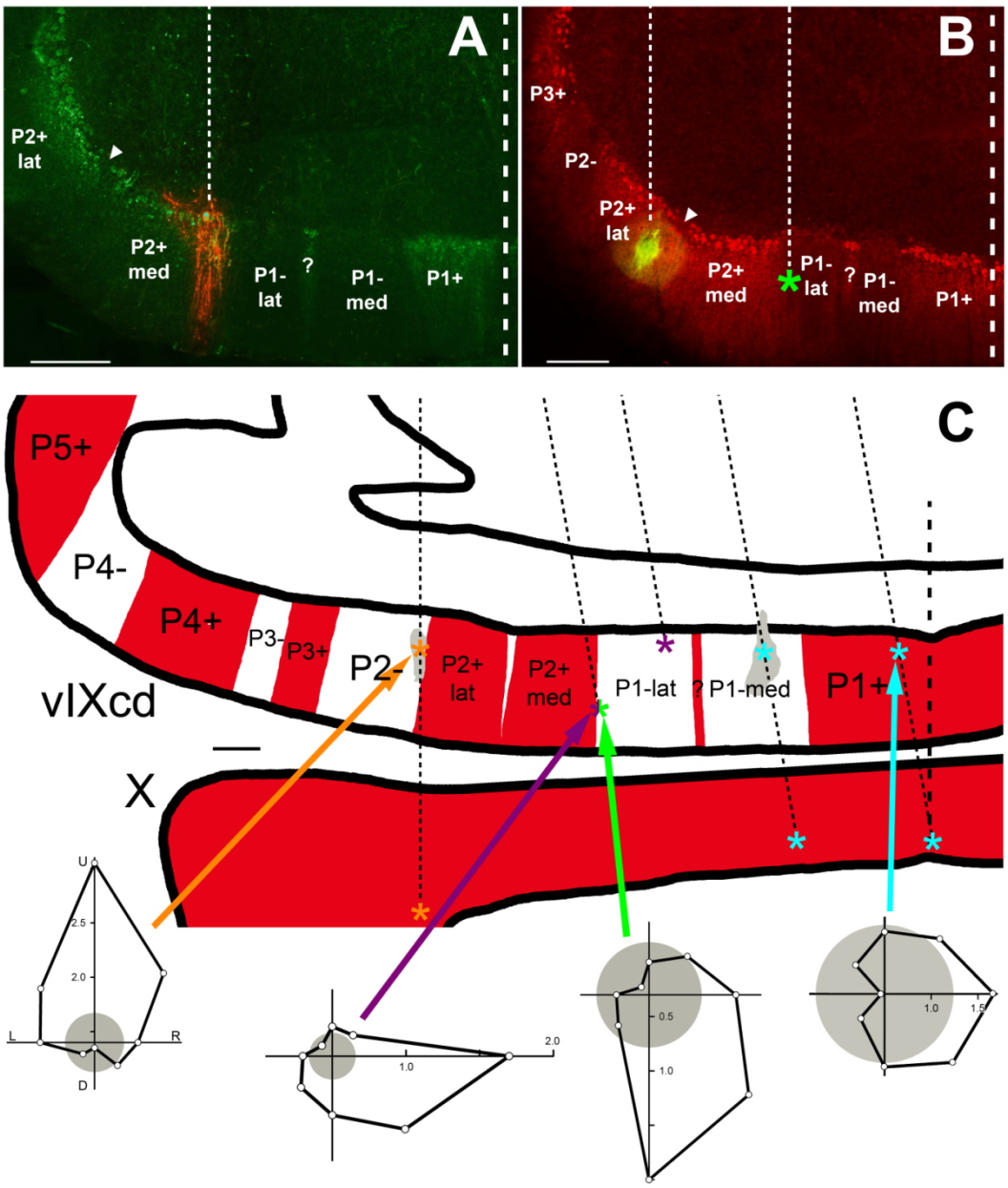

Figure 2.4. Localizing recording sites to zebrin II (ZII) stripes in the ventral uvula. A and B show photomicrographs of a coronal section through the caudal region of folium IXcd. In **A**(**B**) an injection of red (green) CTB is shown with ZII+ labelling in green (red). The thin dashed lines denote the electrode tracks whereas the thick dashed lines indicate the midline. The inverted triangles

indicate the ZII immunonegative notch separating the medial and lateral portions of P2+ (P2+med, P2+ lat). In **A**, an *expansion* cell was recorded at the injection site, located in P2+med. In **B**, a *descent* cell was recorded at the injection site in P2+lat. In the rightmost track, locate 600μm medial to the injection track, an *ascent* cell was recorded as indicated (*) in the lateral portion of the P1- stripe (P1-lat). **C** shows a drawing of coronal section through folia IXcd & X with ZII+ and ZII- stripes indicated, respectively, by red and white shading in the molecular layer. Multiple parallel electrode penetrations are represented by thin dashed lines. The orange, purple and light blue asterisks indicated locations where *descent*, *expansion* and *contraction* cells were recorded, respectively. At the green and purple asterisk on the lateral edge of P1-lat, both *ascent* and *expansion* units were recorded at the same location. (The two units were separated with spike sorting). The two shaded gray areas indicate the locations of two injection sites. Representative direction tuning curves are shown for each type of neuron. Firing rate is plotted as a function of direction of motion in polar coordinates. The gray circles represent the spontaneous rates, and the arrows indicate the preferred direction (i.e. the orientation of the mean vector). Scale bars: = 300 μm in (A, B); 250μm in (C). U, D, R and L = upward, downward, rightward and leftward motion.

part of the flocculus where cells that respond to rotational optic flow are found (see Pakan et al. 2011).

The injections were easily identifiable and could be ascribed to a particular ZII stripe. Figure 2.4A shows an injection of red-CTB, where an *expansion* unit was recorded. The section was immunoreacted for ZII using a green secondary, and the injection can be seen in P2+med. Figure 2.4B shows an injection of green-CTB and the section was processed for ZII using a red secondary. A *descent* cell was recorded at the injection site, which was localized to P2+lat. Within the plane of section, there was a second electrode penetration 600μm medial (thin dashed line). An *ascent* cell was recorded at the location indicated by the green asterisk, located in P1-lat.

When the location of all the recording sites in IXcd were localized to a particular ZII stripe, the results were unambiguous: (i) *contraction* CSA was localized to P1+ and P1-med, (ii) *ascent* and *expansion* CSA was localized to P1-lat and P2+med, and (iii) *descent* cells were localized to P2+lat and P2-. This is illustrated in one case shown in Figure 2.4C where a drawing of a coronal section through IXcd and X is shown, with the ZII+ stripes indicated in red. The locations of eight recording sites along five electrode penetrations (dashed lines) are shown. The orange, purple and light blue asterisks indicated locations where *descent*, *expansion* and *contraction* cells were recorded, respectively. The single purple and green asterisk indicates where both an *ascent* neuron and an *expansion* neuron were recorded at the same location using a single recording electrode. The two shaded gray areas in the ventral lamella of folium IXcd indicate two separate

injection sites. Representative direction tuning curves are shown for each type of neuron. At four sites (one in P1+, one in P1-med and two in folium X), *contraction* neurons were recorded. At two sites (one in P2- and one folium X), *descent* neurons were recorded. At two sites (both in P1-lat), *expansion* neurons were recorded and at one site (in P1-lat), an *ascent* neuron was recorded.

The locations of all 107 recording sites in IXcd from the 24 animals are shown in Figure 2.5A. Because there is variability between animals with respect to the width of the ZII stripes the data have been collapsed onto an average array of stripes. The ZII stripes shown in Figure 2.5A have been averaged from measurements of several cases. The medial-lateral location of a data point was normalized to the width of the stripe in which it was found (i.e. from 0 (medial) to 100% (lateral)) and then scaled to the width of the stripe in Figure 2.5A. For example, blue circle indicated by the asterisk in Figure 2.5A represents a recording site in the P1+ stripe, which measured 439μm in width in that section. The recording site was located 189μm from the medial border of the P1+ stripe, and thus was normalized to 43%. The width of the average P1+ stripe was 400μm, and thus the location was scaled to 172μm lateral to the medial edge of P1+. For the caudo-rostral axis, all measurements are relative to the most caudal section containing folium IXcd.

Of the 13 *contraction* recordings in IXcd, 7 and 6 cells were localized to ZII stripes P1+ and P1-med, respectively. Of the 26 *expansion* recordings in IXcd, 10 and 16 were localized to ZII stripes P1-lat and P2+med, respectively. Of the 15 *ascent* recordings in IXcd, 10 and 5 cells were localized to ZII stripes P1-

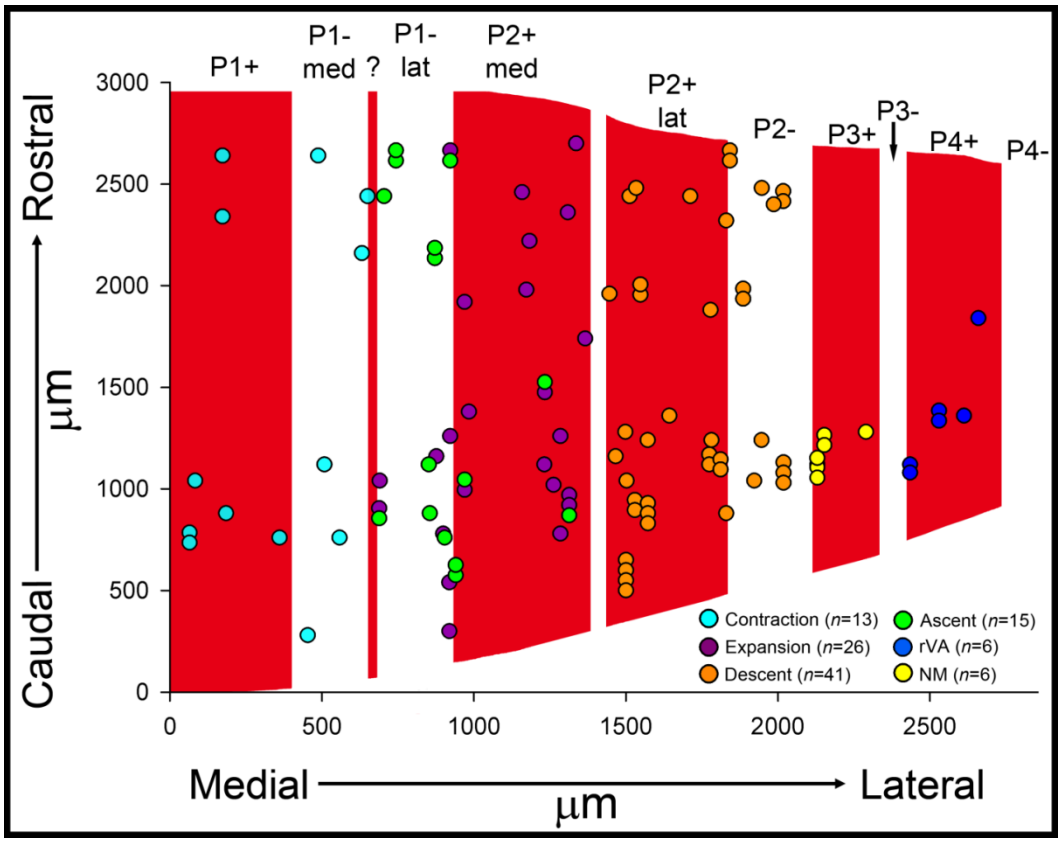

Figure 2.5. Distributions of optic flow neurons in zebrin II (ZII) stripes in the ventral uvula. This figure shows the recording sites of *contraction* (light blue), *expansion* (green), *ascent* (purple), *descent* (orange), cells not modulated to visual stimuli (yellow) and *rVA* (dark blue) cells from all cases are indicated. Both the caudo-rostral (*y*-axis) and medio-lateral (*x*-axis) position are indicated. For the the caudo-rostral axis, all measurements are relative to the most caudal section containing folium IXcd.. For the medial-lateral axis, to permit comparisons between cases, the width of each ZII stripe was normalized (see text for more details). In total 107 recording sites are indicated. The optic flow zones correspond to the ZII stripes as follows: *contraction* = P1+ and P1-med;

expansion/ascent = P1-lat and P2+med; *descent* = P2+lat and P2+. The 6 cells that were not modulated (*NM*) by visual stimuli were all localized to P3+. Consistent with Pakan et al. (2011), the 6 *rVA* cells were localized to P4+.

lat and P2+med, respectively. Of the 41 *ascent* recordings in IXcd, 28 and 13 cells were localized to the ZII stripes P2+lat and P2-, respectively. *rVA* cells were found in the P4+, confirming results found in previous studies (Pakan et al., 2011). In the P3+ stripe, CSA was recorded; however cells in this stripe were not modulated by visual stimulation. Unfortunately, no recordings were obtained from the P3- ZII stripe, which is not surprising as it is so small (<100μm wide). The small size of "?" (about 30 μm wide) and the "notch" in P2+ (about 50 μm wide) also made it impossible for us reliably localize recordings to these stripes.

2.3 Discussion

In the present study we have shown that a given ZII+/- pair in the ventral uvula is 100% concordant to the specific optic flow preference of PCs within that ZII stripe (Table 2.1). We found that (i) *contraction* cells are localized to the P1+ and P1-med stripes; (ii) *expansion* and *ascent* cells are localized to P1-lat and P2+med stripes; and (iii) *descent* cells are localized to the P2+lat and P2- stripes.

There are three points that we need to emphasize. First and foremost, a functional unit in the ventral uvula spans a single ZII+/- pair. This relationship between ZII and functional zones was also shown in the flocculus by Pakan et al. (2011), where they found that *rVA* zones were confined to P4+/- and P6+/-, whereas *rHA* zones were confined to P5+/- and P7+/-. Thus, ZII is related to PC response properties across the entire folium IXcd. Second, the organization revealed in the ventral uvula was not exactly as expected. Within the ventral uvula, our lab has previously grouped the few *ascent* cells that we recorded into

the most lateral functional zone along with *descent* cells (Fig 2.1A; Wylie and Frost, 1993a; Wylie et al., 2003b). However, the present study showed that *ascent* cells were co-localized with *expansion* cells in the zone medial to the *descent* cells (Fig. 2.5) in ZII zones P1-lat and P2+med. Furthermore, we were not able to further subdivide the *expansion* and *ascent* zones, and even recorded both cell types at a single location (see Fig. 2.2 for details). We also found that PCs in ZII zones P3+/- were not responsive to visual stimulation. This could be related to the C2 zone found in the flocculus of mammals, which is non-responsive to optokinetic stimulation, and is proposed to be involved in generating head movements (De Zeeuw and Koekkoek, 1997). It could also be a vestibular zone, similar to those described in the uvula/nodulus of rabbits by Barmack and Sojaku (1995). Finally, the present study reveals a role for satellite bands found in the ventral uvula. Pakan et al. (2007) remarked a small immunopositive band in the middle of P1- (called "?") separating it into P1-med and P1-lat in folium IXcd. Similarly, they also described a natural paucity of PCs in the middle of P2+ dividing it into P2+med and P2+lat. Small satellite bands, or sub-zones, such as this can also been seen in the cerebella of mammals (e.g. Hawkes and Leclerc, 1987; Sanchez et al., 2002). As shown in Figure 2.5, "?" clearly defines the border between the location of *contraction* cells in P1-med, and *expansion* and *ascent* cells in P1-lat. The "notch" in the middle of P2+ provides the boundary between cells responsive to *contraction* and *ascent* cells in P2+med, and *descent* cells in P2+lat. Thus, the "?" in P1- and the "notch" in P2+ play important roles in determining the relationship between functional zones and ZII expression in

the pigeon. However, the optic flow preferences of these satellite zones are beyond the scope of our methods, as we were not able to reliably localize a recording site to these stripes given their small size (often < 50 μm).

2.3.1 ***The Utitlity of the vestibulocerebellum as a General Model for Cerebellar Organization***

The VbC provides an excellent model for cerebellar organization for a number of reasons. First, the zonal organization of the flocculus has been extensively documented and is functionally identical in mammals and birds, and it has been shown that *rVA* and *rHA* cells are organized into parasagittal zones (for review, see Voogd and Wylie, 2004). Furthermore, the uvula/nodulus in birds and mammals is functionally similar (Wylie and Frost, 1993a; Barmack and Shojaku, 1995; Yakusheva et al., 2008). With respect to molecular markers there are nearly identical patterns in both birds and mammals. For example, folium X is uniformly ZII+, while the uvula contains a number of alternating ZII+/- stripes in all species investigated (e.g. Hawkes and Herrup, 1995; Pakan et al., 2007; Marzban and Hawkes, 2010). Though ZII in the flocculus of birds is also expressed in parasagittal bands, the rodent flocculus is uniformly ZII+. However, Fujita et al. (2010) recently found that the flocculus in marmosets contains 4 alternating ZII+/- stripe pairs. Whether the *rVA* and *rHA* zones seen in the marmoset also span a ZII+/- stripe, as in birds, has yet to be determined. A parasagittal expression pattern in the flocculus can also be seen using molecular markers other than ZII. For example, Armstrong et al. (2000) showed that the 25-

kDa heat shock protein (Hsp25) reveals alternating bands of Hsp25-positive (Hsp25+) and Hsp25-negative (Hsp25-) PCs in the flocculus of adult mice. In an attempt to show that Hsp25 is related to PC optokinetic response properties, Schonewille et al., (2006) recorded from *rVA* and *rHA* cells in the mouse flocculus. They showed that a *rHA* or *rVA* stripe could be confined to either an Hsp+, or Hsp- stripe. Whether the same organization of PC response properties and heat shock protein stripes found in the mouse can also be seen in the avian flocculus remains to be seen.

2.3.2 ***Relation of Zebrin II Immunoreactivity to Function in Folium IXcd***

Figure 2.6 shows the organization of PCs responsive to different types of optic flow in relation to ZII stripes. We wish to emphasize that a physiological zone in folium IXcd spans a single ZII+/- band. Though the present study, and that of Pakan et al. (2011) found that CSA of PCs within a given optic flow zone was identical in both the ZII+ and ZII- stripe, recent evidence suggests that ZII+ and ZII- stripes are functionally different. For example, Pakan et al. (2010) showed that MF inputs from two retino-recipient nuclei in pigeons that are responsive to optic flow, the pretectal nucleus lentiformis mesencephali (LM) and the nucleus of the basal optic root (nBOR), project preferentially to ZII+ stripes in IXcd. Therefore, the simple spike activity (SSA) of ZII+ PCs in IXcd should be more responsive to optic flow stimuli, assuming there is greater input to the ZII+ PCs from nBOR and LM through granule cell axons. Whether there are differential connections to ZII+ and ZII- PCs in the pigeon remains to be seen.

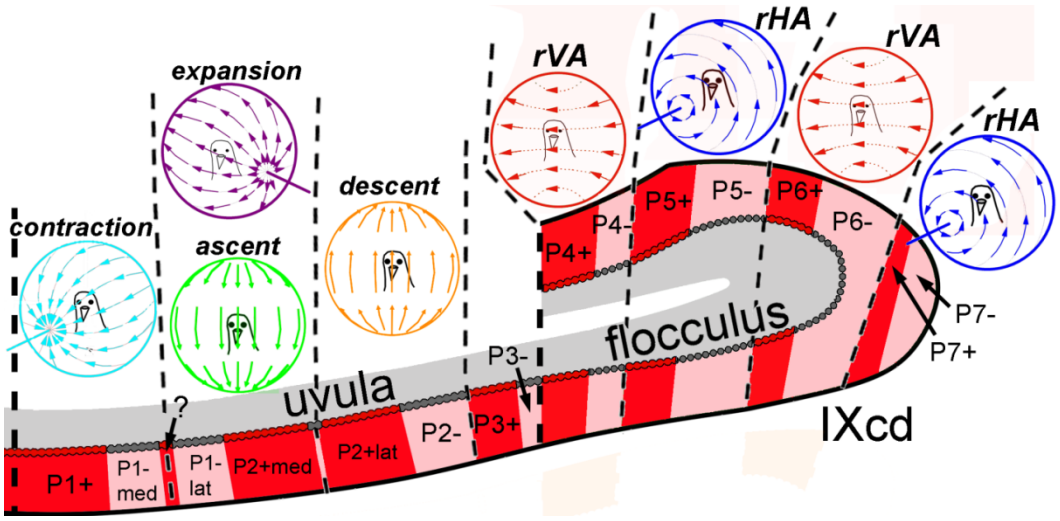

Figure 2.6. Optic flow neurons correspond with zebrin II (ZII) stripes in folium IXcd. ZII-positive Purkinje cells (PCs) are represented as red, whereas ZII-negative PCs are grey and specific zones are indicated from P1+ to P7-. The PCs responsive to *contraction* (light blue), *expansion* (purple), *ascent* (green), *descent* (orange), *rVA* (red) and *rHA* (dark blue) are separated by black dashed lines.

A few other studies have also suggested that ZII+ and ZII- PCs play different roles in the cerebellum. For example, Sugihara et al. (2007) showed that the CSA synchrony was higher among PCs within either a ZII+ or a ZII- band. In a study that did not directly measure PC activity, Gao et al. (2006) found that on-beam and off-beam inhibition evoked by parallel fiber and peripheral stimulation results in parasagittal bands of decreases in activity that correspond to only ZII+ zones along a folium. Paukert et al. (2010) revealed that CFs in ZII+ zones release more glutamate per action potential than CFs in ZII- zones. Mostofi et al. (2010) showed that periocular-evoked CSA was localized to the P5- ZII stripe in the hemisphere of the rabbit cerebellum using an eye-blink conditioning paradigm. The differential projections of various olivary subnuclei to ZII+ and ZII- zones have been investigated in several studies of rodent cerebella (Voogd et al., 2003; Sugihara & Shinoda, 2004; Voogd & Ruigrok, 2004; Pijpers et al., 2006; Sugihara & Quy, 2007). While our methods precluded concurrent recordings at multiple sites, based on the studies above, we believe that there would be higher CSA synchrony in PCs of either a ZII+ or ZII- stripe in folium IXcd of the pigeon. To test this, we could adjust the methods of the present study slightly by making simultaneous recordings of CSA from two sites responsive to the same pattern of optic flow, mark both recording locations, analyze the CSA synchrony, and finally visualize ZII expression to localize the recording sites and compare synchrony results from recordings within ZII zones of the same (or opposite) signature.

2.3.3 *Roles of Sagittal and Transverse Zones in the Vestibulocerebellum*

Finally, while there are clearly sagittal divisions in the cerebellum, one must also consider the transverse zone when looking at cerebellar organization (for review, see Apps and Hawkes, 2009). This is supported by findings of Schwarz and Schwarz (1983), which showed that while primary vestibular inputs project almost exclusively to folium X, neither LM nor nBOR project to this folium. Therefore differential MF projections to IXcd (visual) and X (primary vestibular) suggest a transverse organization of sensory information in the VbC. As MFs from nBOR and LM preferentially innervate ZII+ stripes in IXcd, these projections indicate an interaction between the transverse and sagittal zones. It is also possible that the SSA of PCs in folium X is unlike that in IXcd, where visual and vestibular inputs would drive the SSA of PCs in IXcd and X, respectively. However, visual stimulation would control the CSA in both IXcd and X, while synchrony within and between the ZII+ and ZII- subzones would differ. Therefore, one cannot rely on olivary inputs or CSA responsiveness alone to determine the function of a sagittal zone as the organization within that zone may be further subdivided.

Thus, while our findings certainly contribute to our understanding of cerebellar organization, much more is needed to determine how sensory information is processed in the VbC of pigeons. For example, while the vestibular nuclei, spinal cord, and pontine nuclei also send MF afferents to IXcd (Freedman et al., 1975; Clarke, 1977; Vielvoye & Voogd, 1977; Necker, 1992; Pakan & Wylie, 2008), their relationship to ZII has not been investigated. Do some of

these inputs preferentially target the granular layer subjacent to either ZII+ or ZII- PCs in IXcd? We have previously shown that PCs in VA and HA zones have several non-overlapping projections to different areas in the vestibular and cerebellar nuclei (Wylie et al., 2003). Do the PCs in the ZII+ and ZII- stripes within a physiological zone have differential projections? While in rats ZII+ and ZII- PCs project to different areas in the vestibular and cerebellar nuclei (Sugihara et al., 2009), the story in pigeons remains unclear.

Table 2.1: **Distribution of *contraction*, *expansion*, *ascent*, *descent*, non-modulated to optokinetic stimulation (NM), and rotation about the vertical axis (*rVA*) cells in zebrin II stripes of folium IXcd in the pigeon cerebellum**

	ZII stripe								
	P1+	P1-med	P1-lat	P2+med	P2+lat	P2-	P3+	P3-	P4+
Contraction cells	7	6							
Expansion cells			10	16					
Ascent cells			10	5					
Descent cells					28	13			
NM cells							6		
rVA cells									6

2.4 References

Ahn AH, Dziennis S, Hawkes R, Herrup K. 1994. The cloning of zebrin II reveals its identity with aldolase C. Development 120(8):2081-2090.

Akintunde A, Eisenman LM. 1994. External cuneocerebellar projection and Purkinje cell zebrin II bands: a direct comparison of parasagittal banding in the mouse cerebellum. J Chem Neuroanat 7(1-2):75-86.

Andersson G, Oscarsson O. 1978. Climbing fibre microzones in cerebellar vermis and their projection to different groups of cells in the lateral vestibular nucleus. Exp Brain Res 32(4):565-579.

Apps, R. & Garwicz,M. (2005). Anatomical and physiological foundations of cerebellar information processing. Nature Reviews. Neuroscience 6, 297–311.

Apps R, Garwicz M. 2005. Anatomical and physiological foundations of cerebellar information processing. Nat Rev Neurosci 6(4):297-311.

Armstrong CL, Krueger-Naug AM, Currie RW, Hawkes R. 2000. Constitutive expression of the 25-kDa heat shock protein Hsp25 reveals novel parasagittal bands of purkinje cells in the adult mouse cerebellar cortex. J Comp Neurol 416(3):383-397.

Barmack NH, Shojaku H. 1995. Vestibular and visual climbing fiber signals evoked in the uvula-nodulus of the rabbit cerebellum by natural stimulation. J Neurophysiol 74(6):2573-2589.

Barmack NH, Yakhnitsa V. 2003. Cerebellar climbing fibers modulate simple spikes in Purkinje cells. J Neurosci 23(21):7904–7916.

Barmack NH, Yakhnitsa V. 2008. Distribution of granule cells projecting to focal Purkinje cells in mouse uvula-nodulus. Neurosci 156(1):216–221.

Brecha N, Karten HJ, Hunt SP. 1980. Projections of the nucleus of the basal optic root in the pigeon: an autoradiographic and horseradish peroxidase study. J Comp Neurol 189(4):615-670.

Brochu G, Maler L, Hawkes R. 1990. Zebrin II: a polypeptide antigen expressed selectively by Purkinje cells reveals compartments in rat and fish cerebellum. J Comp Neurol 291(4):538-552.

Chockkan V, Hawkes R. 1994. Functional and antigenic maps in the rat cerebellum: zebrin compartmentation and vibrissal receptive fields in lobule IXa. J Comp Neurol 345(1):33-45.

Clarke PG. 1977. Some visual and other connections to the cerebellum of the pigeon. J Comp Neurol 174(3):535-552.

De Zeeuw CI, Wylie DR, DiGiorgi PL, Simpson JI. 1994. Projections of individual Purkinje cells of identified zones in the flocculus to the vestibular and cerebellar nuclei in the rabbit. J Comp Neurol 349(3):428-447.

Eccles JC, Llinas R, Sasaki K, Voorhoeve PE. 1966. Interaction experiments on the responses evoked in Purkinje cells by climbing fibres. J Physiol 182(2):297-315.

Eisenman LM, Hawkes R. 1993. Antigenic compartmentation in the mouse cerebellar cortex: zebrin and HNK-1 reveal a complex, overlapping molecular topography. J Comp Neurol 335(4):586-605.

Ekerot CF, Larson B. 1973. Correlation between sagittal projection zones of climbing and mossy fibre paths in cat cerebellar anterior lobe. Brain Res 64:446-450.

Freedman SL, Feirabend HK, Vielvoye GJ, Voogd J. 1975. Re-examination of the ponto-cerebellar projection in the adult white leghorn (Gallus domesticus). Acta Morphol Neerl Scand 13(3):236-238.

Gao W, Chen G, Reinert KC, Ebner TJ. 2006. Cerebellar cortical molecular layer inhibition is organized in parasagittal zones. J Neurosci 26(32):8377-8387.

Graf W, Simpson JI, Leonard CS. 1988. Spatial organization of visual messages of the rabbit's cerebellar flocculus. II. Complex and simple spike responses of Purkinje cells. J Neurophysiol 60(6):2091-2121.

Gravel C, Eisenman LM, Sasseville R, Hawkes R. 1987. Parasagittal organization of the rat cerebellar cortex: direct correlation between antigenic Purkinje cell bands revealed by mabQ113 and the organization of the olivocerebellar projection. J Comp Neurol 265(2):294-310.

Gravel C, Hawkes R. 1990. Parasagittal organization of the rat cerebellar cortex: direct comparison of Purkinje cell compartments and the organization of the spinocerebellar projection. J Comp Neurol 291(1):79-102.

Hawkes R, Gravel C. 1991. The modular cerebellum. Prog Neurobiol 36(4):309-327.

Hawkes R, Herrup K. 1995. Aldolase C/zebrin II and the regionalization of the cerebellum. J Mol Neurosci 6(3):147-158.

Herrup K, Kuemerle B. 1997. The compartmentalization of the cerebellum. Annu Rev Neurosci 20:61-90.

Iwaniuk AN, Marzban H, Pakan JM, Watanabe M, Hawkes R, Wylie DR. 2009. Compartmentation of the cerebellar cortex of hummingbirds (Aves: Trochilidae) revealed by the expression of zebrin II and phospholipase C beta 4. J Chem Neuroanat 37(1):55-63.

Ji Z, Hawkes R. 1994. Topography of Purkinje cell compartments and mossy fibre terminal fields in lobules II and III of the rat cerebellar cortex: spinocerebellar and cuneocerebellar projections. Neuroscience 61(4):935-954.

Kano MS, Kano M, Maekawa K. 1990. Receptive field organization of climbing fiber afferents responding to optokinetic stimulation in the cerebellar nodulus and flocculus of the pigmented rabbit. Exp Brain Res 82(3):499-512.

Karten H, Hodos W. 1967. A stereotaxic Atlas of the Brain of the Pigeon (*Columba livia*). Baltimore: Johns Hopkins Press.

Larouche M, Hawkes R. 2006. From clusters to stripes: the developmental origins of adult cerebellar compartmentation. Cerebellum 5(2):77-88.

Llinas R, Sasaki K. 1989. The Functional Organization of the Olivo-Cerebellar System as Examined by Multiple Purkinje Cell Recordings. Eur J Neurosci 1(6):587-602.

Marzban H, Chung SH, Pezhouh MK, Feirabend H, Watanabe M, Voogd J, Hawkes R. 2010. Antigenic compartmentation of the cerebellar cortex in the chicken (*Gallus domesticus*). J Comp Neurol 518(12):2221–2239.

Matsushita M, Ragnarson B, Grant G. 1991. Topographic relationship between sagittal Purkinje cell bands revealed by a monoclonal antibody to zebrin I and spinocerebellar projections arising from the central cervical nucleus in the rat. Exp Brain Res 84(1):133-141.

Mostofi A, Holtzman T, Grout AS, Yeo CH, Edgley SA. 2010. Electrophysiological localization of eyeblink-related microzones in rabbit cerebellar cortex. J Neurosci 30(26):8920–8930.

Nagao S, Kitazawa H, Osanai R, Hiramatsu T. 1997. Acute effects of tetrahydrobiopterin on the dynamic characteristics and adaptability of vestibulo-ocular reflex in normal and flocculus lesioned rabbits. Neurosci Lett 231(1):41-44.

Necker R. 1992. Spinal neurons projecting to anterior or posterior cerebellum in the pigeon. Anat Embryol (Berl) 185(4):325-334.

Ozol K, Hayden JM, Oberdick J, Hawkes R. 1999. Transverse zones in the vermis of the mouse cerebellum. J Comp Neurol 412(1):95-111.

Pakan JM, Graham DJ, Gutiérrez-Ibáñez C, Wylie DR. 2011. Organization of the cerebellum: Correlating zebrin immunochemistry with optic flow zones in the pigeon flocculus. Vis Neurosci 28(2):163-174.

Pakan JM, Graham DJ, Wylie DR. 2010. Organization of visual mossy fiber projections and zebrin expression in the pigeon vestibulocerebellum. J Comp Neurol 518(2):175–198.

Pakan JM, Iwaniuk AN, Wylie DR, Hawkes R, Marzban H. 2007. Purkinje cell compartmentation as revealed by zebrin II expression in the cerebellar cortex of pigeons (*Columba livia*). J Comp Neurol 501(4):619-630.

Pakan JM, Todd KG, Nguyen AP, Winship IR, Hurd PL, Jantzie LL, Wylie DR. 2005. Inferior olivary neurons innervate multiple zones of the flocculus in pigeons (*Columba livia*). J Comp Neurol 486(2):159-168.

Pakan JM, Wylie DR. 2008. Congruence of zebrin II expression and functional zones defined by climbing fibre topography in the flocculus. Neuroscience 157(1):57-69.

Paukert M, Huang YH, Tanaka K, Rothstein JD, Bergles DE. 2010. Zones of enhanced glutamate release from climbing fibers in the mammalian cerebellum. J Neurosci 30(21):7290–7299.

Pijpers A, Apps R, Pardoe J, Voogd J, Ruigrok TJ. 2006. Precise spatial relationships between mossy fibres and climbing fibres in rat cerebellar cortical zones. J Neurosci 26(46):12067-12080.

Ruigrok TJ. 2003. Collateralization of climbing and mossy fibres projecting to the nodulus and flocculus of the rat cerebellum. J Comp Neurol 466(2):278-298.

Ruigrok TJ, Pijpers A, Goedknegt-Sabel E, Coulon P. 2008. Multiple cerebellar zones are involved in the control of individual muscles: A retrograde

transneuronal tracing study with rabies virus in the rat. Eur J Neurosci 28(1):181–200.

Sanchez M, Sillitoe RV, Attwell PJ, Ivarsson M, Rahman S, Yeo CH, Hawkes R. 2002. Compartmentation of the rabbit cerebellar cortex. J Comp Neurol 444(2):159-173.

Schonewille M, Luo C, Ruigrok TJ, Voogd J, Schmolesky MT, Rutteman M, Hoebeek FE, De Jeu MT, De Zeeuw CI. 2006. Zonal organization of the mouse flocculus: physiology, input, and output. J Comp Neurol 497(4):670-682.

Schwarz IE, Schwarz DW. 1983. The primary vestibular projection to the cerebellar cortex in the pigeon (Columba livia). J Comp Neurol 216(4):438-444.

Sillitoe RV, Hawkes R. 2002. Whole-mount immunohistochemistry: a high-throughput screen for patterning defects in the mouse cerebellum. J Histochem Cytochem 50(2):235-244.

Sillitoe RV, Marzban H, Larouche M, Zahedi S, Affanni J, Hawkes R. 2005. Conservation of the architecture of the anterior lobe vermis of the cerebellum across mammalian species. Prog Brain Res 148:283-297.

Simpson J, Graf W, Leonard CS. 1981. The coordinate system of visual climbing fibres to the flocculus. In: Progress in oculomotor research. Fuchs A, Becker W, editors. Amsterdam/New York/Oxford: Elsevier/North Holland.

Sugihara I, Fujita H, Na J, Quy PN, Li BY, Ikeda D. 2009. Projection of reconstructed single Purkinje cell axons in relation to the cortical and nuclear aldolase C compartments of the rat cerebellum. J Comp Neurol 512(2):282–304.

Sugihara I, Marshall SP, Lang EJ. 2007. Relationship of complex spike synchrony bands and climbing fibre projection determined by reference to aldolase C compartments in crus IIa of the rat cerebellar cortex. J Comp Neurol 501(1):13-29.

Sugihara I, Quy PN. 2007. Identification of aldolase C compartments in the mouse cerebellar cortex by olivocerebellar labelling. J Comp Neurol 500(6):1076-1092.

Sugihara I, Shinoda Y. 2004. Molecular, topographic, and functional organization of the cerebellar cortex: a study with combined aldolase C and olivocerebellar labelling. J Neurosci 24(40):8771-8785.

Sugihara I, Shinoda Y. 2007. Molecular, topographic, and functional organization of the cerebellar nuclei: analysis by three-dimensional mapping of the olivonuclear projection and aldolase C labelling. J Neurosci 27(36):9696-9710.

Vielvoye GJ, Voogd J. 1977. Time dependence of terminal degeneration in spino-cerebellar mossy fibre rosettes in the chicken and the application of terminal degeneration in successive degeneration experiments. J Comp Neurol 175(2):233-242.

Voogd J. 1967. Comparative aspects of the structure and fibre connexions of the mammalian cerebellum. Prog Brain Res 25:94-134.

Voogd J, Bigaré F. 1980. Topographical distribution of olivary and cortico nuclear fibres in the cerebellum: a review. Courville J, de Montigny C, Lamarre Y, editors. New York: Raven. 207-234 p.

Voogd J, Broere G, van Rossum J. 1969. The medio-lateral distribution of the spinocerebellar projection in the anterior lobe and the simple lobule in the cat and a comparison with some other afferent fibre systems. Psychiatr Neurol Neurochir 72(1):137-151.

Voogd J, Glickstein M. 1998. The anatomy of the cerebellum. Trends Neurosci 21(9):370-375.

Voogd J, Pardoe J, Ruigrok TJ, Apps R. 2003. The distribution of climbing and mossy fibre collateral branches from the copula pyramidis and the paramedian lobule: congruence of climbing fibre cortical zones and the pattern of zebrin banding within the rat cerebellum. J Neurosci 23(11):4645-4656.

Voogd J, Ruigrok TJ. 2004. The organization of the corticonuclear and olivocerebellar climbing fibre projections to the rat cerebellar vermis: the congruence of projection zones and the zebrin pattern. J Neurocytol 33(1):5-21.

Voogd J, Wylie DR. 2004. Functional and anatomical organization of floccular zones: a preserved feature in vertebrates. J Comp Neurol 470(2):107-112.

Wadiche JI, Jahr CE. 2005. Patterned expression of Purkinje cell glutamate transporters controls synaptic plasticity. Nat Neurosci 8(10):1329-1334.

Waespe W, Henn V. 1987. Gaze stabilization in the primate. The interaction of the vestibulo-ocular reflex, optokinetic nystagmus, and smooth pursuit. Rev Physiol Biochem Pharmacol 106:37-125.

Winship IR, Wylie DR. 2001. Responses of neurons in the medial column of the inferior olive in pigeons to translational and rotational optic flowfields. Exp Brain Res 141(1):63-78.

Winship IR, Wylie DR. 2003. Zonal organization of the vestibulocerebellum in pigeons (Columba livia): I. Climbing fibre input to the flocculus. J Comp Neurol 456(2):127-139.

Wu HS, Sugihara I, Shinoda Y. 1999. Projection patterns of single mossy fibres originating from the lateral reticular nucleus in the rat cerebellar cortex and nuclei. J Comp Neurol 411(1):97-118.

Wylie DR. 2001. Projections from the nucleus of the basal optic root and nucleus lentiformis mesencephali to the inferior olive in pigeons (Columba livia). J Comp Neurol 429(3):502-513.

Wylie DR, Brown MR, Barkley RR, Winship IR, Crowder NA, Todd KG. 2003. Zonal organization of the vestibulocerebellum in pigeons (Columba livia): II. Projections of the rotation zones of the flocculus. J Comp Neurol 456(2):140-153.

Wylie DR, Frost BJ. 1993. Responses of pigeon vestibulocerebellar neurons to optokinetic stimulation. II. The 3-dimensional reference frame of rotation neurons in the flocculus. J Neurophysiol 70(6):2647-2659.

Wylie DR, Kripalani T, Frost BJ. 1993. Responses of pigeon vestibulocerebellar neurons to optokinetic stimulation. I. Functional organization of neurons discriminating between translational and rotational visual flow. J Neurophysiol 70(6):2632-2646.

Wylie DR, Winship IR, Glover RG. 1999b. Projections from the medial column of the inferior olive to different classes of rotation-sensitive Purkinje cells in the flocculus of pigeons. Neurosci Lett 268(2):97-100.

Yakusheva T, Blazquez PM, Angelaki DE. 2008. Frequency-selective coding of translation and tilt in macaque cerebellar nodulus and uvula. J Neurosci 28(40):9997-10009.

Chapter 3: **Correlating Zebrin Expression with Functional Zones Defined by Climbing Fibre Topography in the Ventral Uvula in Pigeons**

As discussed in Chapters 1 and 2 of this thesis, the basic unit of organization in the cerebellum is the parasagittal zone (see Sec. 1.3; 2.1; Voogd and Bigaré, 1980). This parasagittal architecture can be revealed by climbing fiber (CF) and mossy fiber afferent input, Purkinje cell (PC) efferent projection arrangements, and the response properties of PCs (Llinas and Sasaki, 1989; de Zeeuw et al., 1994; Voogd and Glickstein, 1998; Wu et al., 1999; Ruigrok, 2003; Apps and Garwicz, 2005). Several molecular markers also show a parasagittal expression pattern in the cerebellum (for review see Herrup and Kuemerle, 1997). By far the most carefully examined of these is zebrin II (ZII). As described in Chapters 1 and 2, the ZII antibody recognizes the 36-kDa isoenzyme aldolase C which is expressed by PCs (Brochu et al., 1990; Ahn et al., 1994; Hawkes and Herrup, 1995), and the stripey ZII expression pattern is seen in several mammalian and avian species (Hawkes, 1992; Hawkes and Herrup, 1995; Sanchez et al., 2002; Pakan et al., 2007; Iwaniuk et al., 2009; Marzban and Hawkes, 2010), suggesting that the pattern is highly conserved, and is likely critical for fundamental cerebellar function. How ZII stripes relate to functional zones within the cerebellum has been researched extensively (for examples, Chockkan and Hawkes, 1994; Hallem et al., 1999; Voogd et al., 2003; Sugihara and Shinoda, 2004; 2007; Voogd and Ruigrok, 2004; Pijpers et al., 2006; Sugihara et al., 2007), and was the focus of Chapter 2 of this thesis. Breifly, it showed that the four types of visually responsive PCs in the ventral uvula of pigeons are confined to a ZII-immunopositive (ZII+) and ZII-immunonegative (ZII-) pair (see Fig. 2.6). Specifically, PC complex spike activity (CSA)

responsive to *contraction* optic flow was located most medially, in the P1+ and medial portion of P1- (P1-med) stripes, while *descent* PCs were located most laterally, in the lateral portion of P2+ (P2+lat) and P2- stripes. Both *contraction* and *ascent* PCs were confined to the lateral portion of P1- (P1-lat) and the medial portion of P2+ (P2+med). These results are similar to a study by Pakan et al. (2011) of the lateral folium IXcd, where they found that the CSA of PCs responsive to rotational optic flow in the flocculus were confined to a ZII+/- pair.

Given the results of Chapter 2 and Pakan et al. (2011), one would expect that the CF inputs into the VbC would reflect the optic flow preferences found in PC CSA, and would also be related in the same way to ZII expression patterns. As discussed in Chapter 1, the pigeon inferior olive (IO) can be divided into three regions: the ventral and dorsal lamella, and the medial column (mcIO; Arends and Voogd, 1989). Retino-recipient nuclei in the pretectum and the accessory optic system send visual projections to the mcIO, which then carries visual optic flow information to the VbC via CFs (Clarke, 1977; Brecha et al., 1980; Gamlin and Cohen, 1988; Wylie et al., 1997; Wylie, 2001). Previous studies from our lab have determined that neurons in the mcIO respond to optic flow stimuli, as in the VbC (Wylie and Frost, 1993; Winship and Wylie, 2001). Within the mcIO, neurons responsive to translational optic flow are located laterally, whereas neurons responsive to rotational optic flow are located medially (Lau et al., 1998). In the lateral mcIO, *contraction* neurons are located caudally, and *descent* neurons are located rostrally, while *expansion* and *ascent* regions are located between these areas along the rosto-caudal axis in the lateral mcIO (see Fig.

3.1A; Crowder et al., 2000; Winship and Wylie, 2001). In the medial mcIO, *rVA* cells are located caudally, whereas *rHA* neurons are located rostrally (see Fig 3.1A; Wylie et al., 1999; Winship and Wylie, 2001; 2003; Pakan et al., 2005) Recently, Pakan and Wylie (2008) demonstrated the CF input to the flocculus is concordant with ZII banding by making localized injections of anterograde tracer into the caudal and rostral regions of the medial mcIO. The results showed that injections into the *rVA* region of the mcIO resulted in CF labelling in P4+/- and P6+/-, and that injections into the *rHA* region of the mcIO resulted in CF labelling in P5+/- and P7+/-. Thus, this study showed that a CF zone in the pigeon flocculus spans a ZII+/- pair, as does a functional zone in the flocculus (Pakan et al., 2011).

The purpose of Chapter 3 of this thesis was to examine the relationship between CF input and ZII stripes in the ventral uvula of pigeons. We predicted that the CF labelling in the ventral uvula would reflect the results obtained in Chapter 2 of this thesis, which showed that a functional zone in the ventral uvula spans a ZII+/- pair (Fig. 3.1B). Specifically, that (i) CFs from the *contraction* region of the mcIO would project to P1+ and P1-med; (ii) CFs from the *expansion* and *ascent* region of the mcIO would project to P1-lat and P2+med; and (iii) CFs from the *descent* region of the mcIO would project to P2+lat and P2-. In order to determine the relationship between ZII expression patterns and CF projections in the ventral uvula, we made small injections of the anterograde tracer biotinylated dextran amine (BDA) into the caudal (*contraction*), middle (*expansion* and *ascent)* or rostral (*descent*) regions of the lateral mcIO in pigeons

(Fig. 3.1A). We then examined the resulting olivocerebellar CF labelling in relation to the ZII pattern in the ventral uvula.

3.1 Methods

3.1.1 *Surgical and Tracer Injection Procedure*

The methods reported herein conformed to the guidelines established by the Canadian Council on Animal Care and were approved by the Biosciences Animal Care and Use Committee at the University of Alberta. Procedures were optimized for minimizing the number of animals used. Silver King and Homing pigeons (*Columba livia*) obtained from a local supplier were anesthetized with an injection (i.m.) of a ketamine (65 mg/kg)/ xylazine (8 mg/kg) cocktail. Supplemental doses were administered as necessary. Animals were placed in a stereotaxic device with pigeon ear bars and a beak bar adapter so that the orientation of the skull conformed to the atlas of Karten and Hodos (1967). To access the IO, bone and dura were removed from the dorsomedial surface of the cerebellum, lateral to the mid-sagittal sinus. The intent was to make localized injections into the regions of the mcIO that provide CF input to the ventral uvula and nodulus. The pigeon IO is divided into ventral and dorsal lamellae, which are conjoined medially by the mcIO (Arends and Voogd, 1989). The rostro-caudal extent of the mcIO ranges from about 1.4–1.8 mm in length. From our previous work, as discussed above and summarized in Figure 3.1A (Lau et al., 1998; Wylie et al., 1999; Crowder et al., 2000), we showed that injections into the translation

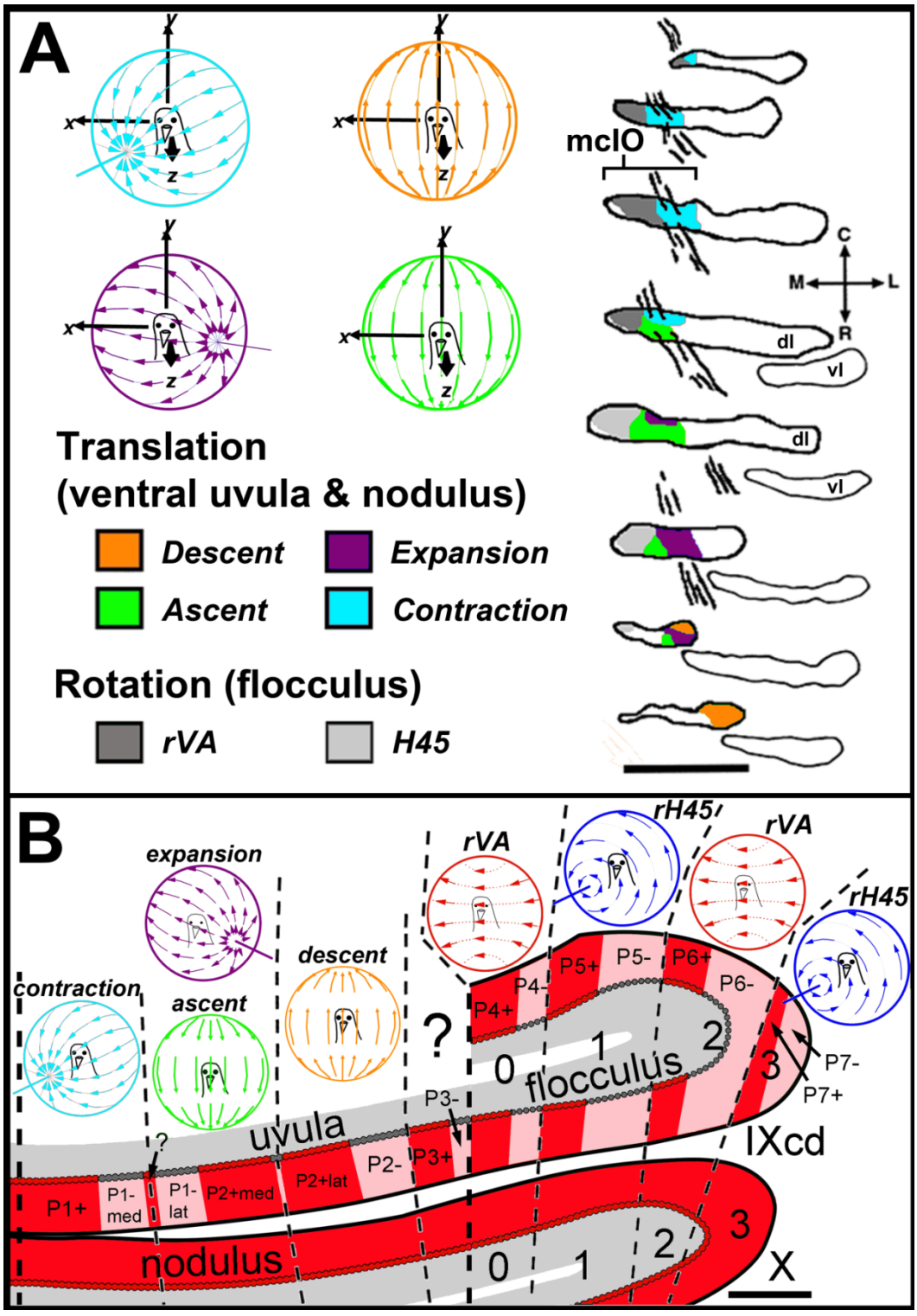
A
mclO
C
M
L
R
dl
vl
dl
vl
Translation
(ventral uvula & nodulus)
Descent
Expansion
Ascent
Contraction
Rotation (flocculus)
rVA
H45
B
expansion
descent
contraction
ascent
rVA
rH45
rVA
rH45
P4+
P4-
P5+
P5-
P6+
P6-
P7-
P7+
?
0
1
2
3
flocculus
P3-
uvula
P2-
P3+
P1+
P1-med
P1-lat
P2+med
P2+lat
IXcd
nodulus
0
1
2
3
X

Figure 3.1. Zebrin II organization and electrophysiological zones in the medial VbC and mcIO of pigeons. A shows the four functional classes of Purkinje cells responsive to patterns of optic flow resulting from self-translation in three-dimensional space: *contraction* (light blue), *expansion* (purple), *ascent* (green), and *descent* (orange). In the mcIO, *contraction* cells are found most caudally, *descent* cells are found most rostrally, and *expansion* and *ascent* cells are found in between *contraction* and *descent* areas, with some rostrocaudal overlap between both the *contraction* and *descent* regions (Crowder et al., 2000). **B** shows a coronal section through folia IXcd and X. The ZII stripes are numbered 1-7 (medial to lateral) from the midline (thick dashed line). ZII+ PCs are indicated in red and ZII- PCs are indicated in grey. P1- is divided into medial and lateral portions by a small satellite immunopositive band 1-2 Purkinje cells wide in the middle of P1- denoted "?". P2+ is divided into medial and lateral portions by a small immunonegative "notch" in the middle of P2+. In medial folium IXcd, (i) *contraction* cells are found in P1+ and P1-med, (ii) *expansion* and *ascent* cells are located in P1-lat and P2+med, and (iii) *descent* cells are located in P2+lat and P2-. Cells responsive to patterns of optic flow resulting from self-rotation are located laterally folium IXcd. Scale bars: = 500 μm in (A); 400 μm in (B). C, R, M and L = caudal, rostral, medial and lateral.

zones of the ventral uvula and nodulus resulted in retrograde labelling of neurons in the lateral half of the mcIO, whereas injections into the rotation zones in the flocculus resulted in retrograde labelling of neurons in the medial half of the mcIO. Furthermore, from injections into the *contraction* zone, retrograde labelling was found caudally in the lateral mcIO, whereas injections into the descent zone resulted in retrograde labelling in the rostral end of the mcIO. Injections into the *expansion* and *ascent* regions resulted in labelling between these areas along the rosto-caudal axis in the lateral mcIO. To ensure that we were in the desired olivary subnuclei, single-unit extracellular recordings were used to confirm the location of the injection sites. To record the activity of optic flow units in the mcIO, glass micropipettes filled with 2 M NaCl, with tip diameters of 4–5 μm, were advanced through the cerebellum and into the brainstem using a hydraulic microdrive (Frederick Haer & Co. Millville, NJ). Extracellular signals were amplified, filtered (10-2000Hz), and a window discriminator was used to isolate complex spikes from simple spikes. Inferior olivary units are easily identified based on their characteristically low firing rate (approximately 1 spike/s) and proximity to the base of the brain. Upon isolation of a unit in the mcIO, the optic flow preference of the unit was qualitatively determined. The direction-selectivity of the olivary neuron was determined by moving a large (90x90°) handheld visual stimulus, consisting of black bars, wavy lines and dots on a white background, in the receptive field of the unit. With such stimuli, *contraction*, *expansion*, *ascent* and *descent* units are qualitatively determined (see Chapter 2; Winship and Wylie, 2001). Once the desired area was

isolated, the recording electrode was replaced with a micropipette (tip diameter 20–30 μm) containing fluorescent BDA: either mini-ruby (red; D-3312) or mini-emerald (green; D-7178; 10,000 molecular weight; Invitrogen, Carlsbad, CA, USA). The tracers (0.01–0.05 μl of 10% solution in 0.1 M phosphate buffer) were pressure injected using a Picospritzer II (General Valve Corporation, Fairfield, NJ). After surgery the craniotomy was filled with bone wax and the wound was sutured. Birds were given an injection of buprenorphine (0.012 mg/kg, i.m.) as an analgesic.

After a recovery period of 3–5 days, the animals were deeply anesthetized with sodium pentobarbital (100 mg/kg) and immediately transcardially perfused with phosphate buffered saline (PBS; 0.9% NaCl, 0.1 M phosphate buffer) followed by 4% paraformaldehyde in 0.1 M PBS (pH 7.4). The brain was extracted from the skull and immersed in paraformaldehyde for 7 days at 4 °C. The brain was then embedded in gelatin and cryoprotected in 30% sucrose in 0.1 M PBS overnight. Using a microtome, frozen serial sections in the coronal plane (40 μm thick) were collected throughout the rostro-caudal extent of the cerebellum.

3.1.2 *Zebrin Immunohistochemistry*

ZII expression was visualized using established immunohistochemical techniques described previously (see Sec. 2.1.2; Pakan et al., 2007). Briefly, tissue sections were rinsed thoroughly in 0.1M PBS and blocked with 10% normal donkey serum (Jackson Immunoresearch Laboratories, West Grove, PA) and 0.4% TritonX-100 in PBS for 1 hour. Tissue was then incubated in PBS

containing 0.1% TritonX-100 and the primary antibody, mouse monoclonal anti-ZII (kindly provided by Richard Hawkes, University of Calgary) for 60-75 hours at room temperature. Sections were then rinsed in PBS and sections were incubated in a fluorescent secondary; either Cy^2 or Cy^3 conjugated donkey anti-mouse antibody (Jackson Immunoresearch Laboratories, West Grove, PA: diluted 1:100 in PBS, 2.5% normal donkey serum, and 0.4% TritonX-100) for 2 hours at room temperature. The tissue was then rinsed in PBS and mounted onto gelatinized slides for viewing.

3.1.3 *Microscopy and Image Analysis*

Sections were viewed with a compound light microscope (Leica DMRE) equipped with the appropriate fluorescence filters (rhodamine and FITC). Images were acquired using a Retiga EXi *FAST* Cooled mono 12-bit camera (Qimaging, Burnaby BC) and analyzed with OPENLAB imaging software (Improvision, Lexington MA). Adobe Photoshop was used to compensate for brightness and contrast.

3.2 Results

3.2.1 *Climbing fibre labelling in the ventral uvula and nodulus*

The results are based on observations in ten animals, where injections of red and/or green fluorescent BDA were made into the mcIO (see Table 3.1). In nine animals, a single injection of red BDA was made in the mcIO: (i) in two of these cases, the injections were aimed at the caudal mcIO (*contraction* region;

cases ZIO2 and ZIO11); (ii) in three of these cases, the injections were aimed at the rostral mcIO (*descent* region; cases ZIO6, ZIO7 and ZIO17); (iii) and in four of these cases, the injections were aimed in the middle of the mcIO (*expansion* and *ascent* region; cases ZIO5, ZIO9, ZIO16, and ZIO19). One animal received two injections: a red injection was aimed into the caudal mcIO and a green injection was aimed into the rostral mcIO (*descent*; case ZIO10). The rostrocaudal extents of the injections as a percentage of the entire mcIO are shown as green bars in Figure 3.4. The sizes of the injections were variable. In some cases the injections were quite discrete, as in ZIO6 where core of the injection covered only 160μm rostrocaudally. In other cases the injections were quite large, as in ZIO9, where the core of the injection covered 480μm rostrocaudally. Fig. 3.2A shows a photomicrograph of a representative injection site from case ZIO16, illustrating a red BDA injection in the middle mcIO (*expansion* and *ascent* region).

The resulting CF labelling from both the red and green BDA was entirely contralateral in all cases, robust, and easily distinguishable in the molecular layer (Fig. 3.2B, C, D, F, G and H). From our injections in the caudal mcIO (*contraction* region) resulting CF labelling was found most medially in both folia IXcd and X. From our injections in the rostral mcIO (*descent* region) we observed CF labelling most laterally in folia IXcd and X (e.g. Fig. 3.3). From our injections in the middle of the mcIO (*expansion* and *ascent* region), the resulting CF labelling in folia IXcd and X was found in lateral to labelling from the caudal mcIO and medial to the labelling from the rostral mcIO.

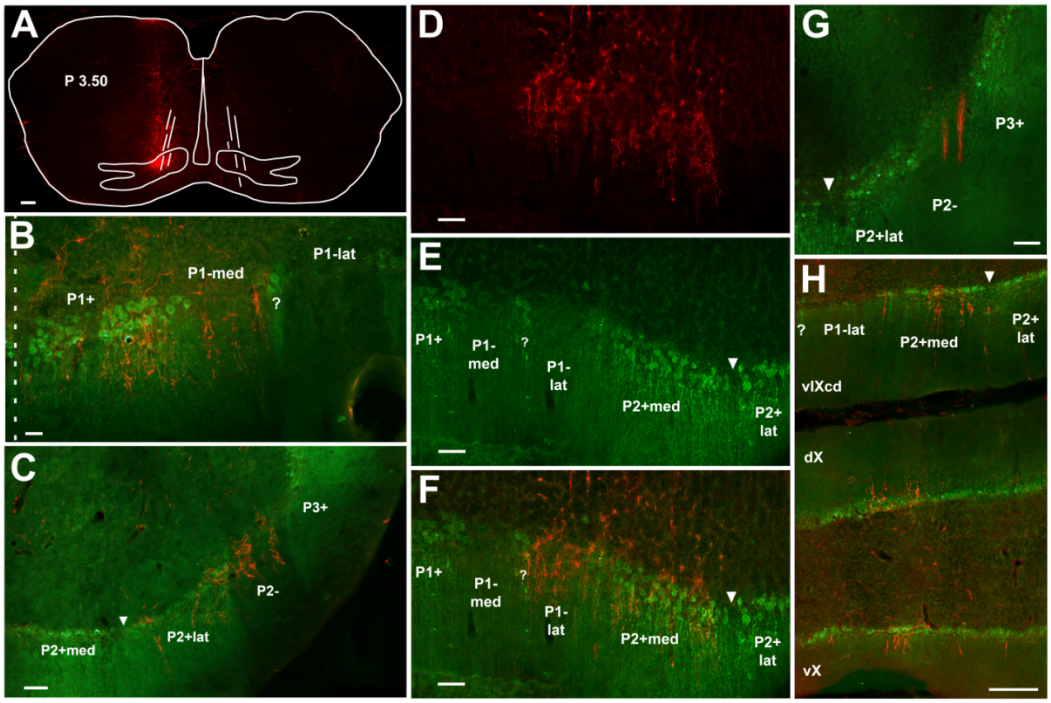

Figure 3.2 Olivary injection site, CF labelling, and ZII immunohistochemistry in medial folium IXcd. A shows a photomicrograph of a coronal section through the brainstem and a red-BDA injection in the middle (*expansion*/*ascent*) region of the mcIO from case ZIO16. P 3.50 refers to the rostrocaudal location of the section in the pigeon atlas of Karten and Hodos (1967). **B-G** show photomicrographs of coronal sections through ventral folium IXcd. The molecular later is represented ventrally, followed by the Purkinje cell layer, and the granule layer dorsally. **B, C** show typical BDA labeled CFs from case ZIO2 (*contraction* region) and ZIO6 (*descent* region), respectively. **D, E, F** Red BDA labeled CFs (D) in ZII zones P1-lat and P2+med (E) from case ZIO5 (*expansion*/*ascent* region). The overlay is shown in (F). **G** shows red BDA labeled CFs on the lateral edge of P2- that do not extend into P3+ from case

ZIO16 (*descent* region). **H** shows red BDA labeled cells in ZII zones P1-lat and P2+med of folium IXcd with subjacent labelling in folium X from case ZIO17 (*expansion*/*ascent* region). Inverted triangle in (E-H) denote ZII immunonegative "notch" separating P2+ into medial and lateral halves. Scale bars: = 200 μm in (A, H); 50 μm in (B); 100 μm in (C, D, E, F, G).

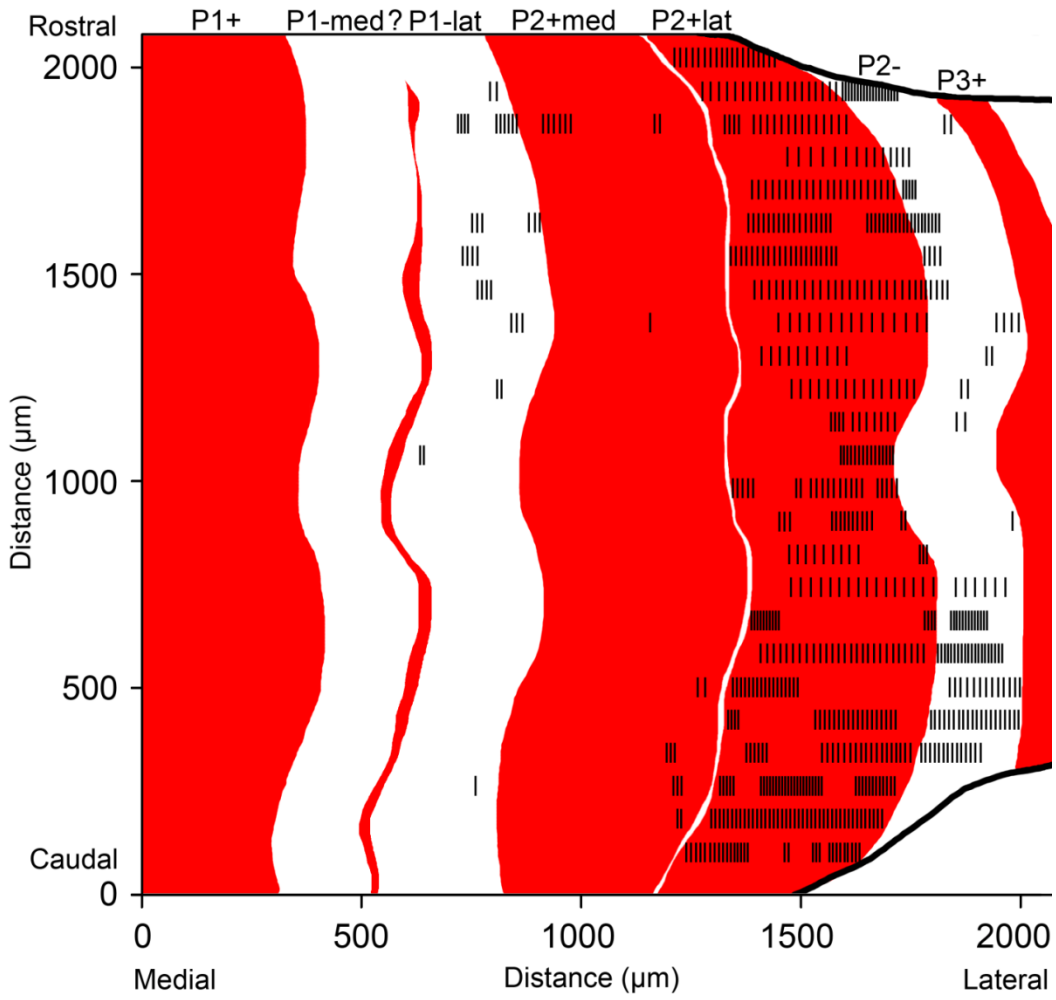

Figure 3.3 A reconstruction of CF projections and ZII expression in medial folium IXcd from case ZIO6. Black lines represent individual CFs labeled in 27 serial coronal sections (40 μm thick and 40 μm apart) throughout the rostrocaudal extent of the ventral folium of the uvula (y-axis). In this case, an injection of red BDA was made in the rostral mcIO (*descent* region). ZII+ zones (in red) are interdigitated by ZII- zones (in white) in the mediolateral plane (x-axis).

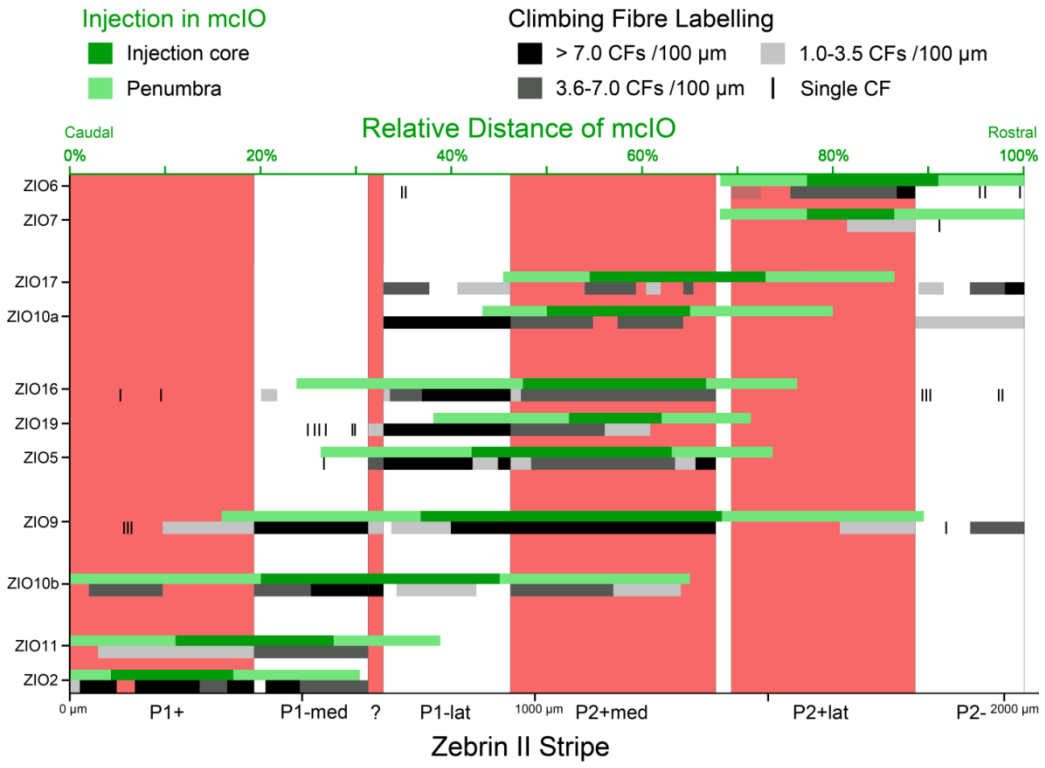

Figure 3.4 Location and extent of the injections sites in the mcIO and the resulting CF labelling in the ventral lamella of medial folium IXcd. Each case is indicated on the y-axis. There are two bar graphs for each case: i) the bottom bar graph represents the location CF labelling in the ZII zones (which are indicated by the bottom x-axis) and the degree of CF labelling (which is indicated by the legend above) from the specified case. The reconstructions of the CF counts from each case were averaged from 5 representative serial sections (40 µm thick and 40 µm apart); ii) the top bar graph represents the location and size of each injection expressed as a proportion of the rostro-caudal extent of the mcIO (which are indicated on the top x-axis, and the legend above). The caudal and rostral borders of mcIO are designated 0% and 100%, respectively. Single

injections of red BDA were made in all cases except for ZIO10, where red BDA was injected more caudally (ZIO10b), and green BDA was injected more rostrally (ZIO10a).

Figures 3.2B-H show representative photomicrographs of ZII expression and CF labelling from red- and green-BDA injections throughout the mcIO. From these injections, along with data from several other cases, there was a clear correspondence with the ZII stripes, which is illustrated in Figures 3.2-3.4. In general, with respect to folium IXcd, (i) injections in the caudal mcIO (*contraction* region) resulted in CF labelling in ZII zones P1+ and P1-med (Figs. 3.2B and 3.4), (ii) injections in the rostral mcIO (*descent* region) resulted in CF labelling in ZII zones P2+lat and P2- (Figs. 3.2C, 3.2G, 3.3, and 3.4), and (iii) injections in the middle mcIO (*expansion* and *ascent* region) resulted in CF labelling in ZII zones P1-lat and P2+med (Figs. 3.2D-F, 3.2H, and 3.4). While many CFs were seen on the very lateral edge of P2- (e.g. Fig. 3.2G), none were observed in ZII zones P3+/- in any of the cases. Labelling in the small immunopositive "?" band in the middle of P1- arose from the injections into the middle mcIO which were closer to the caudal end. Some injections resulted in widespread CF labelling throughout the medial VbC, and some spanned more than one ZII+/- pair. However, these injections tended to be either quite large (e.g. Fig. 3.4; ZIO9, ZIO10b), or the CF labelling in ZII zones outside of the main area of labelling was sparse (e.g. Fig. 3.4; ZIO16, ZIO17). Because there is rostrocaudal overlap of the areas responsive to the different types of translational optic flow in the mcIO (Fig. 3.1A), it is likely that some of the injections spanned more than one electrophysiologically distinct zone in the mcIO.

Our results clearly demonstrate that a CF zone (i.e. a zone that arose from a discrete injection into the caudal, middle or rostral mcIO) spanned a single ZII

stripe including the positive and negative portion. This is illustrated in Figs. 3.2D-F, where a red BDA injection was made in the middle of the mcIO from case ZIO5 (*expansion* and *ascent* region). These photomicrographs show CFs terminating in folium IXcd (Fig. 3.2D), and ZII expression visualized in green (Fig. 3.2E). The overlay of these two photomicrographs shows CF terminals clearly concentrated in P1-lat and P2+med. The presence of CFs in both positive and negative ZII stripes can also be seen in Figures 3.2B, 3.2C, and 3.2H.

Figure 3.3 shows a reconstruction of the pattern of CF labelling in the ventral lamella of folium IXcd as related to the ZII stripes from case ZIO6. 25 serial sections have been combined to illustrate the CF labelling (black marks) from an injection in the rostral mcIO (*descent* region) along with the ZII+ (red) and ZII- (white) stripes. Some CF labelling seen in ZII zones P1-lat and P2+med indicates that not all of the injection was was confined to the *descent* region of the mcIO, however the congruence of the majority of CF labelling with the P2+lat and P2- stripes is evident.

Figure 3.4 shows a diagram representing the injection location and size in the mcIO, and the resulting CF labelling from 5 representative serial sections in the ZII zones P1+ to P2- from each case. The rostrocaudal extents of the injections expressed as a percentage of the entire mcIO (upper x-axis) are shown as dark green (injection core) and light green (injection penumbra) bars. The CF labelling is shown as black, dark gray or light gray bars, or black dashes in relation to the ZII+ (red) and ZII- (white) stripes in which the labelling was found. While there is some overlap of CF labelling in cases with injections in

different areas of the mcIO, again, the correspondence of CF labelling and ZII expression is evident: (i) injections into the caudal mcIO (*contraction* region) resulted in CF labelling primarily in P1+ and P1-med, (ii) injections into the middle mcIO (*expansion* and *ascent* region) resulted in CF labelling primarily in P1-lat and P2+ med, and (iii) injections into the rostral mcIO (*descent* region) resulted in CF labelling primarily in P2+lat and P2-.

3.3 Discussion

3.3.1 ***Climbing fibre zones, functional zones and ZII stripes in Pigeons***

Along with Chapter 2, in this study, by injecting anterograde tracers into the mcIO and comparing the resulting olivocerebellar CF labelling with ZII expression in the ventral uvula, we showed a clear relationship between anatomical inputs, functional zones and biochemical expression in the medial VbC. As with the zones defined by PC CSA, we have shown that there is a clear relationship between CF zones and ZII stripes in folium IXcd in pigeons. Injections of anterograde tracer into: (i) the caudal mcIO resulted in CFs in P1+ and P1-med, (ii) the middle mcIO resulted in CFs in P1-lat and P2+med, and (iii) the rostral mcIO resulted in CFs in P2+lat and P2-. These results parallel findings in the pigeon flocculus by Pakan and Wylie (2008), where they showed that CFs from the *rVA* and *rHA* regions of the medial mcIO each span a ZII+/- stripe. Consistent with this pattern, Chapter 2 and a study by Pakan et al. (2011) showed that the CSA of PCs responsiveness to particular types of optic flow was also

confined to a ZII+/- pair. Figure 3.5 offers a summary schematic of CF and mossy fibre inputs to the VbC and their relationship to ZII stripes. While the concordance between the ZII stripes and the CF zones can be seen in folium IXcd, it cannot be seen in folium X as it is uniformly ZII+ (Fig. 3.2H and 3.5; Pakan et al., 2007). However, the CF zones obviously continue through IXcd and X (e.g. Fig. 3.2H).

It is possible that the CF zones in X are related to some other molecular marker that shows a parasagittal expression in this folium. For example, in the mouse cerebellum, heatshock protein-25 (Hsp 25) is expressed as parasagittal bands of high and low immunoreactivity in the nodulus and flocculus (Armstrong et al., 2000), areas which are homogenously ZII+. While the equivalent to Hsp 25 in rats (Hsp 27) was not detected in the adult rat cerebellum (Wilkinson and Pollard, 1993; Plumier et al., 1997), it remains to be seen whether Hsp 25 is expressed as stripes in the pigeon cerebellum.

3.3.2 Functional differences between climbing fibres projecting to ZII+ and ZII- stripes in mammals

Taken together, Chapter 3 and the study by Pakan et al. (2008) are the first demonstration that a CF zone corresponds to a ZII+/- pair, and conflict with studies of the correspondence of CF afferents and ZII stripes in mammals. Studies in mammals have emphasized that an olivary subnucleus projects to either a ZII+ or ZII- stripe, but never both (Gravel et al., 1987; Sugihara and Shinoda, 2004; Apps and Garwicz, 2005; Pijpers et al., 2006; Sugihara and Quy, 2007). For example, Pijpers et al. (2006) correlated ZII stripes with the pattern of CF

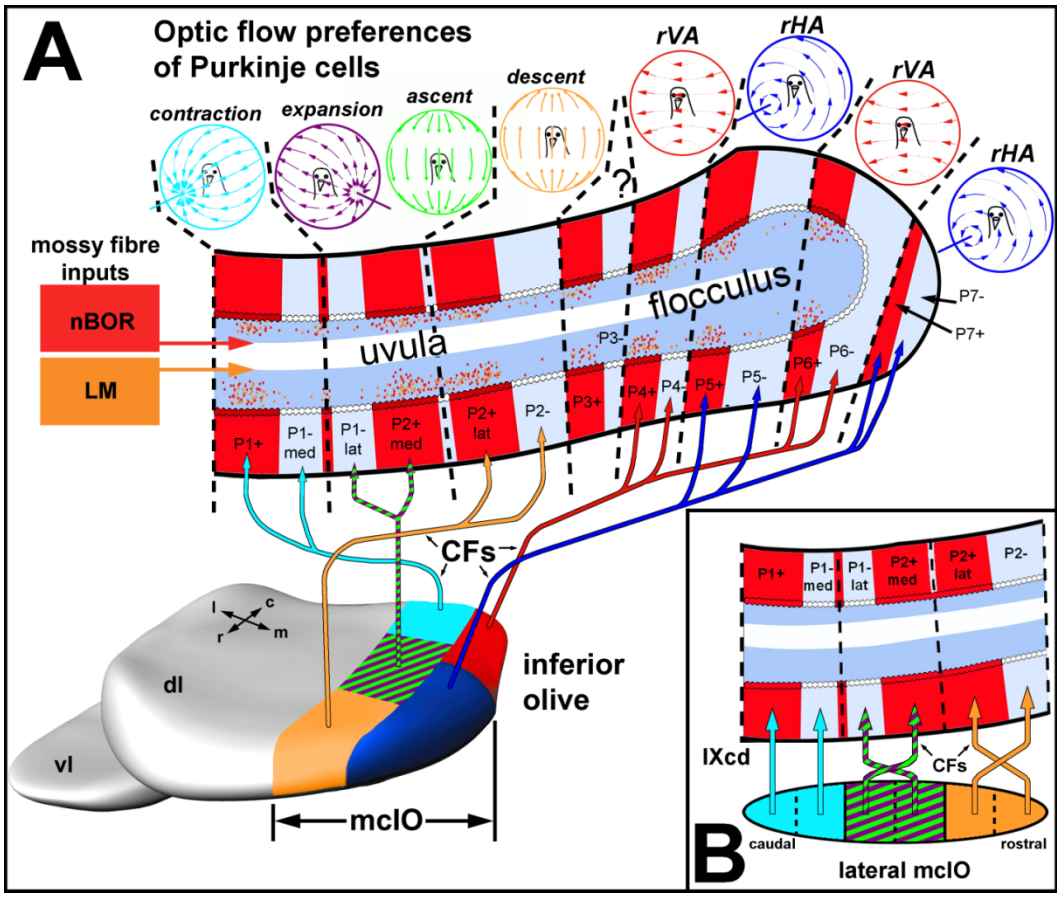

Figure 3.5 Organization of the pigeon vestibulocerebellum: correlating physiology, anatomy, and intrinsic immunochemistry. A shows the organization of the zones containing cells responsive to translational optic flow (*contraction*, *expansion*, *ascent* and *descent*) and rotational optic flow (*rVA* and *rHA*) in relation to mossy fibre (MF) and climbing fibre (CF) inputs and the expression pattern of zebrin II (ZII) in folium IXcd. ZII-positive Purkinje cells (PCs) are represented as red, whereas ZII-negative PCs are white and specific zones are indicated from P1+ to P7-. The visual optic flow preferences of each zone are separated by black dashed lines. Visual inputs to these zones originate in both the nucleus of the basal optic root (nBOR) and pretectal nucleus lentiformis

mesencephali (LM). This optic flow information reaches folium IXcd as CF inputs from the medial column of the inferior olive (mcIO). The lateral portion of the mcIO contains a *contraction* region (light blue), an *expansion*/*ascent* region (green and purple stripes) and a *descent* region (orange), whereas the medial portion contains an *rVA* region (red) and an *rHA* region (dark blue). All areas of the mcIO project to IXcd *via* CFs as indicated by the arrows. nBOR and LM also project directly to IXcd as MFs, which terminate primarily adjacent to ZII+ stripes (orange and yellow dots in the granular layer). **B** shows the hypothesized caudal-to-rostral projections of the translational optic flow neurons in the lateral mcIO to the ZII+ and ZII- zones in the ventral uvula. C, R, M, and L = caudal, rostral, medial and lateral. dl and vl = dorsal lamella and ventral lamella of the inferior olive.

collateral terminations from small retrograde tracer injections in the cerebellar cortex of rats. They found that the terminals of CF collaterals had the same ZII signature as that of the injection site (*i.e.* CF collaterals were in a ZII+ zone if the injection site was in a ZII+ zone). Voogd et al. (2003) compared the distribution of olivocerebellar projections to the copula pyramidis and the paramedian lobule with ZII expression patterns in the rat. They showed that, generally, CFs originating from the rostral dorsal accessory olive innervate the ZII- stripes of the C1 and C3 zones, and that the rostral medial accessory olive and principal olive innervate, respectively, the ZII+ stripes of the C2 and D zones. Voogd and Ruigrok (2004) examined the CF projections to the vermis of the cerebellum in relation to ZII stripes in rats. They showed that localized injections of anterograde tracer in various olivary subnuclei resulted in sagittal CF bands which were confined to either a positive or a negative ZII stripe, but not both. In a comprehensive study of the entire rat cerebellum, Sugihara and Shinoda (2004) injected small amounts of BDA into various areas within the IO and compared the resulting CF labelling with ZII expression. They found that CFs from the principal olive and areas near to it, as well as CFs from several medial subnuclei project to ZII+ zones, while CFs from the centrocaudal portion of the medial accessory olive project to ZII- stripes in the vermis. They also found that the dorsal accessory olive and neighboring regions innervate ZII- and lightly ZII+ stripes in the hemisphere, and the rostral and caudal pars intermedia. That all these studies stress that subnuclei in the inferior olive (IO) innervate either ZII+

or ZII- stripes, but not both, would suggest that ZII+ and ZII- stripes are functionally different.

The efferent projection of a particular region of the IO to either a ZII+ or a ZII- stripe in the cerebellum was not found in the present study. Conversely, in pigeons, a region of the mcIO corresponds to a particular ZII+/- stripe pair. Whether this type of relationship between CFs and ZII expression pattern observed in the VbC is unique to the pigeon remains to be seen. Different olivocerebellar systems might show an alternate correlation between ZII stripes and CF zones. In fact, the current study has revealed a dissimilar relationships betwen ZII expression and CFs in folium IXcd and X. Folium IXcd has alternating ZII+ and ZII- stripes while folium X is uniformly ZII+, however the CF zones in these folia are identical. Futhermore, the results of the present study also suggest that a given optic flow region in the lateral mcIO might in fact be separated into two areas: one that projects to a ZII+ stripe and another that projects to a ZII- stripe. Specifically, (i) within the *contraction* zone of the mcIO more caudal injections led to more CF labelling in P1+, while more rostral injections produced more labelling in P1-med; (i) within the *expansion* and *descent* zone of the mcIO, more caudal injections led to more labelling in P2+med, whereas more rostral injections led to more labelling in P1-lat; and (iii) within the *descent* zone of the mcIO, more caudal injections led to more labelling in P2-, whereas more rostal injections led to more labelling in P2+lat (see Fig. 3.3). A diagram of these proposed sub-regions within the lateral mcIO projecting to either ZII+ or ZII- stripes is shown in Figure 3.5B.

While Chapter 3 of this thesis combined with a study by Pakan and Wylie (2008) describe the first know relationship between CFs and ZII across an entire folium, the story of ZII stripes and function in the pigeon VbC is far from complete. It remains unclear whether ZII+ and ZII- zones of each of the optokinetic zones have different roles in oculomotor function. This is plausible as ZII+ and ZII- cells may differ with respect to plasticity and excitability (Welsh et al., 2002; Wadiche and Jahr, 2005). In our laboratory, research over the past two decades has focused on CSA in response to optokinetic stimulation in PCs and olivary cells that provide CF input to the VbC (e.g. Wylie et al., 1993, 1998; Wylie and Frost, 1991; 1993; Winship and Wylie, 2001), but we have not tested whether these cells in these areas respond to vestibular stimulation, as is the case in the rabbit uvula/nodulus (Shojaku et al., 1991) and flocculus (Simpson et al., 2002). It remains to be seen if either ZII+ or ZII- stripes (or both) also receive vestibular CF information. As results from this Chapter have shown, P3+/- receives no optokinetic CF input from the mcIO, but it is possible that vestibular CFs project to these ZII stripes. As a primary vestibular input has not been seen in the mcIO of pigeons (Schwarz and Schwarz, 1986; Dickman, 1996; Dickman and Fang, 1996), secondary vestibular projections would likely provide this input.

3.3.3 ***Possible functional roles of ZII+ and ZII- stripes in the cerebellum***

Recently, studies have aimed to understand ZII stripes in relation to functional zones in the cerebellum. Sugihara et al. (2004) suggested that ZII+ and ZII- bands have different functional roles because IO subnuclei project to either

ZII+ or ZII- bands and these subnuclei of the IO receive input from particular sensory systems. More specifically, Sugihara et al. (2004) postulated that the ZII- stripes receive input from CFs conveying somatosensory information whereas ZII+ stripes receive input from CFs conveying information from visual, auditory and other sensory systems (see Voogd et al., 2003; Voogd and Ruigrok, 2004; Sugihara and Quy, 2007; Sugihara and Shinoda, 2007). Voogd et al. (1996) provided evidence in support of this hypothesis in showing that the ventral lateral outgrowth, which processes visual-optokinetic information, projects to ZII+ stripes in lobule X and ventral IXcd, while somatosensory olivary subnuclei project to thin ZII- bands in the dorsal margin of IXcd. However, this theory does not pertain to olivocerebellar afferents to the pigeon, VbC as the CF inputs convey only visual information. There are even several challenges to this hypothesis in mammals. For example, the group beta and the dorsomedial cell column carries vestibular information to ZII+ stripes in lobules VIII–X, but the subnucleus B of the caudal medial accessory olive also carries vestibular information to a ZII- stripe in the lateral A subzone of the anterior vermis (Gerrits et al., 1985; Voogd and Ruigrok, 2004; Voogd and Barmack, 2006). Furthermore, nuclei at the midline of the mesodiencephalic junction provide the majority of the CFs to ZII+ stripes and relay information from motor structures (including the red nucleus and accessory oculomotor nuclei; Swenson and Castro, 1983; Onodera, 1984; Holstege and Tan, 1988; de Zeeuw et al., 1989). The subnucleus a, which receives input from the spinal cord, also projects to ZII+ stripes (Matsushita et al., 1991).

The present Chapter, along with the study by Pakan and Wylie (2008), shows a direct relationship between several functional CF zones with clearly defined response properties, and the ZII expression pattern across IXcd. The coordination of CF inputs and a molecular marker throughout an entire folium has not been described in other cerebellar systems in any species (see Chockkan and Hawkes, 1994; Hallem et al., 1999). Nevertheless, a few recent papers have investigated a link between other aspects of cerebellar physiology and ZII stripes, and found functional differences between ZII+ and ZII- stripes (see Discussion, Chapter 2).

Although PCs in the flocculus are uniformly ZII+ in most mammals (e.g., Ozol et al., 1999; Sanchez et al., 2002; Sillitoe and Hawkes, 2002; Marzban et al., 2003), Fujita et al. (2010) recently revealed that the flocculus in marmosets (*Callithrix jacchus*) contains 4 alternating ZII+/- stripe pairs, as in pigeons. It remains to be seen whether the *rVA* and *rHA* CF zones in the marmoset each span a ZII+/- pair. As discussed in Chapter 2, Schonewille et al. (2006) found that physiologically defined zones in the mouse flocculus were organized very differently in relation to heat shock protein 25 (Hsp25) stripes from what Pakan et al. (2011) showed using ZII as a molecular marker. Specifically, an Hsp25 positive stripe comprised zones 1 (*rH45*) and 2 (*rVA*), while an Hsp25 negative stripe comprised zones 3 (*rH45*) and 4 (*rVA*). It remains to be seen whether the pattern of Hsp25 expression and physiological zones in the pigeon flocculus is similar to what Schonewille et al. (2006) have found.

Clearly, the relationship between various molecular markers and the physiological zones in the cerebellum is complex. While the specific function of ZII in the cerebellum has eluded researchers (see Welsh et al., 2002), further studies on the relationship between the unique parasagittal expression of ZII and other areas of cerebellar organization, such as anatomy and physiology, will further our understanding of the fundamental organization of the cerebellar cortex.

Table 3.1 Summary of the Injections in the medial column of the Inferior Olive

Case	mcIO region injected	Tracer Injected	Rostral-caudal location of centre of injection site*
ZIO2	*Contraction*	Red BDA	200 µm
ZIO5	*Expansion*	Red BDA	800 µm
ZIO6	*Descent*	Red BDA	1480 µm
ZIO7	*Descent*	Red BDA	1440 µm
ZIO9	*Expansion*	Red BDA	800 µm
ZIO10	*Expansion* *Contraction*	Green BDA Red BDA	920 µm 480 µm
ZI011	*Contraction*	Red BDA	280 µm
ZIO16	*Ascent*	Red BDA	880 µm
ZIO17	*Expansion*	Red BDA	1120 µm
ZIO19	*Ascent*	Red BDA	960 µm

*Distance from the caudal pole of the inferior olive

3.4 References

Ahn AH, Dziennis S, Hawkes R, Herrup K. 1994. The cloning of zebrin II reveals its identity with aldolase C. Development 120(8):2081-2090.

Apps R, Garwicz M. 2005. Anatomical and physiological foundations of cerebellar information processing. Nat Rev Neurosci 6(4):297-311.

Arends J, Voogd J. 1989. Topographic aspects of the olivocerebellar system in the pigeon. Exp Brain Res, Series 17:52-57.

Armstrong CL, Hawkes R. 2000. Pattern formation in the cerebellar cortex. Biochem Cell Biol 78(5):551-562.

Brecha N, Karten HJ, Hunt SP. 1980. Projections of the nucleus of the basal optic root in the pigeon: an autoradiographic and horseradish peroxidase study. J Comp Neurol 189(4):615-670.

Brochu G, Maler L, Hawkes R. 1990. Zebrin II: a polypeptide antigen expressed selectively by Purkinje cells reveals compartments in rat and fish cerebellum. J Comp Neurol 291(4):538-552.

Chockkan V, Hawkes R. 1994. Functional and antigenic maps in the rat cerebellum: zebrin compartmentation and vibrissal receptive fields in lobule IXa. J Comp Neurol 345(1):33-45.

Clarke PG. 1977. Some visual and other connections to the cerebellum of the pigeon. J Comp Neurol 174(3):535-552.

Crowder NA, Winship IR, Wylie DR. 2000. Topographic organization of inferior olive cells projecting to translational zones in the vestibulocerebellum of pigeons. J Comp Neurol 419(1):87-95.

De Zeeuw CI, Holstege JC, Ruigrok TJ, Voogd J. 1989. Ultrastructural study of the GABAergic, cerebellar, and mesodiencephalic innervation of the cat medial accessory olive: anterograde tracing combined with immunocytochemistry. J Comp Neurol 284(1):12-35.

De Zeeuw CI, Wylie DR, DiGiorgi PL, Simpson JI. 1994. Projections of individual Purkinje cells of identified zones in the flocculus to the vestibular and cerebellar nuclei in the rabbit. J Comp Neurol 349(3):428-447.

Dickman JD. 1996. Vestibular afferent projections to the brain stem in pigeons. Ann N Y Acad Sci 781:611-613.

Dickman JD, Fang Q. 1996. Differential central projections of vestibular afferents in pigeons. J Comp Neurol 367(1):110-131.

Fujita H, Oh-Nishi A, Obayashi S, Sugihara I. 2010. Organization of the marmoset cerebellum in three-dimensional space: Lobulation, aldolase C compartmentalization and axonal projection. J Comp Neurol 518(10):1764–1791.

Gamlin PD, Cohen DH. 1988. Projections of the retinorecipient pretectal nuclei in the pigeon (Columba livia). J Comp Neurol 269(1):18-46.

Gerrits NM, Voogd J, Magras IN. 1985. Vestibular afferents of the inferior olive and the vestibulo-olivo-cerebellar climbing fibre pathway to the flocculus in the cat. Brain Res 332(2):325-336.

Gravel C, Eisenman LM, Sasseville R, Hawkes R. 1987. Parasagittal organization of the rat cerebellar cortex: direct correlation between antigenic Purkinje cell bands revealed by mabQ113 and the organization of the olivocerebellar projection. J Comp Neurol 265(2):294-310.

Hallem JS, Thompson JH, Gundappa-Sulur G, Hawkes R, Bjaalie JG, Bower JM. 1999. Spatial correspondence between tactile projection patterns and the distribution of the antigenic Purkinje cell markers anti-zebrin I and anti-zebrin II in the cerebellar folium crus IIA of the rat. Neuroscience 93(3):1083-1094.

Hawkes R. 1992. Antigenic markers of cerebellar modules in the adult mouse. Biochem Soc Trans 20(2):391-395.

Hawkes R, Blyth S, Chockkan V, Tano D, Ji Z, Mascher C. 1993. Structural and molecular compartmentation in the cerebellum. Can J Neurol Sci 20 Suppl 3:S29-35.

Hawkes R, Herrup K. 1995. Aldolase C/zebrin II and the regionalization of the cerebellum. J Mol Neurosci 6(3):147-158.

Herrup K, Kuemerle B. 1997. The compartmentalization of the cerebellum. Annu Rev Neurosci 20:61-90.

Holstege G, Tan J. 1988. Projections from the red nucleus and surrounding areas to the brainstem and spinal cord in the cat. An HRP and autoradiographical tracing study. Behav Brain Res 28(1-2):33-57.

Iwaniuk AN, Marzban H, Pakan JM, Watanabe M, Hawkes R, Wylie DR. 2009. Compartmentation of the cerebellar cortex of hummingbirds (Aves: Trochilidae) revealed by the expression of zebrin II and phospholipase C beta 4. J Chem Neuroanat 37(1):55-63.

Karten H, Hodos W. 1967. A stereotaxic Atlas of the Brain of the Pigeon (Columba livia). Baltimore: Johns Hopkins Press.

Lau KL, Glover RG, Linkenhoker B, Wylie DR. 1998. Topographical organization of inferior olive cells projecting to translation and rotation zones in the vestibulocerebellum of pigeons. Neuroscience 85(2):605-614.

Llinas R, Sasaki K. 1989. The Functional Organization of the Olivo-Cerebellar System as Examined by Multiple Purkinje Cell Recordings. Eur J Neurosci 1(6):587-602.

Marzban H, Hawkes R. 2010. On the Architecture of the Posterior Zone of the Cerebellum. Cerebellum. Accepted for publication Sept 14 2010.

Marzban H, Zahedi S, Sanchez M, Hawkes R. 2003. Antigenic compartmentation of the cerebellar cortex in the syrian hamster Mesocricetus auratus. Brain Res 974(1-2):176-183.

Matsushita M, Ragnarson B, Grant G. 1991. Topographic relationship between sagittal Purkinje cell bands revealed by a monoclonal antibody to zebrin I

and spinocerebellar projections arising from the central cervical nucleus in the rat. Exp Brain Res 84(1):133-141.

Onodera S. 1984. Olivary projections from the mesodiencephalic structures in the cat studied by means of axonal transport of horseradish peroxidase and tritiated amino acids. J Comp Neurol 227(1):37-49.

Ozol K, Hayden JM, Oberdick J, Hawkes R. 1999. Transverse zones in the vermis of the mouse cerebellum. J Comp Neurol 412(1):95-111.

Pakan JM, Graham DJ, Gutiérrez-Ibáñez C, Wylie DR. 2011. Organization of the cerebellum: Correlating zebrin immunochemistry with optic flow zones in the pigeon flocculus. Vis Neurosci 28(2):163-174.

Pakan JM, Iwaniuk AN, Wylie DR, Hawkes R, Marzban H. 2007. Purkinje cell compartmentation as revealed by zebrin II expression in the cerebellar cortex of pigeons (Columba livia). J Comp Neurol 501(4):619–630.

Pakan JM, Todd KG, Nguyen AP, Winship IR, Hurd PL, Jantzie LL, Wylie DR. 2005. Inferior olivary neurons innervate multiple zones of the flocculus in pigeons (Columba livia). J Comp Neurol 486(2):159-168.

Pakan JM, Wylie DR. 2008. Congruence of zebrin II expression and functional zones defined by climbing fiber topography in the flocculus. Neurosci 157(1):57–69.

Pijpers A, Apps R, Pardoe J, Voogd J, Ruigrok TJ. 2006. Precise spatial relationships between mossy fibres and climbing fibres in rat cerebellar cortical zones. J Neurosci 26(46):12067-12080.

Plumier JC, Hopkins DA, Robertson HA, Currie RW. 1997. Constitutive expression of the 27-kDa heat shock protein (Hsp27) in sensory and motor neurons of the rat nervous system. J Comp Neurol 384(3):409-428.

Ruigrok TJ. 2003. Collateralization of climbing and mossy fibres projecting to the nodulus and flocculus of the rat cerebellum. J Comp Neurol 466(2):278-298.

Sanchez M, Sillitoe RV, Attwell PJ, Ivarsson M, Rahman S, Yeo CH, Hawkes R. 2002. Compartmentation of the rabbit cerebellar cortex. J Comp Neurol 444(2):159-173.

Schonewille M, Luo C, Ruigrok TJ, Voogd J, Schmolesky MT, Rutteman M, Hoebeek FE, De Jeu MT, De Zeeuw CI. 2006. Zonal organization of the mouse flocculus: physiology, input, and output. J Comp Neurol 497(4):670-682.

Schwarz DW, Schwarz IE. 1986. Projection of afferents from individual vestibular sense organs to the vestibular nuclei in the pigeon. Acta Otolaryngol 102(5-6):463-473.

Shojaku H, Barmack NH, Mizukoshi K. 1991. Influence of vestibular and visual climbing fibre signals on Purkinje cell discharge in the cerebellar nodulus of the rabbit. Acta Otolaryngol Suppl 481:242-246.

Sillitoe RV, Hawkes R. 2002. Whole-mount immunohistochemistry: a high-throughput screen for patterning defects in the mouse cerebellum. J Histochem Cytochem 50(2):235-244.

Simpson JI, Belton T, Suh M, Winkelman B. 2002. Complex spike activity in the flocculus signals more than the eye can see. Ann N Y Acad Sci 978:232-236.

Sugihara I, Ebata S, Shinoda Y. 2004. Functional compartmentalization in the flocculus and the ventral dentate and dorsal group y nuclei: an analysis of single olivocerebellar axonal morphology. J Comp Neurol 470(2):113-133.

Sugihara I, Marshall SP, Lang EJ. 2007. Relationship of complex spike synchrony bands and climbing fibre projection determined by reference to aldolase C compartments in crus IIa of the rat cerebellar cortex. J Comp Neurol 501(1):13-29.

Sugihara I, Quy PN. 2007. Identification of aldolase C compartments in the mouse cerebellar cortex by olivocerebellar labelling. J Comp Neurol 500(6):1076-1092.

Sugihara I, Shinoda Y. 2004. Molecular, topographic, and functional organization of the cerebellar cortex: a study with combined aldolase C and olivocerebellar labelling. J Neurosci 24(40):8771-8785.

Sugihara I, Shinoda Y. 2007. Molecular, topographic, and functional organization of the cerebellar nuclei: analysis by three-dimensional mapping of the olivonuclear projection and aldolase C labelling. J Neurosci 27(36):9696-9710.

Swenson RS, Castro AJ. 1983. The afferent connections of the inferior olivary complex in rats. An anterograde study using autoradiographic and axonal degeneration techniques. Neuroscience 8(2):259-275.

Voogd J, Barmack NH. 2006. Oculomotor cerebellum. Prog Brain Res 151:231-268.

Voogd J, Bigaré F. 1980. Topographical distribution of olivary and cortico nuclear fibres in the cerebellum: a review. Courville J, de Montigny C, Lamarre Y, editors. New York: Raven. 207-234 p.

Voogd J, Gerrits NM, Ruigrok TJ. 1996. Organization of the vestibulocerebellum. Ann N Y Acad Sci 781:553-579.

Voogd J, Glickstein M. 1998. The anatomy of the cerebellum. Trends Neurosci 21(9):370-375.

Voogd J, Pardoe J, Ruigrok TJ, Apps R. 2003. The distribution of climbing and mossy fibre collateral branches from the copula pyramidis and the paramedian lobule: congruence of climbing fibre cortical zones and the pattern of zebrin banding within the rat cerebellum. J Neurosci 23(11):4645-4656.

Voogd J, Ruigrok TJ. 2004. The organization of the corticonuclear and olivocerebellar climbing fibre projections to the rat cerebellar vermis: the congruence of projection zones and the zebrin pattern. J Neurocytol 33(1):5-21.

Wadiche JI, Jahr CE. 2005. Patterned expression of Purkinje cell glutamate transporters controls synaptic plasticity. Nat Neurosci 8(10):1329-1334.

Welsh JP, Yuen G, Placantonakis DG, Vu TQ, Haiss F, O'Hearn E, Molliver ME, Aicher SA. 2002. Why do Purkinje cells die so easily after global brain ischemia? Aldolase C, EAAT4, and the cerebellar contribution to posthypoxic myoclonus. Adv Neurol 89:331-359.

Wilkinson JM, Pollard I. 1993. Immunohistochemical localisation of the 25 kDa heat shock protein in unstressed rats: possible functional implications. Anat Rec 237(4):453-457.

Winship IR, Wylie DR. 2001. Responses of neurons in the medial column of the inferior olive in pigeons to translational and rotational optic flowfields. Exp Brain Res 141(1):63-78.

Winship IR, Wylie DR. 2003. Zonal organization of the vestibulocerebellum in pigeons (Columba livia): I. Climbing fibre input to the flocculus. J Comp Neurol 456(2):127-139.

Wu HS, Sugihara I, Shinoda Y. 1999. Projection patterns of single mossy fibres originating from the lateral reticular nucleus in the rat cerebellar cortex and nuclei. J Comp Neurol 411(1):97-118.

Wylie DR. 2001. Projections from the nucleus of the basal optic root and nucleus lentiformis mesencephali to the inferior olive in pigeons (Columba livia). J Comp Neurol 429(3):502-513.

Wylie DR, Bischof WF, Frost BJ. 1998. Common reference frame for neural coding of translational and rotational optic flow. Nature 392(6673):278-282.

Wylie DR, Frost BJ. 1991. Purkinje cells in the vestibulocerebellum of the pigeon respond best to either translational or rotational wholefield visual motion. Exp Brain Res 86(1):229-232.

Wylie DR, Frost BJ. 1993. Responses of pigeon vestibulocerebellar neurons to optokinetic stimulation. II. The 3-dimensional reference frame of rotation neurons in the flocculus. J Neurophysiol 70(6):2647-2659.

Wylie DR, Frost BJ. 1999a. Complex spike activity of Purkinje cells in the ventral uvula and nodulus of pigeons in response to translational optic flow. J Neurophysiol 81(1):256-266.

Wylie DR, Kripalani T, Frost BJ. 1993. Responses of pigeon vestibulocerebellar neurons to optokinetic stimulation. I. Functional organization of neurons discriminating between translational and rotational visual flow. J Neurophysiol 70(6):2632-2646.

Wylie DR, Linkenhoker B, Lau KL. 1997. Projections of the nucleus of the basal optic root in pigeons (Columba livia) revealed with biotinylated dextran amine. J Comp Neurol 384(4):517-536.

Wylie DR, Winship IR, Glover RG. 1999. Projections from the medial column of the inferior olive to different classes of rotation-sensitive Purkinje cells in the flocculus of pigeons. Neurosci Lett 268(2):97-100.

Chapter 4: **Summary and Future Directions**

The fundamental architecture of the cerebellum is the sagittal zone, and this organization can be seen in afferent projections to the cerbellar cortex and Purkinje cell response properties (Llinas and Sasaki, 1989; De Zeeuw et al., 1994; Voogd and Glickstein, 1998; Wu et al., 1999; Ruigrok, 2003; Apps and Garwicz, 2005), as well as expression patterns of several biochemical markers (for review, see Herrup & Kuemerle, 1997). Thoroughly characterizing the relationship between the anatomy, physiology and biochemical composition of the cerebellum will provide insight into how this poorly understood brain region processes massive amounts of sensory information from several sensory systems.

4.1 Summary of Chapters

This thesis contained two studies that investigated the relationship between the molecular, anatomical and physiological organization of the pigeon vestibulocerebellum (VbC).

In Chapter 2, electrophysiological and immunohistochemical techniques were used to investigate the organization Purkinje cells responsive to different types of translational optic flow and its relationship to the molecular marker zebrin II (ZII) in the medial VbC (uvula/nodulus). Previous studies have shown that Purkinje cells express ZII (Hawkes et al., 1988; Brochu et al., 1990; Dore et al., 1990; Leclerc et al., 1990; Lannoo et al., 1991a,b; 1992; Hawkes, 1992; Meek

et al., 1992; Ahn et al., 1994; Hawkes and Herrup, 1995; Sanchez et al., 2002; Marzban et al., 2003; Sillitoe et al., 2003; 2005). The pattern of ZII expression in the cerebellum is evolutionarily conserved, with seven alternating immunopositive (ZII+) and immunonegative (ZII-) stripes designated P1+/- medially to P7+/- laterally (for review see Hawkes and Herrup, 1995; Marzban and Hawkes, 2010). Previous research has shown that the cells in the uvula/nodulus respond to four patterns of optic flow resulting from self-translation: *contraction*, *expansion*, *ascent*, and *descent* cells (Wylie and Frost, 1991; 1993; Wylie et al., 1998). These cells are topographically organized into parasagittal zones (Wylie and Frost, 1999; Wylie et al., 2003). To investigate the relationship between these physiologically distinct zones and the ZII stripes, we made single unit recordings of Purkinje cell complex spike activity in response to optic flow stimuli, injected small amounts of fluorescent tracer to mark our recording sites, then cut the brain and immunoprocessed it for ZII in order to localize the recording sites to a particular ZII zone. We found a clear relationship between the optic flow preferences of Purkinje cells and ZII labelling: (i) recordings from *contraction* cells were localized to ZII bands P1+ and P1-med; (ii) recordings from *expansion* and *ascent* cells were localized to ZII bands P1-lat and P2+med; and (iii) recordings from *descent* cells were localized to ZII bands P2+lat and P2-. Thus, this study demonstrated that a ZII+/- stripe pair comprises a functional zone in the VbC. This finding was also seen in a study comparing ZII bands to rotational optic flow zones in the pigeon flocculus (Pakan et al., 2011).

In Chapter 3, we investigated the organization of the olivocerebellar climbing fibre inputs to the uvula/nodulus, and examined the relationship of these projections to the ZII expression pattern. Previous research has shown that visual climbing fibre afferents projecting to the uvula/nodulus arise from the lateral mcIO (Lau et al., 1998; Crowder et al., 2000). Pakan and Wylie (2008) made localized injections of anterograde tracer into the caudal and rostral regions of the medial mcIO, as these areas are responsive to *rVA* and *rHA* optic flow, respectively. The results from that study showed that injections into the *rVA* region of the mcIO resulted in CF labelling in P4+/- and P6+/-, and that injections into the *rHA* region of the mcIO resulted in CF labelling in P5+/- and P7+/-. To investigate the relationship between climbing fibre zones responsive to translational optic flow and ZII stripes, we made small injections of a fluorescent anterograde tracer into different areas of the lateral mcIO after determining the optic flow preference of cells in that region, and visualized ZII expression in the VbC. We found a strict concordance between climbing fibre organization and ZII labelling: (i) the most caudal injections into the lateral mcIO resulted in climbing fibres in ZII zones P1+ and P1-med; (ii) injections into the middle portion of the lateral mcIO resulted in climbing fibres in ZII zones P1-lat and P2+med; and (iii) the most rostral injections into the lateral mcIO resulted in climbing fibres in ZII zones P2+lat and P2-. Thus, as in the flocculus, a climbing fibre zone responsive to a particular type of optic flow in the uvula/nodulus spans a ZII+/- pair. this finding was one of the first studies in any species to correlate the biochemical, anatomical and functional organization in a cerebellar system.

The results from the Chapters in this thesis, taken together with the studies of Pakan and Wylie (2008) and Pakan et al. (2011), constitute the first demonstration relating functional and anatomical zones to the ZII expression pattern across an entire cerebellar folium in any species.

4.2 Future Directions

Several interesting questions arise as a result of the work presented in this thesis. Though a functional zone in the pigeon medial VbC was found to span a ZII+/- pair in Chapter 2, it remains to be seen if there are any functional differences between a ZII+ and ZII- responsive to the same type of optic flow. Studies in mammals suggest that ZII+ and ZII- Purkinje cells are functionally different. For example, Sugihara et al. (2007) measured the complex spike activity in Purkinje cells of the rat cerebellum and found that synchrony was higher within either a ZII+ or a ZII- band. Because a given optic flow zone in folium IXcd of pigeons spans a ZII+/- stripe, it would be interesting to see how the synchrony of complex spike activity differs in Purkinje cells within and between ZII+ and ZII- stripes of the same optic flow preference. Sugihara and Shinoda (2004) showed that ZII+ and ZII- bands have receive different inputs from IO subnuclei. Though Chapter 3 of this thesis found that climbing fibres from functionally identical areas of the lateral mcIO span a ZII+/- stripe, it is possible that there are differences between climbing fibres of the same optic flow zone that project to ZII+ and ZII- bands. In order to test this, discrete injections of different coloured retrograde tracers would be made into ZII+ and ZII- zones with

the same optic flow preference in order to visualize the cells that project to them. In a similar experiment, anterograde tracers could be used intead of retrograde tracers to determine if there are differences in the projections of ZII+ and ZII- Purkinje cells within the same optic flow zone. A finding that ZII+ and ZII- Purkinje cells within the same optic flow zone have subtle functional distinction would bring us closer to determining the exact cerebellar role of an enzyme whose function remains largely unknown.

Which leads us to a very important question: what are the exact cellular functions of ZII within the cerebellum? While we know that it cleaves fructose-l,6-biphosphate in glycolosis in vitro (Ahn et al., 1994), its actual function in vivo may be quite different. We know that many molecular markers are also expressed in a complementary fashion to the expression pattern of ZII Purkinje cells. For example, the excitatory amino acid transporter EAAT4 is expressed in a parasagittal pattern that is identical to the ZII (Welsh et al., 2002). This is fascinating, as recent evidence has shown that EAAT4 plays a direct role in synaptic plasticity in Purkinje cells and protects them against excitotoxic cell death during ischemia (Welsh et al., 2002; Wadiche and Jahr, 2005; Yamashita et al., 2006). In an effort to relate this evidence to ZII expression, Paukert et al. (2010) revealed that more glutamate is released per action potential by CFs in ZII+ zones than CFs in ZII- zones. The calcium-buffer Parvalbumin has also been shown to be expressed in a parasagittal pattern complementary to ZII in birds, where Parvalbumin-positive Purkinje cells are generally ZII- (Wylie et al., 2011). Beyond helping maintain the synapse at its resting level during sustained

excitation (Bastianelli, 2003), Schwaller et al. (2002) has also proposed a role for Parvalbumin in synaptic plasticity. All these findings point back to a central problem: why are ZII and other molecular markers differentially expressed in the cerebellum, and what is the functional difference between the zones that either express or do not express them? While these questions are at the forefront of cerebellar research, because of our poor understanding of basic cerebellar function, much work needs to be done before they will ever be answered.

4.3 Conclusions

The connections from AOS and associated pretectal structures to the VbC are highly conserved, and the functional response properties of this pathway show a parasagittal zonal organization that is remarkably similar between mammals and birds (Voogd and Wylie, 2004). In addition to its role in compensatory responses to the visual motion created by an organisms movement throughout its environment, recent studies on the AOS and associated pretectum suggest that these structures are involved in the estimation of direction and speed of self-motion, spatial cognition, postural control, and visual obstacle avoidance (for review see Gamlin, 2006; Giolli et al., 2006). Thus, research into the organization and function of this visual pathway provides an opportunity to discover how extremely complex stimuli, such as visual motion of the environment across the retina, can be broken down into simpler elements by a sensory system to process information important for guiding an organisms behaviour.

Though traditional views of the cerebellum have undervalued its role in the central nervous system, likely due to its uniform structure, a complex

parasagittal organization has been revealed by its intrinsic functional, anatomical and molecular arrangement (see section 1.2.2). Increasingly, systems within the cerebellar cortex have become ideal models for determining the fundamental organization of the entire nervous system. Throughout the cerebellar cortex there is a basic cytoarchitecture, therefore properties of organization in one region of the cerebellum can usually be generalized to other regions, a principle that is not usually found between different regions of the cerebral cortex. However, while recent studies have begun to dissect the complex anatomical, biochemical and functional arrangement of the cerebellar cortex, we are still far from understanding how exactly the cerebellum works.

4.4 References

Ahn AH, Dziennis S, Hawkes R, Herrup K. 1994. The cloning of zebrin II reveals its identity with aldolase C. Development 120(8):2081-2090.

Apps R, Garwicz M. 2005. Anatomical and physiological foundations of cerebellar information processing. Nat Rev Neurosci 6(4):297-311.

Bastianelli E. 2003. Distribution of calcium-binding proteins in the cerebellum. Cerebellum. 2(4):242-62.

Brochu G, Maler L, Hawkes R. 1990. Zebrin II: a polypeptide antigen expressed selectively by Purkinje cells reveals compartments in rat and fish cerebellum. J Comp Neurol 291(4):538-552.

Crowder NA, Winship IR, Wylie DR. 2000. Topographic organization of inferior olive cells projecting to translational zones in the vestibulocerebellum of pigeons. J Comp Neurol 419(1):87-95.

De Zeeuw CI, Wylie DR, DiGiorgi PL, Simpson JI. 1994. Projections of individual Purkinje cells of identified zones in the flocculus to the vestibular and cerebellar nuclei in the rabbit. J Comp Neurol 349(3):428-447.

Dore L, Jacobson CD, Hawkes R. 1990. Organization and postnatal development of zebrin II antigenic compartmentation in the cerebellar vermis of the grey opossum, Monodelphis domestica. J Comp Neurol 291(3):431-449.

Gamlin PD. 2006. The pretectum: connections and oculomotor-related roles. Prog Brain Res 151:379-405.

Giolli RA, Blanks RH, Lui F. 2006. The accessory optic system: basic organization with an update on connectivity, neurochemistry, and function. Prog Brain Res 151:407-440.

Hawkes R. 1992. Antigenic markers of cerebellar modules in the adult mouse. Biochem Soc Trans 20(2):391-395.

Hawkes R, Herrup K. 1995. Aldolase C/zebrin II and the regionalization of the cerebellum. J Mol Neurosci 6(3):147-158.

Hawkes RA, Roehrig JT, Hunt AR, Moore GA. 1988. Antigenic structure of the Murray Valley encephalitis virus E glycoprotein. J Gen Virol 69 (Pt 5):1105-1109.

Herrup K, Kuemerle B. 1997. The compartmentalization of the cerebellum. Annu Rev Neurosci 20:61-90.

Lannoo MJ, Brochu G, Maler L, Hawkes R. 1991a. Zebrin II immunoreactivity in the rat and in the weakly electric teleost Eigenmannia (gymnotiformes) reveals three modes of Purkinje cell development. J Comp Neurol 310(2):215-233.

Lannoo MJ, Maler L, Hawkes R. 1992. Zebrin II distinguishes the ampullary organ receptive map from the tuberous organ receptive maps during development in the teleost electrosensory lateral line lobe. Brain Res 586(1):176-180.

Lannoo MJ, Ross L, Maler L, Hawkes R. 1991b. Development of the cerebellum and its extracerebellar Purkinje cell projection in teleost fishes as

determined by zebrin II immunocytochemistry. Prog Neurobiol 37(4):329-363.

Lau KL, Glover RG, Linkenhoker B, Wylie DR. 1998. Topographical organization of inferior olive cells projecting to translation and rotation zones in the vestibulocerebellum of pigeons. Neuroscience 85(2):605-614.

Leclerc N, Dore L, Parent A, Hawkes R. 1990. The compartmentalization of the monkey and rat cerebellar cortex: zebrin I and cytochrome oxidase. Brain Res 506(1):70-78.

Llinas R, Sasaki K. 1989. The Functional Organization of the Olivo-Cerebellar System as Examined by Multiple Purkinje Cell Recordings. Eur J Neurosci 1(6):587-602.

Marzban H, Zahedi S, Sanchez M, Hawkes R. 2003. Antigenic compartmentation of the cerebellar cortex in the syrian hamster Mesocricetus auratus. Brain Res 974(1-2):176-183.

Meek J, Hafmans TG, Maler L, Hawkes R. 1992. Distribution of zebrin II in the gigantocerebellum of the mormyrid fish Gnathonemus petersii compared with other teleosts. J Comp Neurol 316(1):17-31.

Pakan JM, Graham DJ, Gutiérrez-Ibáñez C, Wylie DR. 2011. Organization of the cerebellum: Correlating zebrin immunochemistry with optic flow zones in the pigeon flocculus. Vis Neurosci 28(2):163-174.

Pakan JM, Wylie DR. 2008. Congruence of zebrin II expression and functional zones defined by climbing fiber topography in the flocculus. Neurosci 157(1):57–69.

Ruigrok TJ. 2003. Collateralization of climbing and mossy fibres projecting to the nodulus and flocculus of the rat cerebellum. J Comp Neurol 466(2):278-298.

Sanchez M, Sillitoe RV, Attwell PJ, Ivarsson M, Rahman S, Yeo CH, Hawkes R. 2002. Compartmentation of the rabbit cerebellar cortex. J Comp Neurol 444(2):159-173.

Schwaller B, Meyer M, Schiffmann S. 2002. 'New' functions for 'old' proteins: the role of the calcium-binding proteins calbindin D-28k, calretinin and parvalbumin, in cerebellar physiology. Studies with knockout mice. Cerebellum. 1(4):241-58.

Sillitoe RV, Kunzle H, Hawkes R. 2003. Zebrin II compartmentation of the cerebellum in a basal insectivore, the Madagascan hedgehog tenrec Echinops telfairi. J Anat 203(3):283-296.

Sillitoe RV, Marzban H, Larouche M, Zahedi S, Affanni J, Hawkes R. 2005. Conservation of the architecture of the anterior lobe vermis of the cerebellum across mammalian species. Prog Brain Res 148:283-297.

Sugihara I, Marshall SP, Lang EJ. 2007. Relationship of complex spike synchrony bands and climbing fiber projection determined by reference to aldolase C compartments in crus IIa of the rat cerebellar cortex. Journal Comp Neurol 50(1):13–29.

Sugihara I, Shinoda Y. 2004. Molecular, topographic, and functional organization of the cerebellar cortex: a study with combined aldolase C and olivocerebellar labelling. J Neurosci 24(40):8771-8785.

Voogd J, Glickstein M. 1998. The anatomy of the cerebellum. Trends Neurosci 21(9):370-375.

Voogd J, Wylie DR. 2004. Functional and anatomical organization of floccular zones: a preserved feature in vertebrates. J Comp Neurol 470(2):107-112.

Wadiche JI, Jahr CE. 2005. Patterned expression of Purkinje cell glutamate transporters controls synaptic plasticity. Nat Neurosci 8(10):1329-1334.

Welsh JP, Yuen G, Placantonakis DG, Vu TQ, Haiss F, O'Hearn E, Molliver ME, Aicher SA. 2002. Why do Purkinje cells die so easily after global brain ischemia? Aldolase C, EAAT4, and the cerebellar contribution to posthypoxic myoclonus. Adv Neurol 89:331-359.

Wu, H.S., Sugihara, I. & Shinoda, Y. (1999). Projection patterns of single mossy fibers originating from the lateral reticular nucleus in the rat cerebellar cortex and nuclei. The Journal of Comparative Neurology 411, 97–118.

Wylie DR, Bischof WF, Frost BJ. 1998. Common reference frame for neural coding of translational and rotational optic flow. Nature 392(6673):278-282.

Wylie DR, Brown MR, Barkley RR, Winship IR, Crowder NA, Todd KG. 2003. Zonal organization of the vestibulocerebellum in pigeons (Columba livia): II. Projections of the rotation zones of the flocculus. J Comp Neurol 456(2):140-153.

Wylie DR, Frost BJ. 1991. Purkinje cells in the vestibulocerebellum of the pigeon respond best to either translational or rotational wholefield visual motion. Exp Brain Res 86(1):229-232.

Wylie DR, Frost BJ. 1993. Responses of pigeon vestibulocerebellar neurons to optokinetic stimulation. II. The 3-dimensional reference frame of rotation neurons in the flocculus. J Neurophysiol 70(6):2647-2659.

Wylie DR, Frost BJ. 1999. Complex spike activity of Purkinje cells in the ventral uvula and nodulus of pigeons in response to translational optic flow. J Neurophysiol 81(1):256-266.

Wylie DR, Gutierrez-Ibanez C, Graham DJ, Kreuzer MB, Pakan JM, Iwaniuk AN. 2011. Heterogeneity of parvalbumin expression in the avian cerebellar cortex and comparisons with zebrin II. Neurosci 185:73-84.

Yamashita A, Makita K, Kuroiwa T, Tanaka K. 2006. Glutamate transporters GLAST and EAAT4 regulate postischemic Purkinje cell death: an in vivo study using a cardiac arrest model in mice lacking GLAST or EAAT4. Neurosci Res 55(3):264-270.